

**Forward Osmosis as an Approach to Manage Oil Sands Produced Water:  
Membrane Fouling and Organic Removal**

By  
Shu Zhu

A thesis submitted in partial fulfillment of the requirements for the degree of  
Doctor of Philosophy  
in  
Environmental Engineering

Department of Civil and Environmental Engineering

University of Alberta

©Shu Zhu, 2017

## ABSTRACT

Currently, large amounts of oil sands process-affected water (OSPW) are stored in tailing ponds, leaving its environmental impact a significant concern. To better manage OSPW, numerous treatment approaches have been investigated including adsorption, advanced oxidation and biological treatment, among others. Forward osmosis (FO) as an emerging membrane desalination technology is gaining increasing research interests. FO utilizes only the osmotic difference between two solutions to draw the water molecules from the less concentrated side to the concentrated side, which potentially reduces the energy consumption and eliminates the membrane fouling. To date, the application of FO has already been evaluated on water and wastewater treatment, especially for the oil and gas wastewater. The overall objective of the current research is to better understand the feasibility of using FO in the treatment of OSPW in terms of membrane fouling and organic removal.

In the first set of investigations, FO was proposed to manage OSPW, using on-site waste basal depressurization water (BDW) as the draw solution. To investigate its feasibility, both short and long-term OSPW desalination experiments were carried out. By applying FO process, the volume of OSPW was decreased >40% and high rejections were achieved, especially, the major organic toxicity source — naphthenic acids (NAs). Although comparable low water flux ( $\geq 3$  L/m<sup>2</sup> hr) was obtained, water flux caused by membrane fouling can be completely recovered using clean water backwash. Moreover, calcium carbonate precipitation was observed on OSPW-oriented membrane side and with respect to flux decline, FO (active layer facing feed solution) and PRO (support layer facing draw solution) mode did not demonstrate a significant difference on anti-fouling performance. The advantages provided by this approach include zero

draw solution cost, less and reversible membrane fouling and beneficial reuse/recycle of diluted BDW.

In the second set of investigations, the effects of pH and draw solutions on the rejection of NA model compounds including cyclohexane carboxylic acid (CHA), 1-adamantaneacetic acid (AAA) and the refined Merichem mixture of NAs in forward osmosis were studied. The rejection behavior of CHA and AAA were pH-depend (from pH = 3 to 9), which further suggested that electrostatic repulsion was the dominant rejection mechanism. The rejection efficiency of Merichem NAs was maintained above 95%, which was not affected by the pH range from 6 to 9. A decline trend was observed on water flux using AAA and Merichem NAs as feed solution and surface fouling on Merichem NAs rejected membrane was confirmed by scanning electron microscopy (SEM) analysis. Four inorganic salts — sodium chloride (NaCl), ammonia chloride (NH<sub>4</sub>Cl), sodium sulphate (Na<sub>2</sub>SO<sub>4</sub>), and calcium chloride (CaCl<sub>2</sub>) — were introduced as the draw salts and no significant difference was found between the these draw solutes regarding the CHA rejection. Furthermore, the reverse salt diffusions for the draw solutes remained stable, except CaCl<sub>2</sub>. The reverse salt flux along with the water decline indicated that using CaCl<sub>2</sub> as the draw solution caused membrane surface precipitation. Our experimental results also suggested that the exposure of NA model compounds might alter the membrane characteristics, which needs to be further investigated.

In the third set of investigations, aquaporin (AQP)-based and cellulose triacetate (CTA)-based FO membranes, used to treat oil sands produced water, were compared in terms of membrane characteristics, NA model compounds adsorption and rejection, membrane fouling, and NA and inorganic salt rejections. Results of the nano-filtration (NF) test indicated the AQP membrane had higher water permeability than the CTA membrane. At pH = 9, each of the membranes

showed low adsorption and high rejection of NA model compounds, due to the electrostatic forces between the negatively charged membrane surface and the model compounds. Our study demonstrated that CTA membrane was more anti-fouling in treating OSPW. OSPW fouling associated with the presence of calcium was observed on both membranes, evidencing the possibility of cake enhanced concentration polarization. In addition, it was seen that the rejections of NAs and salt were more related to pretreatment methods and produced water type than membrane selection.

In the last set of investigations, to understand better the fouling mechanism in FO in terms of membrane materials and functional groups in NAs, which are the main source of organic concentration in OSPW, the direct force measurement was conducted using surface force apparatus (SFA) between three membranes including cellulose triacetate (CTA)-FO, aquaporin (AQP)-FO and polyamide (PA)-RO membrane and three functional groups including carboxyl, hydroxyl and hydrophobic functional group. Moreover, the adsorption phenomenon of the tested membranes using two NA model compounds (cyclohexanecarboxylic acid and cholic acid) was investigated and the FO fouling test using 0.45  $\mu\text{m}$  filtered OSPW as the feed solution was also performed. In the force measurement, only repulsive force was observed on -OH and -COOH functional group regardless of membrane types. It was also found that the adhesive forces caused by hydrophobic-hydrophobic interaction and compared to the other two membranes, AQP-FO exhibited the strongest hydrophobic interaction. The results from OSPW fouling experiment showed that AQP-FO suffered a more severe flux decline, which supported the observations in the interactive force analysis and subsequently suggested that the AQP-FO membrane might be easier to cause membrane fouling, comparing two other membranes.

## **PREFACE**

All of the research conducted in this thesis was designed and planned by myself and supervised by Dr. Mohamed Gamal El-Din at the University of Alberta. One part of this thesis was attributed to the collaboration with Dr. Hongbo Zeng's research group in the Department of Chemical Engineering.

### Chapter 2:

- Dr. Mingyu Li and Dr. Pamela Chelme-Ayala contributed to the manuscript edits.
- Dr. Rongfu Huang performed ultra-pressure liquid chromatography-high resolution mass spectrometry (UPLC/HRMS) analysis.

### Chapter 3:

- Dr. Mingyu Li and Dr. Pamela Chelme-Ayala contributed to the manuscript edits.
- Dr. Rongfu Huang performed ultra-pressure liquid chromatography-high resolution mass spectrometry (UPLC/HRMS) analysis.
- Dr. Mingyu Li and Dr. Selamawit Ashagre Messele helped with liquid chromatography–mass spectrometry (LC-MS) analysis.

### Chapter 4:

- Dr. Mingyu Li and Dr. Pamela Chelme-Ayala contributed to the manuscript edits.
- Dr. Rongfu Huang performed ultra-pressure liquid chromatography-high resolution mass spectrometry (UPLC/HRMS) analysis.
- Dr. Mingyu Li and Dr. Selamawit Ashagre Messele helped with liquid chromatography–mass spectrometry (LC-MS) analysis.

Chapter 5:

- Dr. Hongbo Zeng and Dr. Li Xiang contributed to the experimental planning.
- Dr. Mingyu Li and Dr. Pamela Chelme-Ayala contributed to the manuscript edits.
- Dr. Li Xiang conducted the surface force apparatus (SFA) analysis.

All the research work was conducted by myself except the above-mentioned contributions from collaborators and coauthors.

## **DEDICATION**

I dedicate my thesis work to my family and friends. I would like to express my sincere gratitude to my lovely father for letting me fulfill my dream of being a Ph.D. student. I would also like to thank my dear aunt for supporting me throughout all the stress while accepting the fact I still cannot get married. Also, this work is dedicated to my dear grandpa who had a great influence on my life but no longer has any opportunities to witness my achievements.

## **ACKNOWLEDGEMENT**

Firstly, I would like to express my sincere and great appreciation to my supervisor, Dr. Mohamed Gamal El-Din for his guidance and financial support through my 4-year program. Thank you for letting me to be part of your research group.

Secondly, I would like to thank all the post-doctoral fellows in our research group, Dr. Alla Alpatova, Dr. Mingyu Li, Dr. Pamela Chelme-Ayala, Dr. Rongfu Huang, Dr. Yanyan Zhang, Dr. Kerry N. McPhedran, and Dr. Selamawit Ashagre Messele for their support toward my research.

Thirdly, I appreciate all the technical staff in the Department of Civil and Environmental Engineering who always helped with my research: Maria Demeter, Nian Sun, Liang Chen, and all my other colleagues.

Fourthly, I would thank all the professors who gave insightful instruction with my course studies including Dr. Ania Ulrich, Dr. Ian Buchanan, Dr. Leonidas Perez-Estrada, and Dr. Keith Tierney. Especially, I would express my deep appreciation to Dr. Buchanan for letting be his teaching assistant in EnvE 440 and 421 for three years. I have learned a lot by being his teaching assistant.

Also, I would like to acknowledge my previous supervisor Dr. Susan J. Masten at the Michigan State University. Her strong recommendation gave me a great opportunity to accomplish my Ph.D. dream at the University of Alberta.

Lastly, I would like to acknowledge all the industrial and government institutions that supported my research including Napier-Reid Ltd., Shell Canada Limited, Helmholtz-Alberta Initiative (HAI) through the Alberta Environment and Parks' ecoTrust Program, Natural Sciences and Engineering Research Council of Canada (NSERC) Industrial Research Chair (IRC) Program in Oil Sands Tailings Water Treatment through the support by Syncrude Canada Ltd., Suncor



Energy Inc., Shell Canada, Canadian Natural Resources Ltd., Total E&P Canada Ltd., EPCOR  
Water Services, IOWC Technologies Inc., Alberta Innovates - Energy and Environment Solution,  
and Alberta Environment and Parks.

# Table of Contents

|         |  |    |
|---------|--|----|
| 1       | Chapter 1 General introduction and objectives .....  | 1  |
| 1.1     | Background and Motivation.....   | 1  |
| 1.1.1   | Oil sands process-affected water (OSPW).....   | 1  |
| 1.1.2   | OSPW treatment .....   | 2  |
| 1.1.3   | Forward osmosis (FO) .....   | 5  |
| 1.2     | Research Scopes and Objectives .....   | 8  |
| 1.3     | Thesis Organization.....   | 9  |
| 1.4     | Reference.....   | 11 |
| 2       | Chapter 2 Forward osmosis as an approach to manage oil sands tailings water and on-site basal depressurization water ..... | 18 |
| 2.1     | Introduction .....   | 18 |
| 2.2     | Materials and methods .....  | 21 |
| 2.2.1   | OSPW and BDW characteristics .....   | 21 |
| 2.2.2   | FO membrane characteristics and system setup .....   | 21 |
| 2.2.3   | Experimental procedures .....  | 24 |
| 2.2.3.2 | The evaluation of OSPW desalination.....   | 25 |
| 2.2.3.3 | Analytical methods .....   | 26 |
| 2.3     | Results and discussion.....  | 27 |
| 2.3.1   | Evaluation of BDW as the draw solution .....   | 27 |
| 2.3.2   | Evaluation of OSPW desalination .....  | 30 |
| 2.3.3   | Draw solute diffusion.....   | 35 |
| 2.3.4   | Organic rejection.....   | 36 |
| 2.4     | Sustainability of using FO to treat BDW and OSPW .....   | 39 |
| 2.5     | Conclusions .....  | 40 |
| 2.6     | Reference.....   | 41 |
| 3       | Chapter 3 Rejection of naphthenic acids by forward osmosis: Effect of pH value and draw solutes .....                      | 50 |
| 3.1     | Introduction .....   | 50 |
| 3.2     | Materials and methods .....  | 52 |
| 3.2.1   | Bench-scale FO system.....   | 52 |

|       |  |     |
|-------|--|-----|
| 3.2.2 | NA model compound rejection experiments .....  | 53  |
| 3.2.3 | Analytical methods .....   | 56  |
| 3.3   | Results and discussion.....  | 57  |
| 3.3.1 | Effect of pH on NA model compound and OSPW NA rejection .....  | 57  |
| 3.3.2 | Specific reverse salt diffusion.....   | 61  |
| 3.3.3 | NA model compound rejection.....   | 62  |
| 3.3.4 | Effect of draw solute on NA model compound rejection .....   | 68  |
| 3.4   | Conclusions.....   | 73  |
| 3.5   | Reference.....   | 73  |
| 4     | Chapter 4 Forward osmosis desalination of oil sands produced water: comparison between cellulose triacetate-based and aquaporin-based membranes.....                           | 80  |
| 4.1   | Introduction .....   | 80  |
| 4.2   | Materials and methods .....  | 83  |
| 4.2.1 | NA model compounds .....   | 83  |
| 4.2.2 | Oil sands produce water.....   | 84  |
| 4.2.3 | Membrane properties and FO operating system .....  | 84  |
| 4.2.4 | Determination of membrane characteristics .....  | 86  |
| 4.2.5 | NA model compound adsorption and rejection experiment protocol.....  | 87  |
| 4.2.6 | OSPW/BDW fouling experiment .....  | 88  |
| 4.2.7 | Analytical methods .....   | 89  |
| 4.3   | Results and discussion.....  | 90  |
| 4.3.1 | Membrane characterization.....   | 90  |
| 4.3.2 | Membrane performance .....   | 93  |
| 4.3.3 | NA model compounds adsorption and rejection experiment.....  | 94  |
| 4.3.4 | FO performance treating oil sands produced water .....   | 98  |
| 4.4   | Conclusions .....  | 106 |
| 4.5   | Reference.....   | 106 |
| 5     | Chapter 5 Probing oil sands process-affected water fouling mechanism of forward osmosis membrane: impact of membrane materials and functional groups in naphthenic acids ..... | 113 |
| 5.1   | Introduction .....   | 113 |
| 5.2   | Materials and methods .....  | 115 |

|       |  |     |
|-------|--|-----|
| 5.2.1 | FO membrane and sample preparation .....                                   | 115 |
| 5.2.2 | SFA interaction force measurements and AFM imaging .....                   | 116 |
| 5.2.3 | OSPW .....   | 118 |
| 5.2.4 | NA model compound adsorption experiment .....                              | 119 |
| 5.2.5 | Membrane performance in OSPW fouling experiment .....                      | 120 |
| 5.3   | Results and discussion.....  | 121 |
| 5.3.1 | Morphology of membrane polymer coated and functionalized micas.....        | 121 |
| 5.3.2 | Interaction between polymeric membrane surface and functional groups ..... | 122 |
| 5.3.3 | NA model compound adsorption experiment .....                              | 125 |
| 5.3.4 | Membrane fouling experiment using OSPW as the feed solution.....           | 126 |
| 5.4   | Conclusions .....  | 128 |
| 5.5   | Reference.....   | 129 |
| 6     | Chapter 6 General conclusions and recommendations.....                     | 133 |
| 6.1   | Thesis overview.....   | 133 |
| 6.2   | Conclusions .....  | 134 |
| 6.3   | Recommendations .....  | 136 |
| 7.    | Bibliography .....   | 140 |
| 8.    | Appendices.....  | 158 |

## List of Figures

|   |    |
|---|----|
| Figure 1-1 The schematic of FO compared to RO (Modified from (Cath, Childress, & Elimelech, 2006)). $\Delta\pi$ refers to the osmotic pressure difference between feed and brine. $\Delta P$ is the hydraulic pressure that requires forcing water diffuses to the less concentrated side. ....   | 6  |
| Figure 2-1 The schematic of the proposed process using BDW as the draw solution to treat OSPW. ....   | 21 |
| Figure 2-2 SEM images of (a) active layer and (b) support layer. ....   | 22 |
| Figure 2-3 Results of EDS analysis for two sides of membrane: (a) active layer, (b) support layer. ....   | 22 |
| Figure 2-4 ATR-FTIR spectra of membrane active and support layers. ....   | 23 |
| Figure 2-5 Schematic of the FO system.....  | 24 |
| Figure 2-6 Results of short-term OSPW desalination test at a crossflow velocity of 14 cm/s. (a) The experiments were conducted using clean DI as feed solution and BDW as draw solution in FO and PRO mode. 0.23 M NaCl as draw solution and clean DI water as feed solution in FO mode. (b) Natural settled OSPW as the feed and BDW as the draw solution. The shown data were corrected by the baseline experiments using BDW as draw solution and clean DI as feed solution in FO and PRO mode, respectively. Error bars represent standard deviation from triplicate experiments..... | 29 |
| Figure 2-7 Results of long-term OSPW desalination test. The experiment was conducted using BDW as draw solution and natural settled OSPW as the feed solution. (a): Water flux presented as a function of time. (b): Water flux/normalized flux presented as a function of permeate volume. The data shown in (b) were corrected by baseline experiments (using BDW as draw solution and clean DI as feed solution in FO and PRO mode, respectively).....   | 31 |

Figure 2-8 SEM images of membrane surfaces after long-term desalination experiment in FO mode: (a) active layer facing with OSPW (b) support layer facing BDW, and PRO mode: (c) active layer facing BDW (d) support layer facing OSPW ..... 33

Figure 2-9 EDS analysis of foulants found on the sides orienting OSPW. (a) active layer (FO mode); (b) support layer (PRO mode). In Figure 2-8 a, strong peaks of carbon, oxygen and calcium (O 50.64%, Ca 25.61%, and C 21.96%) were detected on the tested foulants. In Figure 2-8 b, same elements were observed on the precipitations of the support layer. Same elements (O 48.14%, Ca 24.86%, and C 24.16%) still attributed to the major compositions, while other inorganic elements ranked as Cl 1.16% > Na 0.84% > Mg 0.53% > S 0.18% > K 0.12% > Si 0.02%. ..... 34

Figure 2-10 The concentrations of COD, TOC and NA species before and after desalination (a) OSPW, (b) BDW. Error bar represents standard deviation from triplicate experiments..... 37

Figure 2-11 The concentration of NA species in BDW with the corresponding carbon and Z numbers before and after desalination. Before desalination (a), after FO mode desalination (b), after PRO mode desalination (c)..... 38

Figure 2-12 The SFS of OSPW and BDW taken before and after desalination ..... 39

Figure 2-13 Maximum capability of using BDW as the draw to desalinate OSPW. The experiment was conducted at the crossflow velocity of 14 cm/s in PRO mode. 1L of natural settled OSPW was used as the feed solution and 1L of BDW was used as the draw solution. .... 40

Figure 3-1 Schematic of FO system set-up..... 53

Figure 3-2 Water flux at various pH values as a function of permeate volume. (a) CHA (b) AAA (c) Merichem NAs, and (d) OSPW (NA concentration = 25.4 mg/L) as the feed solution. 1M NaCl was the draw solution. The presented water flux was baseline corrected. The baseline

experiments were conducted using corresponding buffer solution only as the feed solution and 1M NaCl solution as the draw. .... 59

Figure 3-3 SEM images taken before and after the rejection experiment for each NA model compound (100 ppm at pH = 9)..... 60

Figure 3-4 Contact angle analysis before and after the rejection experiment for each NA model compound (100 mg/L at pH = 9) ..... 60

Figure 3-5 Specific reverse salt flux of NaCl at different pH values with presence of NA model compound. Experimental condition: Draw solution = 1M NaCl, initial feed solutions (a) 100 mg/L of CHA at pH = 3, 6, 9; 25 mg/L of CHA at pH = 3 (b) 100 mg/L of AAA at pH = 3, 6, 9; 25 mg/L of AAA at pH = 3 (c) 100 mg/L of Merichem NAs at pH = 6, 9. The specific reverse diffusion of 1M NaCl as draw solution and corresponding buffer solution only as the feed solution was also plotted as a reference..... 62

Figure 3-6 Rejection of CHA (a) and AAA (b) as a function of time. The experimental conditions were as follows: the initial concentrations of CHA and AAA were  $100 \pm 3.2$  ppm and  $25 \pm 1.3$  ppm, draw solution was 1M NaCl. .... 63

Figure 3-7 Rejection of Merichem NAs as a function of hydrogen deficiency (-Z) (a) and carbon number (n) (b). 3D-rejection image along with corresponding carbon number and -Z number at pH =6 (c) and pH =9 (d), respectively. The experimental conditions were as follows: the initial concentrations of were 93.7 and 96.2 mg/L, respectively. Draw solution was 1M NaCl. .... 66

Figure 3-8 Rejection of OSPW NAs as a function of (a) hydrogen deficiency (-Z) and (b) carbon number (n). 3D-rejection image (c) along with corresponding carbon number and -Z number at pH =6, respectively. The experimental conditions were as follows: the initial concentrations of OSPW NAs were 25.4 mg/L and draw solution was 1M NaCl..... 66

Figure 3-9 Concentration of NAs in Merichem NA aqueous solution (a) pH = 9, (b) pH = 6 and (c) in oil sands process-affected water (OSPW) at pH = 9. .... 67

Figure 3-10 Normalized flux (baseline corrected) as a function of permeate volume using 1M NaCl, NH<sub>4</sub>Cl, Na<sub>2</sub>SO<sub>4</sub>, and 0.6 M CaCl<sub>2</sub> as the draw solution. The initial flux generated by these draw solutions was around 7.3±0.2 L/m<sup>2</sup> hr. Experimental condition: initial CHA concentration =92.6±3.7 mg/L, pH =9. Baseline experiments were conducted using the corresponding concentrations of inorganic salt solutions as the draw solutions and clean DI water as the feed at the same operating condition. .... 68

Figure 3-11 (a) Reverse salt flux as a function of water flux. Experimental conditions: using 0.1, 0.2, 0.5 and 1 M inorganic salt solutions (NaCl, NH<sub>4</sub>Cl, Na<sub>2</sub>SO<sub>4</sub>, and CaCl<sub>2</sub>) as draw and DI water as the feed (b) Specific reverse draw solute flux for NaCl, NH<sub>4</sub>Cl, Na<sub>2</sub>SO<sub>4</sub>, and CaCl<sub>2</sub>. Experimental condition: initial feed solution with CHA concentration = 92.6±3.7 mg/L, pH = 9. .... 71

Figure 3-12 Rejection of CHA as a function of time using 1M NaCl, NH<sub>4</sub>Cl, Na<sub>2</sub>SO<sub>4</sub>, and 0.6 M CaCl<sub>2</sub> as the draw solution. The initial water flux was maintained at 7.46±0.32 L/m<sup>2</sup> hr. .... 72

Figure 4-1 (a) SEM images of AQP-FO membrane and (b) ATR-FTIR image of AQP-FO membrane active layer. .... 91

Figure 4-2 (a) XPS results and (b) AFM images of AQP-FO membrane surface. The roughness of AQP-FO membrane was 36.30±0.34 nm. .... 92

Figure 4-3 Comparison of CTA-FO and AQP-FO membranes on NA model compounds adsorption (a) CHA, (b) AAA, (c) CA, and (d) TPCA. Experimental conditions: the initial concentration of each compound was 50 mg/L. Effective area was 4 cm<sup>2</sup> and the adsorption experiment lasted for 7 hours. .... 93



Figure 4-4 Comparison between CTA-FO and AQP-FO membranes on NA model compounds rejection efficiency (a) CHA, (b) AAA, (c) CA, and (d) TPCA. Experimental condition: Initial concentration of each model compound was 50 mg/L. Cross-flow velocity = 2.3 cm/s, the experiment lasted for 7 hours..... 97

Figure 4-5 The comparison between CTA and AQP-FO membranes on water flux applying NA model compound solutions. (a) CHA, (b) AAA, (c) CA, and (d) TPCA. Experimental condition: Initial concentration of each model compound was 50 mg/L. Cross-flow velocity = 2.3 cm/s, the experiments lasted for 7 hours. .... 98

Figure 4-6 The comparison of CTA-FO and AQP-FO membranes on water flux when using (b) OSPW, (c) OSPW (0.45  $\mu\text{m}$  filtered), and (d) BDW (0.45  $\mu\text{m}$  filtered) as feed solution. Experimental condition: FO membrane was operated in active layer facing the feed solution. Crossflow velocity = 2.3 cm/s, draw solution: 1 M NaCl. Baseline experiment (a) was conducted using 0.23 M and 0.01 M NaCl to mimic the osmotic pressure level of BDW and OSPW, respectively. 1M NaCl was used as the draw solution..... 101

Figure 4-7 SEM and EDX images taken after the FO performance experiment: (a), (c) raw OSPW and (b), (d) 0.45  $\mu\text{m}$  filtered OSPW. .... 102

Figure 4-8 3-D matrix of NA concentration in OSPW (0.45  $\mu\text{m}$  filtered). The concentration of NA was 25.4 mg/L..... 104

Figure 4-9 The comparison between CTA and AQP-FO membranes on OSPW-NA rejection efficiency..... 105

Figure 4-10 The comparison between CTA and AQP membranes on rejection of inorganic ions in (a) 0.45  $\mu\text{m}$  filtered OSPW (b) 0.45  $\mu\text{m}$  filtered BDW (c) concentration of each ion in 0.45  $\mu\text{m}$  filtered OSPW and BDW, respectively. .... 106

|   |     |
|---|-----|
| Figure 5-1 FT-IR spectra of the three tested membranes. ....  | 116 |
| Figure 5-2 NA concentration in OSPW at corresponding n and -Z number. ....  | 119 |
| Figure 5-3 AFM images of membrane polymer films: (a) AQP-FO (b) PA-RO (c) CTA-FO and<br>AFM images of functionalized mica: (d) hydrophobilized and (e) carboxylated surface. ....   | 122 |
| Figure 5-4 The results of direct force measurement between three membrane polymer films and<br>functional groups. (a) to (c) -OH, (d) to (f) -COOH and (g) to (i) -CH <sub>3</sub> . ....   | 124 |
| Figure 5-5 The comparison between CTA-FO, AQP-FO and PA-RO on NA model compound<br>adsorption. The concentrations of initial NA model compound were 49.6 mg/L and 46.8 mg/L<br>for both CHA and CA. ....  | 126 |
| Figure 5-6 Comparison between three membranes (CTA-FO, AQP-FO and PA-RO) on the<br>treatment of 0.45 μm OSPW. Experimental condition: 1 M NaCl was used as the draw solution<br>and the FO system was operating at a crossflow velocity of 2.3 cm/s. .... | 127 |
| Figure 6-1 The conceptual schematic of the integrated system.....   | 138 |
| Figure 8-1 Curve fitting of SFA force measurement.....  | 160 |

## List of Tables

|   |     |
|---|-----|
| Table 1-1 The general characteristics of OSPW (Y. Zhang, 2016).....                         | 2   |
| Table 1-2 Brief summary of the advantages and disadvantage of OSPW treatment technology ... | 5   |
| Table 2-1 Characteristics of raw OSPW, natural settled OSPW and BDW. ....                   | 28  |
| Table 3-1 Characteristics of NA model compounds.....  | 54  |
| Table 4-1 Characteristics of NA model compounds at pH = 9.....                              | 84  |
| Table 4-2 Characteristics of OSPW and BDW.....  | 85  |
| Table 4-3 Membrane properties.....  | 86  |
| Table 4-4 FO and NF performances of CTA and AQP membranes.....                              | 94  |
| Table 5-1 Water matrices of 0.45 $\mu\text{m}$ filtered OSPW .....                          | 119 |
| Table 8-1 Ion composition of OSPW and BDW before and after desalination.....                | 158 |
| Table 8-2 Characteristic of CHA and CA at pH = 9.....                                       | 159 |

## List of Abbreviations

|       |  |
|-------|--|
| AAA   | 1-adamantaneacetic acid                    |
| AEF   | Acid extractable fraction                  |
| AFM   | Atomic force microscopy                    |
| AOP   | Advanced oxidation process                 |
| AQP   | Aquaporin                                  |
| BDW   | Basal depressurization water               |
| BTEX  | Benzene, toluene, ethylbenzene, and xylene |
| CA    | Cellulose acetate                          |
| CECP  | Cake enhanced concentration polarization   |
| CHA   | Cyclohexane carboxylic acid                |
| CP    | Concentration polarization                 |
| CTA   | Cellulose triacetate                       |
| DMF   | Dimethylformamide                          |
| DOM   | Dissolved organic matter                   |
| EDX   | Energy dispersive x-ray spectroscopy       |
| FECO  | Fringes of equal chromatic order           |
| FO    | Forward osmosis                            |
| ICP   | Internal concentration polarization        |
| LC/MS | Liquid chromatography - mass spectrometric |
| MBI   | Multiple beam interferometry               |
| NAs   | Naphthenic acids                           |
| PAHs  | Polycyclic aromatic hydrocarbons           |
| PA    | Polyamide                                  |
| PES   | Polyethersulfone                           |

|      |   |
|------|---|
| PC   | Petroleum coke                          |
| OSPW | Oil sands process-affected water        |
| RMS  | Root mean square                        |
| RO   | Reverse osmosis                         |
| SEM  | Scanning electron microscopy            |
| SFA  | Surface force apparatus                 |
| TDS  | Total dissolved solids                  |
| TPCA | Trans-4-pentacyclohexanecarboxylic acid |
| TFC  | Thin film composite                     |
| TOC  | Total organic carbon                    |
| TSS  | Total suspended solids                  |
| UPLC | Ultra-performance liquid chromatography |

# 1 Chapter 1 General introduction and objectives

## 1.1 Background and Motivation

### 1.1.1 Oil sands process-affected water (OSPW)

The Athabasca oil sands deposit located in Alberta, Canada ranks as the world's third largest oil sands deposit (Kannel & Gan, 2012). In Canada, the Clark process known as hot water extraction process is continuously applied to produce crude oil from oil sands. In this process, warm water and caustic soda are introduced to separate the bitumen from oil sands, generating also oil sands process-affected water (OSPW). OSPW contains both organic and inorganic components. Sodium, bicarbonate, chloride and sulphate are four major components of its dissolved inorganic solids. The organic content of OSPW is made up of naphthenic acids (NAs), polycyclic aromatic hydrocarbons (PAHs), benzene, toluene, ethylbenzene, xylene (BTEX) and phenols (Mikula, Kasperski, Burns, & MacKinnon, 1996). NAs contribute to the majority (~80%) of dissolved organic matter (DOM) in OSPW and it is considered as one of dominant sources of toxicity toward aquatic biota and mammal (Garcia-Garcia et al., 2011; Pourrezaei et al., 2014). The general formula used to describe the chemical structure of NAs is  $(C_nH_{2n+z}O_2)$ , where n represents the carbon number and Z demonstrates its hydrogen deficiency. The concentration of NAs in tailing pond depends on their age and composition and usually, it ranges from 40 to 70 mg/L (Allen, 2008a; Holowenko, MacKinnon, & Fedorak, 2002). Currently, OSPW is stored in tailing ponds and cannot be discharged directly to the environment (zero-discharge policy). In the year of 2013, the total area of tailing ponds covered approximately 180 km<sup>2</sup> (El-Din et al., 2011) and the surface is increasing yearly as new ponds are being developed. The general characteristics of OSPW are summarised in Table 1-1.

**Table 1-1** The general characteristics of OSPW (Y. Zhang, 2016)

| <b>Parameter</b>                                     | <b>Range</b> |
|--|--------------|
| pH   | 8.3-8.7      |
| Turbidity (NTU)                                      | 71.6-213.3   |
| Conductivity ( $\mu\text{S}/\text{cm}$ )             | 3459-4500    |
| Total suspended solids (TSS) (mg/L)                  | 97-221       |
| Total dissolved solids (TDS) (mg/L)                  | 2477-2859    |
| Alkalinity (mg/L)                                    | 609.3-776.9  |
| Chloride (mg/L)                                      | 641.0-715.7  |
| Sulfate (mg/L)                                       | 274.7-602.6  |
| Sodium (mg/L)  | 840.6-846.7  |
| Potassium (mg/L)                                     | 14.7-17.0    |
| Magnesium (mg/L)                                     | 8.6-15.1     |
| Calcium (mg/L)                                       | 10.1-25.3    |
| Chemical oxygen demand (COD) (mg/L)                  | 204-302      |
| Total organic carbon (TOC) (mg/L)                    | 48.3-75.0    |
| Biochemical oxygen demand (BOD <sub>5</sub> ) (mg/L) | 2.7-3.30     |
| Naphthenic acids (NAs) (mg/L)                        | 8.92-39.2    |

### 1.1.2 OSPW treatment

Various physical, chemical and biological methods have been investigated to efficiently treat OSPW, especially, to eliminate the negative impact caused by NAs and other organic component in OSPW. Four categories of oil sands produced water treatments are summarized as follows.

- **Adsorption**

The most common adsorption process used in oil sand produced water is physical adsorption where the contaminants diffuse into the adsorbents and get adsorbed into the surface of adsorbents. The common adsorbents include active carbon, natural organic matter, zeolites, clays, and synthetic polymers (Allen, 2008b). The performances of those adsorbents were not consistent with all the organic target pollutants. For example, it is reported that active carbon showed high removal efficiency on NAs, but weak removal of

benzene, toluene, ethylbenzene, and xylene (BTEX) compared to carbonaceous adsorbent (Gallup, Isacoff, & Smith, 1996). Another example was using organic matter — peat as adsorbent. Couillard (Couillard, 1994) compared the removals between emulsified oil, benzene, toluene, and m-xylene. The results indicated that peat was more efficient in removing emulsified oil than benzene, toluene, and m-xylene. Petroleum coke (PC) was also evaluated as an adsorbent in Zubot et al.'s (Zubot, MacKinnon, Chelme-Ayala, Smith, & El-Din, 2012) study. The authors reported that PC adsorbent can be used in OSPW treatment directly due to its high efficiency on NAs and total acid-extractable organics (TAO) adsorption.

- **Advanced oxidation**

Compared to conventional chemical oxidation process, advanced oxidation processes (AOPs) were preferable when dealing with complex wastewater matrix (Ribeiro, Nunes, Pereira, & Silva, 2015). AOPs usually refer to the oxidation reactions with hydroxyl radicals ( $\cdot\text{OH}$ ) and they can be combined not only with oxidants but other process such as  $\text{O}_3/\text{H}_2\text{O}_2$ ,  $\text{UV}/\text{O}_3$ , and  $\text{UV}/\text{H}_2\text{O}_2$  etc. to maintain and enhance the efficiency of produced hydroxyl radicals (Allen, 2008b). The application of AOPs to the treatment of recalcitrant organic compounds in OSPW has been widely studied. Shu et al. (Shu, Li, Belosevic, Bolton, & El-Din, 2014) employed a solar UV/Chlorine AOP to remediate OSPW and the experimental results indicated that 75 to 84% of OSPW NAs were removed, along with the OSPW toxicity reduction. The AOP study conducted by Afzal et al. (Afzal et al., 2012) demonstrated that the performance of  $\text{UV}/\text{H}_2\text{O}_2$  process varied with carbon and ring numbers in terms of NAs degradation.

- **Biological treatment**



The principle of biological treatment for OSPW is to employ microorganism to removal the organics. Biological treatments such as active sludge, membrane bioreactor, trickling filter etc. have been investigated on oilfield produced water (Scholzy & Fuchs, 2000; Tellez, Nirmalakhandan, & Gardea-Torresdey, 2002). The research findings showed that the performance of biological treatment depended on the toxicity and high salinity tolerance (e.g. phenol) of microbes. Therefore, combined processes, for example granular activated carbon – fluidized bed reactor, were introduced to eliminate the impact of toxic organic compound and significant improvements were observed (Allen, 2008b). Another example is using ozonation combined with integrated fixed-film activated sludge (IFAS) (Huang, Shi, El-Din, & Liu, 2015) to treat OSPW. The authors reported that pre-ozonation enhanced the removal of NAs and the acid extractable fraction (AEF) in OSPW from 43.14% and 12.06% to 80.17% and 41.97%, respectively.

- **Membrane filtration**

Pressure-driven membrane processes including micro-, ultra-, nano-filtration and reverse osmosis, electrical-driven membrane process—electrodialysis have been studied as OSPW treatment alternatives. The performance of membrane process builds upon the membrane pore size, reverse osmosis (RO) can reject approximately all undesirable contaminants due to its non-porous structure (E. S. Kim, Liu, & El-Din, 2011). However, membrane treatments still suffers a few disadvantages including membrane fouling, high operational cost, and low permeate water flux (Allen, 2008b; Campos, Borges, Oliveira, Nobrega, & Sant'Anna, 2002).

The various advantages and disadvantages associated with each OSPW treatment technologies are summarized in Table 1-2 (Allen, 2008b).

**Table 1-2** Brief summary of the advantages and disadvantage of OSPW treatment technology

| OSPW treatment technology | Examples of each treatment  | Advantages   | Disadvantages   |
|---------------------------|---|--|---|
| Adsorption                | Adsorbents: activated carbon, carbonaceous adsorbents, natural organic adsorbents | Low environmental impact with limited waste production   | Inconstant treatment efficiency for organic removal   |
| Advanced oxidation        | Photocatalytic oxidation, sonochemical oxidation                                  | Degradation of both organic and inorganic pollutants     | High energy and cost consumption, incomplete degradation, by-product formation                  |
| Biological treatment      | Active sludge, membrane bioreactor, trickling filter                              | High degradation efficiency, comparative low cost        | Unstable removal efficiency because of the toxicity   |
| Membrane filtration       | Micro-, nano-, ultra-filtration and reverse osmosis                               | Efficiency rejection of organic and inorganic components | High energy input, efficiency might be affected of feed water pH, increased waste disposal cost |

### 1.1.3 Forward osmosis (FO)

The principle of FO is to utilize osmotic pressure difference as a driving force to transport water molecules from a low-concentration solution (feed solution) to a high-concentration solution (draw solution). A schematic of FO compared with reverse osmosis (RO) is shown in Figure 1-1. As a result, the feed solution is concentrated while the draw solution is diluted (Cath, Childress, & Elimelech, 2006). In FO process, little or no extra hydraulic pressure is required, which potentially reduces the operational cost and lowers the energy consumption. Another potential advantage of FO is low and reversible fouling propensity, which indirectly decreases the overall energy consumption (S. F. Zhao, Zou, Tang, & Mulcahy, 2012). To date, its application feasibility has been reported intensively on power generation, water and wastewater treatment, and food industry (Lutchmiah, Verliefde, Roest, Rietveld, & Cornelissen, 2014; S. F. Zhao et al.,

2012; Zhou, Gingerich, & Mauter, 2015). Moreover, applying FO as a treatment method for oil and gas wastewater has also been investigated by numerous researchers (Coday, Almaraz, & Cath, 2015; Duong & Chung, 2014; Minier-Matar et al., 2015). These studies include the reclamation of oil and gas drilling wastewater (Coday, Xu, et al., 2014; Hickenbottom et al., 2013), separation of emulsified oil–water (Duong & Chung, 2014), and recovery water from petroleum/water emulsions (S. Zhang, Wang, Fu, & Chung, 2014), among others.

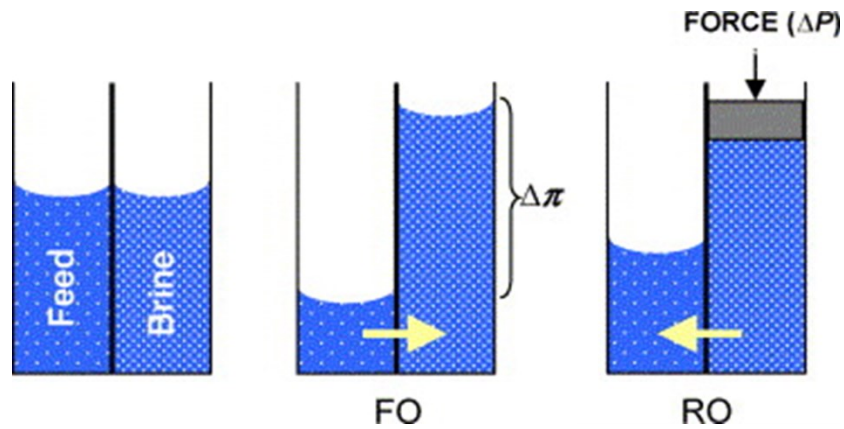


**Figure 1-1** The schematic of FO compared to RO (Adapted and modified from Cath, Childress, & Elimelech, 2006).  $\Delta\pi$  refers to the osmotic pressure difference between feed and brine.  $\Delta P$  is the hydraulic pressure that requires forcing water diffuses to the less concentrated side.

Despite all the potential benefits, several challenges still cast a shadow over FO application. Due to the nature of osmosis, no clean permeate can be directly obtained, leaving the separation process an inevitable concern (Shaffer, Werber, Jaramillo, Lin, & Elimelech, 2015). Moreover, draw solution selection, FO membrane properties and membrane fouling control are all key issues needed to be addressed in practice (Chung et al., 2012; Shaffer et al., 2015). Limited FO membranes are commercial available. Asymmetric cellulose triacetate (CTA) membrane manufactured by Hydration Technology Innovation, USA is a one of popular FO membranes

reported in several membrane studies. Flat sheet aquaporin (AQP) inside membrane (Aquaporin A/S, DK) is a biomimic membrane which attracts more research interests for its higher water permeability and contaminant rejection rate. However, these two FO membranes have their own drawbacks. CTA membrane suffers a high fouling propensity and low water flux because of its membrane materials and structure (D. T. Qin et al., 2015). Although AQP membranes showed high water flux and contaminant rejection efficiency, the mechanical strength was comparatively weak, thereby leaving its stability an important concern. The mean pore radius of CTA-FO membrane is 0.25–0.30 nm (Fang, Bian, Bi, Li, & Wang, 2014) while the pore size of AQP-FO has not been studied yet.

To date, employing membrane processes to manage oil and gas wastewater has been intensively studied. Hickenbottom et al. (Hickenbottom et al., 2013) studied the treatment of drilling mud and fracturing wastewater from oil and gas industry using cellulose triacetate (CTA) membrane. The results demonstrated that 80% volume of drilling wastewater was recovered and high inorganic and organic rejections were achieved. Coday et al. (Coday et al., 2016) studied the effect of FO membrane types (one CTA membrane and two polyamide-based TFC membranes) and operating conditions on the treatment of oil and gas wastewater. The results indicated that, compared to the direct influences of initial water flux and cross-flow velocity, membrane types had little impact on membrane fouling. However, CTA and TFC membranes performed distinctively different on pharmaceutical rejection (Jin, Shan, Wang, Wei, & Tang, 2012). Compared to CTA membranes, TFC showed steadier rejections (>95%) of carbamazepine, diclofenac, ibuprofen and naproxen at various pH values and permeate fluxes. Additionally, a comparison between CTA, TFC and two Porifera membranes had been carried out by Blandin et al. (Blandin, Vervoort, Le-Clech, & Verliefde, 2016) in aspects of membrane fouling and

cleaning. It was reported that two Porifera membranes showed higher water permeability than CTA and TFC but suffered more severe fouling.

## **1.2 Research Scopes and Objectives**

As discussed above, FO has been widely studied in different research areas. However, few studies have applied FO for OSPW treatment. Only Jiang et al. (Jiang, Liang, & Liu, 2016) evaluated the feasibility of using FO as a OSPW desalination method; the authors concluded that 85% water can be recovered from OSPW, and 80 to 100% of metallic and organic contaminants were rejected. They also mentioned that the water recovery efficiencies of a cleaned membrane and clean pristine membrane were comparable. Besides the significant research gaps between FO applicability and OSPW management, the selection of proper draw solution remains under investigation from the perspective of cost reduction and its recycle and/or safe discharge (Cath et al., 2006). To solve this problem, some researchers introduced ammonia salts including ammonia—carbon dioxide and ammonia bicarbonate as draw solutions so that the draw solutes could be recycled by moderate heating (M. H. Qin & He, 2014; Yip, Tiraferri, Phillip, Schiffman, & Elimelech, 2010). However, the thermal recycle is still considered as an energy-intensive process (Ge, Ling, & Chung, 2013). Accordingly, similar to other pressure-driven membrane processes, research gaps in understanding the organic rejection and membrane fouling mechanism are worthy noting.

This Ph.D. thesis focused on applying FO to OSPW desalination and the overall objective was to investigate the feasibility of FO as an approach for OSPW management. Also, other perspectives including operating condition, membrane and draw solution types, organic rejection mechanism, and membrane fouling were evaluated as important factors affecting the FO performance on OSPW management. The objectives of the research were as follows:

- To test the feasibility of FO as a desalination method of OSPW;
- To evaluate the treatment efficiency in terms of permeate flux, draw solute and organic rejection;
- To study the FO membrane fouling propensity using different NA model compounds;
- To investigate the feasibility of using basal depressurization water (BDW) as the draw solution in OSPW desalination process;
- To evaluate the effect of membrane orientation and membrane fouling behavior by permeate flux pattern and membrane fouling morphology;
- To study the rejection of three NA model compounds on aspects of feed solution pH and draw solution types;
- To further understand the rejection mechanism of FO membrane toward NA model compound;
- To investigate the membrane rejection efficiency of NA model compounds, OSPW-NAs, and heavy metals;
- To compare the performance of two types of commercially available FO membranes in terms of membrane own characteristics, membrane fouling, and inorganic and organic rejections; and
- To study the interaction force between membrane surface and major functional groups in NAs.

### **1.3 Thesis Organization**

The current thesis consists of six chapters. Chapter 1 provides a brief introduction and research motivations followed by research scope and objectives. Chapter 2 presents a published paper in which BDW was used as the draw solution to desalinate OSPW. Both short- and long-term batch

experiments were conducted to evaluate the performance of BDW as the draw solution. Water flux, membrane surface morphology, organic and inorganic rejection efficiency were all evaluated as important parameters to determine the proposed FO process. Chapter 3 contains an investigation on rejection of NAs by forward osmosis in aspects of effect of pH value and draw solutes. To be more specific, the effects of pH on the rejection of NA model compounds including cyclohexane carboxylic acid (CHA), 1-adamantaneacetic acid (AAA) and the refined Merichem mixture of NAs in forward osmosis were studied and four inorganic salts— sodium chloride (NaCl), ammonia chloride (NH<sub>4</sub>Cl), sodium sulfate (Na<sub>2</sub>SO<sub>4</sub>), and calcium chloride (CaCl<sub>2</sub>) were introduced as the draw salts to evaluate their impacts of the removal of NA compounds. Chapter 4 presents a comparison of the performance two FO membranes (CTA and aquaporin inside) for the treatment of oil sands produced water (i.e., OSPW and BDW). Membrane fouling, organic and inorganic rejections as well as the adsorption of NA model compounds were evaluated. Chapter 5 introduces a study of the interactive forces between membrane polymeric surface and major functional groups in NAs to evaluate the mechanism of organic fouling on FO membrane. Three commercially available membranes including CTA-FO, AQP-FO and PA-RO were investigated and compared in terms of the adhesion and repulsion forces between membrane materials and three functional groups, including –COOH, –OH and –(CH<sub>2</sub>)<sub>17</sub>CH<sub>3</sub>. Chapter 6 presents the general conclusions and recommendations obtained from the experimental results, which give suggestions for future work in the current research scope. Finally, some of the experimental methodologies and supplementary figures and tables are provided in the Appendices.

## 1.4 Reference

- Afzal, A., Drzewicz, P., Perez-Estrada, L. A., Chen, Y., Martin, J. W., & El-Din, M. G. (2012). Effect of Molecular Structure on the Relative Reactivity of Naphthenic Acids in the UV/H<sub>2</sub>O<sub>2</sub> Advanced Oxidation Process. *Environmental Science & Technology*, 46(19), 10727-10734.
- Allen, E. W. (2008a). Process water treatment in Canada's oil sands industry: I. Target pollutants and treatment objectives. *Journal of Environmental Engineering and Science*, 7(2), 123-138.
- Allen, E. W. (2008b). Process water treatment in Canada's oil sands industry: II. A review of emerging technologies. *Journal of Environmental Engineering and Science*, 7(5), 499-524. doi: Doi 10.1139/S08-020
- Blandin, G., Vervoort, H., Le-Clech, P., & Verliefde, A. R. D. (2016). Fouling and cleaning of high permeability forward osmosis membranes. *Journal of Water Process Engineering*, 9, 161-169. doi: <http://dx.doi.org/10.1016/j.jwpe.2015.12.007>
- Campos, J. C., Borges, R. M. H., Oliveira, A. M., Nobrega, R., & Sant'Anna, G. L. (2002). Oilfield wastewater treatment by combined microfiltration and biological processes. *Water Research*, 36(1), 95-104.
- Cath, T. Y., Childress, A. E., & Elimelech, M. (2006). Forward osmosis: Principles, applications, and recent developments. *Journal of Membrane Science*, 281(1-2), 70-87. doi: 10.1016/j.memsci.2006.05.048



- Chung, T. S., Li, X., Ong, R. C., Ge, Q. C., Wang, H. L., & Han, G. (2012). Emerging forward osmosis (FO) technologies and challenges ahead for clean water and clean energy applications. *Current Opinion in Chemical Engineering*, 1(3), 246-257.
- Coday, B. D., Almaraz, N., & Cath, T. Y. (2015). Forward osmosis desalination of oil and gas wastewater: Impacts of membrane selection and operating conditions on process performance. *Journal of Membrane Science*, 488, 40-55. doi: 10.1016/j.memsci.2015.03.059
- Coday, B. D., Hoppe-Jones, C., Wandera, D., Shethji, J., Herron, J., Lampi, K., . . . Cath, T. Y. (2016). Evaluation of the transport parameters and physiochemical properties of forward osmosis membranes after treatment of produced water. *Journal of Membrane Science*, 499, 491-502.
- Coday, B. D., Xu, P., Beaudry, E. G., Herron, J., Lampi, K., Hancock, N. T., & Cath, T. Y. (2014). The sweet spot of forward osmosis: Treatment of produced water, drilling wastewater, and other complex and difficult liquid streams. *Desalination*, 333(1), 23-35. doi: 10.1016/j.desal.2013.11.014
- Couillard, D. (1994). The Use of Peat in Waste-Water Treatment. *Water Research*, 28(6), 1261-1274.
- Duong, P. H. H., & Chung, T. S. (2014). Application of thin film composite membranes with forward osmosis technology for the separation of emulsified oil-water. *Journal of Membrane Science*, 452, 117-126. doi: 10.1016/j.memsci.2013.10.030

- El-Din, M. G., Fu, H. J., Wang, N., Chelme-Ayala, P., Perez-Estrada, L., Drzewicz, P., . . . Smith, D. W. (2011). Naphthenic acids speciation and removal during petroleum-coke adsorption and ozonation of oil sands process-affected water. *Science of the Total Environment*, 409(23), 5119-5125.
- Gallup, D. L., Isacoff, E. G., & Smith, D. N. (1996). Use of Ambersorb(R) carbonaceous adsorbent for removal of BTEX compounds from oil-field produced water. *Environmental Progress*, 15(3), 197-203.
- Garcia-Garcia, E., Pun, J., Perez-Estrada, L. A., Din, M. G. E., Smith, D. W., Martin, J. W., & Belosevic, M. (2011). Commercial naphthenic acids and the organic fraction of oil sands process water downregulate pro-inflammatory gene expression and macrophage antimicrobial responses. *Toxicology Letters*, 203(1), 62-73.
- Ge, Q. C., Ling, M. M., & Chung, T. S. (2013). Draw solutions for forward osmosis processes: Developments, challenges, and prospects for the future. *Journal of Membrane Science*, 442, 225-237. doi: 10.1016/j.memsci.2013.03.046
- Hickenbottom, K. L., Hancock, N. T., Hutchings, N. R., Appleton, E. W., Beaudry, E. G., Xu, P., & Cath, T. Y. (2013). Forward osmosis treatment of drilling mud and fracturing wastewater from oil and gas operations. *Desalination*, 312, 60-66. doi: 10.1016/j.desal.2012.05.037
- Holowenko, F. M., MacKinnon, M. D., & Fedorak, P. M. (2002). Characterization of naphthenic acids in oil sands wastewaters by gas chromatography-mass spectrometry. *Water Research*, 36(11), 2843-2855. doi: Pii S0043-1354(01)00492-4

- Huang, C. K., Shi, Y. J., El-Din, M. G., & Liu, Y. (2015). Treatment of oil sands process-affected water (OSPW) using ozonation combined with integrated fixed-film activated sludge (IFAS). *Water Research*, 85, 167-176.
- Jiang, Y., Liang, J., & Liu, Y. (2016). Application of forward osmosis membrane technology for oil sands process-affected water desalination. *Water Science and Technology*, 73(7), 1-8. doi: 10.2166/wst.2016.014
- Jin, X., Shan, J. H., Wang, C., Wei, J., & Tang, C. Y. Y. (2012). Rejection of pharmaceuticals by forward osmosis membranes. *Journal of Hazardous Materials*, 227, 55-61. doi: 10.1016/j.jhazmat.2012.04.077
- Kannel, P. R., & Gan, T. Y. (2012). Naphthenic acids degradation and toxicity mitigation in tailings wastewater systems and aquatic environments: A review. *Journal of Environmental Science and Health Part a-Toxic/Hazardous Substances & Environmental Engineering*, 47(1), 1-21. doi: 10.1080/10934529.2012.629574
- Kim, E. S., Liu, Y., & El-Din, M. G. (2011). The effects of pretreatment on nanofiltration and reverse osmosis membrane filtration for desalination of oil sands process-affected water. *Separation and Purification Technology*, 81(3), 418-428. doi: DOI 10.1016/j.seppur.2011.08.016
- Lutchmiah, K., Verliefde, A. R. D., Roest, K., Rietveld, L. C., & Cornelissen, E. R. (2014). Forward osmosis for application in wastewater treatment: A review. *Water Research*, 58, 179-197. doi: 10.1016/j.watres.2014.03.045

- Mikula, R. J., Kasperski, K. L., Burns, R. D., & MacKinnon, M. D. (1996). Nature and fate of oil sands fine tailings. *Suspensions: Fundamentals and Applications in the Petroleum Industry*, 251, 677-723.
- Minier-Matar, J., Hussain, A., Janson, A., Wang, R., Fane, A. G., & Adham, S. (2015). Application of forward osmosis for reducing volume of produced/Process water from oil and gas operations. *Desalination*, 376, 1-8.
- Pourrezaei, P., Alpatova, A., Khosravi, K., Drzewicz, P., Chen, Y., Chelme-Ayala, P., & El-Din, M. G. (2014). Removal of organic compounds and trace metals from oil sands process-affected water using zero valent iron enhanced by petroleum coke. *Journal of Environmental Management*, 139, 50-58.
- Qin, M. H., & He, Z. (2014). Self-Supplied Ammonium Bicarbonate Draw Solute for Achieving Wastewater Treatment and Recovery in a Microbial Electrolysis Cell-Forward Osmosis-Coupled System. *Environmental Science & Technology Letters*, 1(10), 437-441. doi: 10.1021/ez500280c
- Ribeiro, A. R., Nunes, O. C., Pereira, M. F. R., & Silva, A. M. T. (2015). An overview on the advanced oxidation processes applied for the treatment of water pollutants defined in the recently launched Directive 2013/39/EU. *Environment International*, 75, 33-51.
- Scholzy, W., & Fuchs, W. (2000). Treatment of oil contaminated wastewater in a membrane bioreactor. *Water Research*, 34(14), 3621-3629.
- Shaffer, D. L., Werber, J. R., Jaramillo, H., Lin, S. H., & Elimelech, M. (2015). Forward osmosis: Where are we now? *Desalination*, 356, 271-284. doi: 10.1016/j.desa.2014.10.031

- Shu, Z. Q., Li, C., Belosevic, M., Bolton, J. R., & El-Din, M. G. (2014). Application of a Solar UV/Chlorine Advanced Oxidation Process to Oil Sands Process-Affected Water Remediation. *Environmental Science & Technology*, 48(16), 9692-9701.
- Tellez, G. T., Nirmalakhandan, N., & Gardea-Torresdey, J. L. (2002). Performance evaluation of an activated sludge system for removing petroleum hydrocarbons from oilfield produced water. *Advances in Environmental Research*, 6(4), 455-470.
- Yip, N. Y., Tiraferri, A., Phillip, W. A., Schiffman, J. D., & Elimelech, M. (2010). High Performance Thin-Film Composite Forward Osmosis Membrane. *Environmental Science & Technology*, 44(10), 3812-3818. doi: 10.1021/es1002555
- Zhang, S., Wang, P., Fu, X. Z., & Chung, T. S. (2014). Sustainable water recovery from oily wastewater via forward osmosis-membrane distillation (FO-MD). *Water Research*, 52, 112-121. doi: 10.1016/j.watres.2013.12.044
- Zhang, Y. (2016). Development and application of Fenton and UV-Fenton processes at natural pH using chelating agents for the treatment of oil sands process-affected water (Doctor of Philosophy ), University of Alberta.
- Zhao, S. F., Zou, L., Tang, C. Y. Y., & Mulcahy, D. (2012). Recent developments in forward osmosis: Opportunities and challenges. *Journal of Membrane Science*, 396, 1-21. doi: 10.1016/j.memsci.2011.12.023
- Zhou, X. S., Gingerich, D. B., & Mauter, M. S. (2015). Water Treatment Capacity of Forward-Osmosis Systems Utilizing Power-Plant Waste Heat. *Industrial & Engineering Chemistry Research*, 54(24), 6378-6389. doi: 10.1021/acs.iecr.5b00460

Zubot, W., MacKinnon, M. D., Chelme-Ayala, P., Smith, D. W., & El-Din, M. G. (2012). Petroleum coke adsorption as a water management option for oil sands process-affected water. *Science of the Total Environment*, 427, 364-372.

## **2 Chapter 2 Forward osmosis as an approach to manage oil sands tailings water and on-site basal depressurization water<sup>1</sup>**

### **2.1 Introduction**

The bitumen extraction process for the oil sands in Alberta, Canada requires large volumes of water intake (Mohamed, Wilson, Peru, & Headley, 2013). The created process water, oil sand process-affected water (OSPW), cannot currently be directly discharged into the environment due to a zero discharge practice implemented by the industry (Allen, 2008a). Similar to other petroleum refinery and hydraulic fracturing wastewaters, OSPW contains both dissolved inorganic (e.g., heavy metals) and organic compounds (e.g., naphthenic acids) which are acute and chronic toxic to various aquatic organisms (Frank et al., 2008; Garcia-Garcia et al., 2012). To date, tailing ponds cover an area of 180 square kilometers and the surface is increasing yearly as new ponds are being developed. Due to the large quantities of stored OSPW, different treatment approaches on biological (Huang et al., 2015; Islam, Zhang, McPhedran, Liu, & El-Din, 2015), chemical (Anderson et al., 2012; Klamerth et al., 2015) and physicochemical (Alpatova et al., 2014; Dong et al., 2014) aspects have been investigated for their safe discharge and recycle. Conventional pressure-driven membrane processes including micro-, ultra-, nano-filtration (NF) and reverse osmosis (RO) as typical physical treatment methods were investigated for OSPW management (Allen, 2008b). NF and RO were reported to be effective, but membrane

---

<sup>1</sup> A version of this chapter has been published previously: Shu Zhu, Mingyu Li & Mohamed Gamal El-Din. (2017). Forward osmosis as an approach to manage oil sands tailings water and on-site basal depressurization water. *Journal of Hazardous Materials*, 327, 18-27

fouling, high energy consumption, complicated system maintenance are still affecting their popularization in the oil sands industry (E. S. Kim et al., 2011).

Recent researches have shown great promise in an emerging membrane desalination technology — forward osmosis (FO) (Rastogi & Nayak, 2011). In FO process, clean permeate from feed solution (less concentrated) can be attracted into draw solution (high concentrated) by osmotic pressure difference through semi-permeable membrane. Therefore, less or no extra hydraulic pressure is required, which minimizes the membrane fouling potential and reduces the energy input. While its potential application has been reported intensively on power generation, food industry and water and wastewater treatment (Lutchmiah et al., 2014; S. F. Zhao et al., 2012; Zhou et al., 2015), especially high salinity industrial wastewaters (Shaffer et al., 2013), the selection of proper draw solution remains under investigation from the perspective of cost reduction and its recycle and/or safe discharge (Cath et al., 2006). To solve this problem, some researchers have introduced ammonia salts including ammonia—carbon dioxide and ammonia bicarbonate as draw solutions so that the draw solutes can be recycled by moderate heating (M. H. Qin & He, 2014; Yip et al., 2010). However, the thermal recycle is still considered an energy-intensive process (Ge et al., 2013). In the current study, we proposed a novel approach of using basal depressurization water (BDW), one of the on-site brackish wastewaters, to drive OSPW desalination through semi-permeable membrane. BDW, the depressurized groundwater, was produced in open mining to control surface runoff and seepage water accumulation (E. S. Kim, Dong, Liu, & Gamal El-Din, 2013). By employing FO process, the concentration of OSPW and dilution of BDW could be achieved at one process. Consequently, the volume of OSPW can be reduced while sufficient diluted BDW can be reused/recycled, which would potentially lower both the energy input and environmental impact.



Low fouling propensity was highlighted in FO process over other pressure-driven membrane processes; however, the complex compositions of OSPW and BDW including organic species, inorganic salts and colloidal particles cast a shadow over its performance. In FO process, concentration polarization, divalent ion binding, membrane materials and structure, reverse salt diffusion (Y. Kim, Lee, Shon, & Hong, 2015; J. Lee, Kim, & Hong, 2014; S. Lee, Boo, Elimelech, & Hong, 2010; B. Mi & Elimelech, 2008; B. X. Mi & Elimelech, 2010; Motsa, Mamba, D'Haese, Hoek, & Verliefde, 2014) along with the presence of organic and inorganic species were reported to accelerate membrane fouling and salt saturation (scaling). Boo et al. (Boo, Lee, Elimelech, Meng, & Hong, 2012) suggested that the reverse salt diffusion enhanced the particle aggregation and destabilisation, which led to an irreversible flux decline. Liu and Mi (Liu & Mi, 2012) assessed the membrane fouling with the coexistence of gypsum and alginate and discovered that alginate combined with gypsum crystal formed larger size compounds, gypsum scaling. Accordingly, membrane fouling phenomenon caused by OSPW desalination driven by BDW requires further investigation.

The main objective of the paper is to study the feasibility of managing OSPW in FO process using BDW as the draw solution. To achieve that, the effect of membrane orientation and membrane fouling behavior were evaluated through the permeate flux pattern and membrane surface morphology. The salt diffusion and organic rejection were also examined. The schematic of the proposed process is shown in Fig. 2-1.

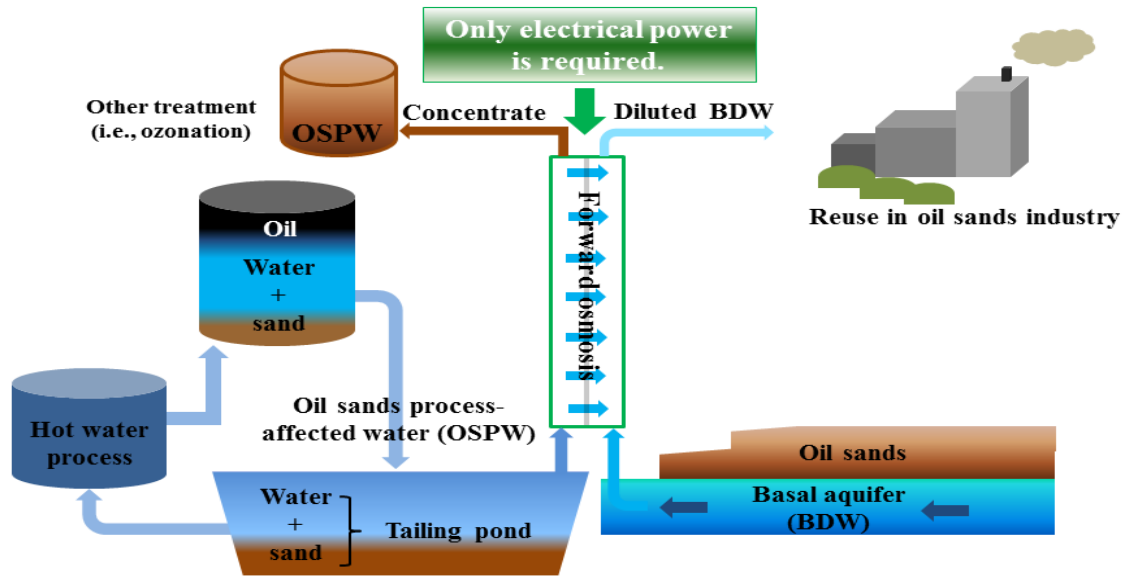


**Figure 2-1** The schematic of the proposed process using BDW as the draw solution to treat OSPW.

## 2.2 Materials and methods

### 2.2.1 OSPW and BDW characteristics

Raw OSPW and BDW were both collected from Fort McMurray, AB, Canada, and stored in polyvinyl chloride barrels at 4°C. The water properties are presented in Table 2-1. Tested OSPW used in the following experiments was naturally settled by gravity to reduce the suspended solids. Compared to OSPW, the turbidity of BDW was lower ( $1.0 \pm 0.1$  NTU). Hence, no extra pre-treatment was conducted. Water samples were warmed to the room temperature ( $21 \pm 1^\circ\text{C}$ ) before used.

### 2.2.2 FO membrane characteristics and system setup

The FO membrane used in this study was provided by HTI (Hydration Technologies, Inc., Albany, OR, USA). The cellulose triacetate (CTA) membrane was fabricated asymmetrically with a shiny active layer supported by embedded polyester mesh. Detailed membrane properties

are described elsewhere (Arkhangelsky et al., 2014; C. Kim, Lee, & Hong, 2012). Membrane surface characterization could be found in the Fig. 2-1 to Fig. 2-3.

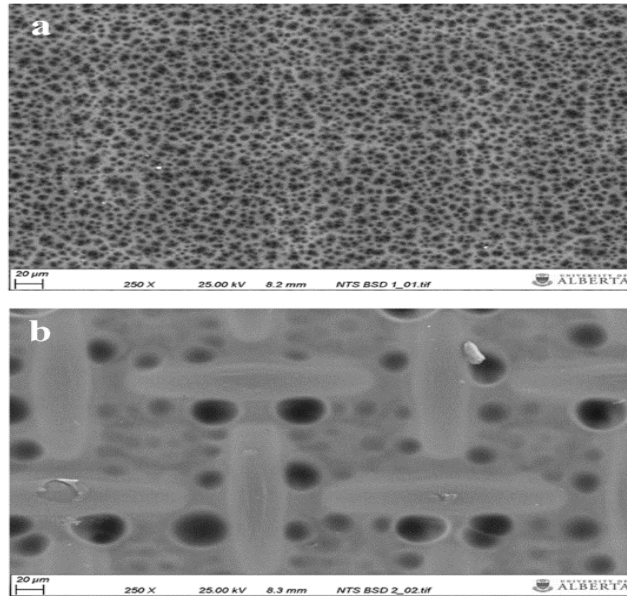


**Figure 2-2** SEM images of (a) active layer and (b) support layer.

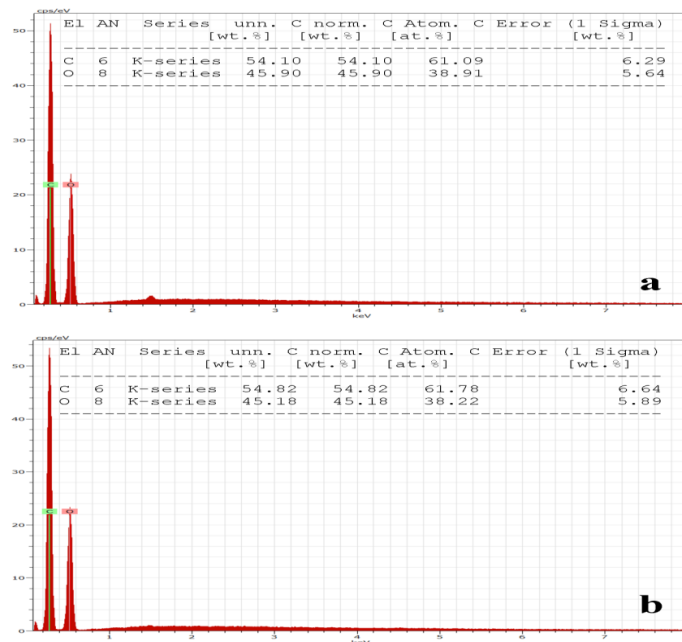


**Figure 2-3** Results of EDS analysis for two sides of membrane: (a) active layer, (b) support layer.

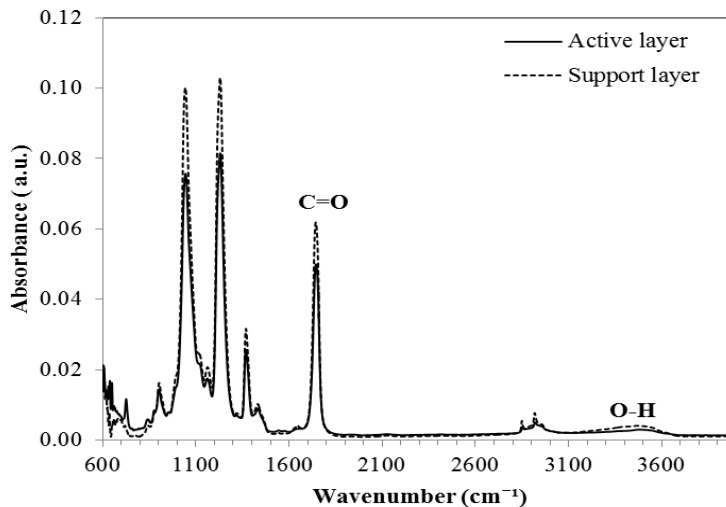


**Figure 2-4** ATR-FTIR spectra of membrane active and support layers.

The schematic of FO system setup is shown in Fig. 2-4. The membrane was placed in a SEPA FO cell (active area dimension: 0.97 mm × 14.7 cm × 9.53 cm) provided by Sterlitech Corporation (WA, USA) without using feed spacer or permeate carrier. Two speed-variable peristaltic pumps (Cole-Palmer, Vernon Hills, IL, USA) were applied to control the crossflow velocities on each side of the membrane. A digital balance (Scout Pro, Ohaus Corp., Parsippany, NJ, USA) connected to a computer was used to monitor the weight change of the draw solution. Membrane orientations including active layer facing the feed solution (FO mode) and active layer facing draw solution (PRO mode) were tested as an important factor affecting the membrane performance. All the experiments were carried out under 21±1°C.

In our previous test, two different cross-flow velocities (7 and 14 cm/s) and two cell configurations (horizontal and vertical) were studied as two factors which may influence membrane fouling. The obtained water flux indicated that the cell configuration showed little effect on membrane fouling compared to the cross-flow velocity. Therefore, the higher cross-

flow velocity (14 cm/s) was applied in the following desalination experiment to eliminate the impact of membrane fouling.

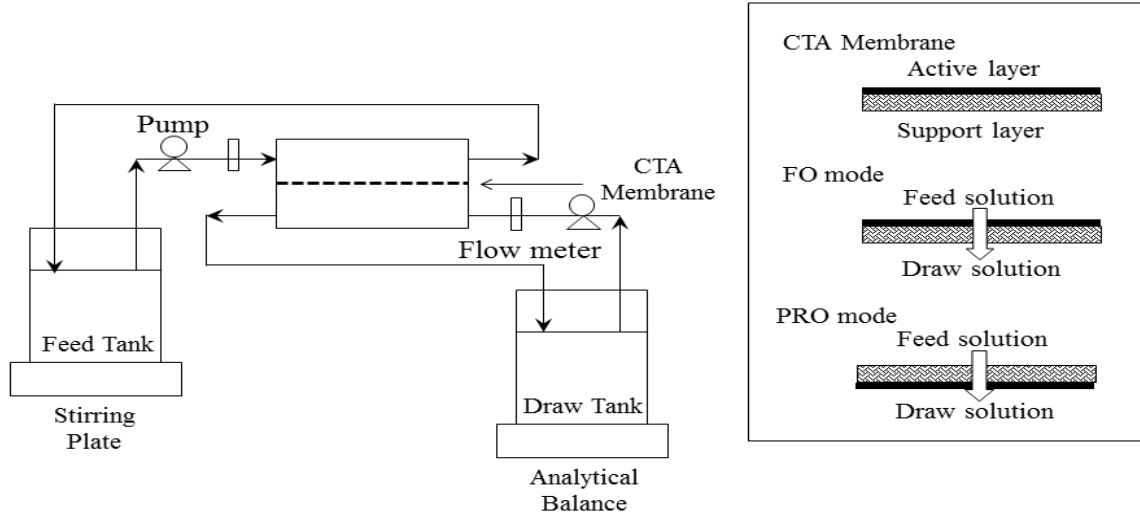


**Figure 2-5** Schematic of the FO system

## 2.2.3 Experimental procedures

### 2.2.3.1 The evaluation of using BDW as the draw solution

BDW was examined as the potential draw solution in terms of water flux in two membrane orientations (FO and PRO mode) at crossflow velocity of 14 cm/s. The experiments were conducted using BDW as draw solution and clean deionized (DI) water as feed solution. The obtained water flux was also used to eliminate the impact of draw solution dilution (baseline experiment). Furtherly, to evaluate the fouling propensity of BDW, NaCl solution was introduced as a comparable draw solution. The water flux was calculated based on the mass change of the draw solution:

$$J_w = \frac{V_P}{A_m \times t} \quad (1)$$

Where  $J_w$  is the water flux,  $V_p$  is the permeate volume,  $A_m$  is the effective area of membrane (140 cm<sup>2</sup>), and  $t$  is the operating time.

### 2.2.3.2 The evaluation of OSPW desalination

An 8-hour OSPW desalination experiment using natural settled OSPW as the feed and BDW as the draw was conducted in both FO and PRO modes at fixed crossflow velocity of 14 cm/s. After that, an OSPW desalination test lasting 7 days was conducted in both modes. The experiments started with 1 L of OSPW and 1 L of BDW. After 24 hours of operation, the pumps were interrupted and the diluted BDW and concentrated OSPW were switched to 1L of fresh BDW and natural settled OSPW. The water samples for salt diffusion and organic rejection analysis were taken after the first 24 hours of operation. The rejection (R) of organic species was calculated by mass balance in draw solution (4).

$$C_p \times V_p + C_{d,0} \times V_{d,0} = C_{d,t} \times V_{d,t} \quad (2)$$

$$R (\%) = \left(1 - \frac{C_p}{C_{f,0}}\right) \times 100\% \quad (3)$$

$$R (\%) = \left(1 - \frac{C_{d,t} \times V_{d,t} - C_{d,0} \times V_{d,0}}{C_{f,0} \times V_p}\right) \times 100\% \quad (4)$$

Where  $C_{d,t}$  and  $C_{d,0}$  are the concentrations of organic species in draw solution at time =  $t$  and 0, respectively.  $V_{d,t}$  and  $V_{d,0}$  are the volumes of draw solution at time =  $t$  and 0, respectively.  $C_{f,0}$  is the concentration of organic species in feed solution at time = 0.  $V_p$  is the permeate volume and  $C_p$  is the permeate concentration of organic species.

The diffusion of draw solute was evaluated by the specific reverse solute flux which can be determined by equation (3).

$$J_{\text{specific solute}} = J_{\text{solute}}/J_w = \frac{C_{f,t}V_{f,t} - C_{f,0}V_{f,0}}{A_m t} / J_w \quad (5)$$

Where  $C_{\text{feed},f}$  and  $C_{\text{feed},0}$  are the concentration of the solute in feed solution at time = t and 0, respectively;  $V_{\text{feed},t}$  and  $V_{\text{feed},0}$  are the volume of feed solution at time = t and 0, respectively. t is the operating time and  $J_w$  is water flux and can be determined by eq.1.

Because of the asymmetric structure of FO membrane, membrane support layer proceeded in PRO mode suffered a higher inner pore fouling propensity. Therefore, the cleaning process was performed only in PRO mode after long-term OSPW desalination immediately. During the 15-min physical cleaning (P. Zhao, Gao, Yue, & Shon, 2015), both draw and feed sides were circulated with clean DI water under a crossflow rate of 14 cm/s. After the cleaning, the same experimental condition was applied for one extra hour to test the cleaning efficiency. The water flux recovery (R) is determined by equation (4).

$$R = \left( \frac{J_{w,\text{cleaned}} - J_{w,\text{fouled}}}{J_{w,\text{pristine}} - J_{w,\text{fouled}}} \right) \times 100\% \quad (6)$$

Where  $J_{w,\text{cleaned}}$  is the water flux obtained after cleaning process,  $J_{w,\text{fouled}}$  is the water flux after membrane was fouled, and  $J_{w,\text{pristine}}$  is the water flux obtained using pristine membrane.

### 2.2.3.3 Analytical methods

The conductivity and pH value were measured with a pH /conductivity meter (Fisher Scientific, Ottawa, ON, Canada). The turbidity was determined by an OcbecoHellige 956 Digital Nephelometric Turbidimeter (Orberco Analytical System Inc., Sarasota, FL, USA). The total organic carbon (TOC) concentration was quantified by an Apollo 9000 TOC combustion analyzer (FOLIO Instrument Inc., Kitchener, ON, Canada) and chemical oxygen demand (COD) were measured using a COD reagent kit (Hatch Co., Loveland, CO). The naphthenic acids (NAs)

concentrations were evaluated by an ultra-performance liquid chromatograph (Waters Corp., Milford, MA, USA) according to the method described elsewhere (Alpatova et al., 2014; Moustafa et al., 2014). Total suspended solids (TSS) and total dissolved solids (TDS) of OSPW and BDW were determined following the standard methods (Standard method 2540-Solids) (Clesceri, Greenberg, Eaton, & American Public Health Association., 1998). The concentrations of ion species were quantified by inductively coupled plasma mass spectrometry (ICP-MS, Elan 6000 ICP mass spectrometer, PerkinElmer, Waltham, MA, USA) and ion chromatography (ICS-2000, Dionex, Sunnyvale, CA, USA). The aromatic organic fraction was characterized using Agilent Cary Eclipse Fluorescence Spectrophotometer (Markham, ON, Canada). Attenuated total reflectance Fourier transform infrared spectroscopy (ATR-FTIR) (Nicolet 8700, Thermo Electron Corp., West Palm Beach, FL, USA) was used to analyze the functional groups on both active and support layers. The membrane morphology was analyzed using Zeiss Sigma 300 VP-FESEM (Carl Zeiss Microscopy GmbH, Jena, Germany) and the element analysis was conducted by a Bruker energy dispersive X-ray spectroscopy (EDS) system (Bruker Corp., Billerica, MA, USA).

## **2.3 Results and discussion**

### **2.3.1 Evaluation of BDW as the draw solution**

BDW contained more inorganic solutes (i.e., sodium and chloride), resulting a much higher conductivity value and total dissolved solids (TDS) concentration than OSPW (Table 2-1). Theoretically, it could be used as the draw solution to desalinate OSPW in FO. To examine the capability of using BDW as the draw, we used clean deionized water (DI) as the feed solution at the crossflow velocity of 14 cm/s in both FO and PRO modes. Directly facing the support layer (FO mode), the colloidal particles and organic components from BDW might cause inner pore



blocking. Hence, 0.23 M NaCl solution was introduced as synthetic BDW to evaluate its fouling propensity. The molarity of NaCl solution was determined by the major ion distribution (i.e., Na, Cl) of BDW to mimic its osmotic driving force. In the support layer fouling test, the 0.23 M NaCl was facing with support layer while DI water was used as the feed facing the active layer (FO mode).

**Table 2-1** Characteristics of raw OSPW, natural settled OSPW and BDW.

| Parameters                         | Raw OSPW    | Natural settled OSPW | BDW          |
|------------------------------------|-------------|----------------------|--------------|
| pH                                 | 8.7±0.1     | 8.9±0.0              | 9.2±0.1      |
| Conductivity, mS/cm                | 3.9±0.3     | 3.7±0.2              | 20.1±2.2     |
| Chemical oxygen demand (COD), mg/L | 361.3±3.1   | 263.8±15.0           | 167.3±15.4   |
| Total organic carbon (TOC), mg/L   | 69.4±8.5    | 58.6±0.1             | 12.9±0.5     |
| Naphthenic acids (NAs), mg/L       |             | 35.5                 | 3.0          |
| Total dissolved solids (TDS), mg/L | 2511.4±15.3 | 2375.2±42.5          | 14739.2±86.2 |
| Total suspended solids (TSS), mg/L | 589.0±45.1  | 145.3±10.8           | 107.4±11.7   |

OSPW: oil sands process-affected water; BDW: basal depressurization water

It can be seen in Fig. 2-5 (a) that the water flux in PRO mode was higher than FO water flux because of the less severe impact of internal concentration polarization (ICP) (Tang, She, Lay, Wang, & Fane, 2010; P. Zhao et al., 2015). The presented water flux demonstrated that no distinct difference was observed between using 0.23 M NaCl and BDW as draw solutions in FO mode, indicating the support layer was not fouled or the occurred fouling did not significantly affect the water flux under current operating condition. As shown in Table 2-1, BDW exhibited a turbidity of 1.0±0.1 NTU and a TSS concentration of 107.4±11.7 mg/L. The presence of small particles in BDW could increase the risk of inner pore blocking on the support layer. However, it was not necessarily fouled because the permeate water might flush away those foulants hidden in the pores (Boo, Elimelech, & Hong, 2013). Although the support layer against BDW was not

fouled using DI water as the feed, it was still unclear if membrane fouling could be completely excluded in OSPW desalination. The reduced driven force and membrane fouling could lead to a lower flux. The obtained water flux files using BDW as the draw and DI water as the feed solution were set as the baseline to correct the water flux when OSPW was applied as the feed solution in FO and PRO mode (Fig. 2-5 (b)), respectively.

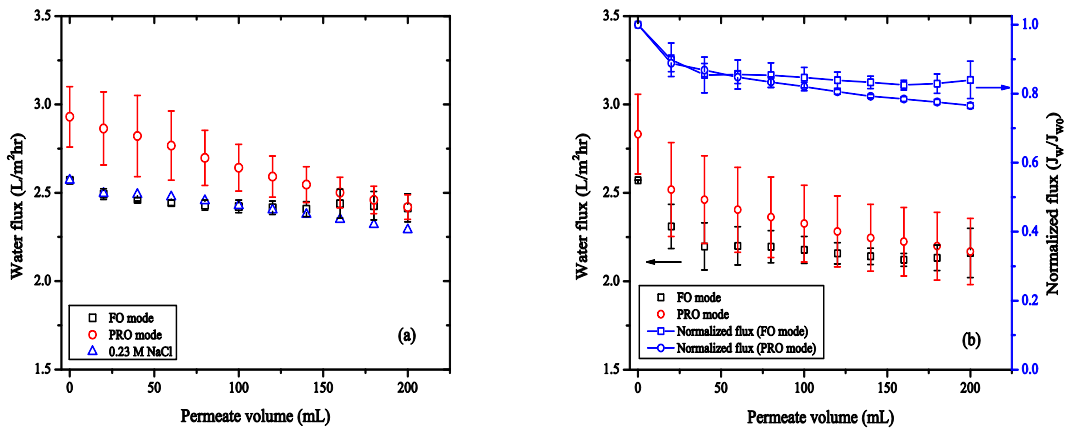


**Figure 2-6** Results of short-term OSPW desalination test at a crossflow velocity of 14 cm/s. (a) The experiments were conducted using clean DI as feed solution and BDW as draw solution in FO and PRO mode. 0.23 M NaCl as draw solution and clean DI water as feed solution in FO mode. (b) Natural settled OSPW as the feed and BDW as the draw solution. The shown data were corrected by the baseline experiments using BDW as draw solution and clean DI as feed solution in FO and PRO mode, respectively. Error bars represent standard deviation from triplicate experiments.

## **2.3.2 Evaluation of OSPW desalination**

### **2.3.2.1 Short-term OSPW desalination**

The short-term FO experiment using OSPW as the feed and BDW as the draw was carried out at crossflow velocity of 14 cm/s. The water flux and normalized flux were shown as a function of permeate volume in Fig. 2-5 (b) with baseline correction.

In good agreement with previous publications suggesting that FO mode is more fouling resistant (B. Mi & Elimelech, 2008; P. Zhao, Gao, Yue, Liu, & Shon, 2016), we found that the water flux declined faster in PRO mode in spite of a higher initial water flux. To obtain 200 mL of permeate water; the water flux declined approximately 15% in FO mode and 25% in PRO mode, respectively. Interestingly, in FO mode, the water flux started to level-off after reduced by 12% while the flux in PRO mode kept decreasing. The continuous flux drop might be caused by the membrane surface fouling or inner pore blocking on the support layer facing OSPW (PRO mode). Membrane pore blocking could decrease water permeability (A) and increase the salt resistivity (K), thereby intensifying concentration polarization and reducing the water flux furtherly (Yeo et al., 2014).

### **2.3.2.2 Long-term OSPW desalination performance**

The long-term batch experiments lasted for 7 days followed by a 15 minutes DI water cleaning in only PRO mode. To maintain the osmotic pressure difference, the concentrated feed (OSPW) and the diluted draw (BDW) solutions were switched to fresh supplies every 24 hours. After 7 days operating, the accumulated permeate water volume were 2622.3 mL and 2800.6 mL in FO and PRO mode, respectively. The raw water flux versus time (Fig. 2-6 (a)) was summarized into the following three stages: stage 1: DI water flux (baseline experiment): DI water as the feed and BDW as the draw; stage 2: OSPW water flux: OSPW as the feed and BDW as the draw (7 days);

stage 3: the recovered OSPW flux after clean water backwashing: OSPW as the feed and BDW as the draw.

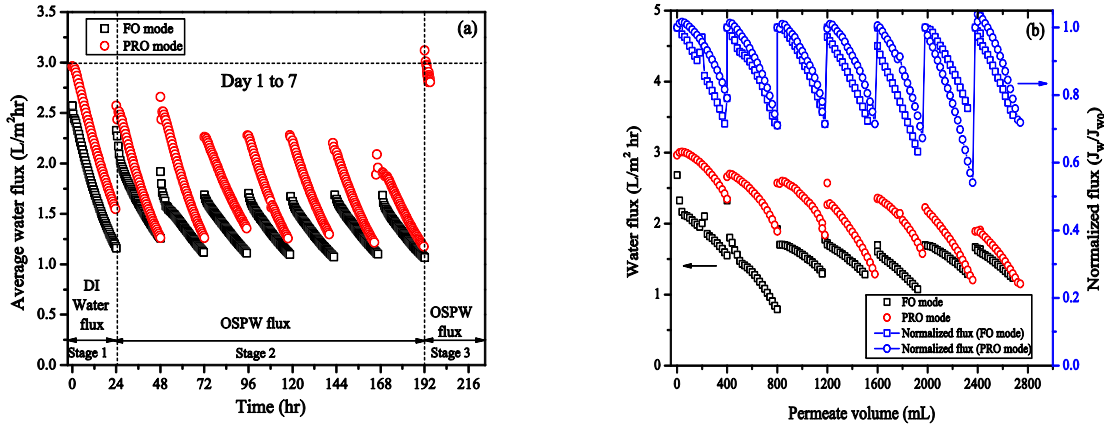


**Figure 2-7** Results of long-term OSPW desalination test. The experiment was conducted using BDW as draw solution and natural settled OSPW as the feed solution. (a): Water flux presented as a function of time. (b): Water flux/normalized flux presented as a function of permeate volume. The data shown in (b) were corrected by baseline experiments (using BDW as draw solution and clean DI as feed solution in FO and PRO mode, respectively).

As shown in Fig. 2-6 (a) stage 2, the highest initial water flux was found on 1<sup>st</sup> day (2.57 L/m<sup>2</sup> hr in FO mode and 2.95 L/m<sup>2</sup> hr in PRO mode). On 2<sup>nd</sup> day, the initial fluxes sharply declined to 2.25 L/m<sup>2</sup> hr (by 12.4%) and 2.57 (by 12.9%) observed in FO and PRO modes, respectively. The sharp flux drop suggested that the immediate membrane pore blocking or scaling happened in the first 24 hours. After that, foulants kept accumulating, thereby gradually decreasing the initial water fluxes on the following days. Compared to 1<sup>st</sup> day, the initial water fluxes of day 7 were reduced 36% in FO and 28% in PRO mode, respectively. After 15-minute cleaning process, the

initial water flux in PRO mode recovered to the original flux level (Fig. 2-6 (a) stage 3). Calculated from eq. (3), the water flux recovery (R) was 100%.

To better elucidate the data, we plotted stage 2 (7-days OSPW desalination) separately in Fig. 2-6 (b) as baseline corrected water flux and normalized flux in 7 batches with corresponding permeate volume of 400 mL per batch to eliminate the concentration and dilution effects. The permeate fluxes varied from 3~0.8 L/m<sup>2</sup> hr in both modes. The average normalized flux at the end of each batch was 73.2±4.7% in FO mode and 67.1±7.9% in PRO mode, respectively. In contradiction with previous finding indicating that FO fouling was negligible under lower permeate flux using 10 mM NaCl with latex particle as the feed and various concentrations of sodium chloride as the draw (Wang, Wicaksana, Tang, & Fane, 2010), we observed that the approximately 30% of flux decline in both modes might be contributed to membrane fouling or the coupled effect of external concentration polarization (ECP) and membrane fouling. Furtherly, in comparison with the short-term performance, the water flux decline observed in the long-term experiment failed to distinguish the anti-fouling performance of two membrane orientations. This could be attributed to the complex water matrix of OSPW which might trigger a different fouling behavior in terms of salt and particle deposition, penetration and diffusion.

Fig. 2-7 showed the membrane morphology of the active and support layers after long-term desalination. In FO mode (Fig. 2-7 (a) and (b)), scattered or clustered white foulants were observed on the side facing with OSPW while no intensive surface foulants were found on the support layer against BDW. Similar with FO mode, some accumulated precipitates were only observed surrounded by the pores on the support layer against OSPW in PRO mode. The foulants might flow with the permeate water and loosely accumulated near the membrane pores as shown in Fig. 2-7 (d). Those results indicated that the membrane fouling was mainly caused

by the feed—OSPW. SEM images along with the recovered water flux after cleaning (Fig 2-6. (a) Stage 3) in PRO mode might reveal that surface fouling, rather than inner pore blocking, was the main reason causing continuously flux decrease. Because the foulants trapped inside of the support layer could not be exacerbated under physical cleaning method. On the other perspective, the recovered water flux also suggested that the adhesive force of the OSPW foulants on CTA membrane might be weakened, which would simplify membrane cleaning process and furtherly, reduce the membrane consumption and operational cost. The adhesive force of the foulant on FO membranes would be investigated in our future work.

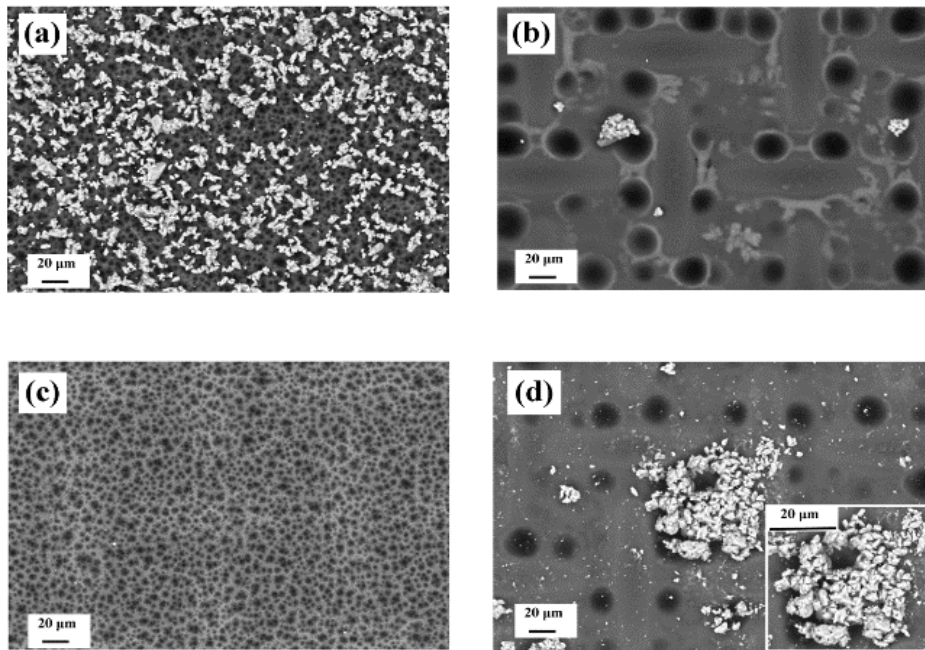


**Figure 2-8** SEM images of membrane surfaces after long-term desalination experiment in FO mode: (a) active layer facing with OSPW (b) support layer facing BDW, and PRO mode: (c) active layer facing BDW (d) support layer facing OSPW

In addition, EDS analysis was performed to find out the chemical distribution of the foulants (Fig. 2-8). Interestingly, the OSPW foulants shared an identical chemical element profile: strong peaks

of carbon, oxygen and calcium (chemical weight > 20%), weak peaks (chemical weight  $\leq$  1%) of other elements including magnesium, sodium, etc. The EDS results might evidence the formation of calcium carbonate. Anhydrous  $\text{CaCO}_3$  has three common polymorphs including aragonite, calcite and vaterite (Yashina, Meldrum, & deMello, 2012) . The observed foulant showed a rhombic shape which was similar to the typical pattern of calcite crystal. During the operating process, we also observed that some floating white flakes formed in feed solution, which might also be attributed to the formation of calcium carbonate. OSPW contained a calcium concentration of  $7.54 \pm 1.99$  mg/L, external concentration polarization (ECP) was a possible factor that promoted its precipitation. Meanwhile, the existence of organic matters in OSPW might affect the  $\text{CaCO}_3$  precipitation as well (M. M. Zhang, Hou, She, & Tang, 2014).

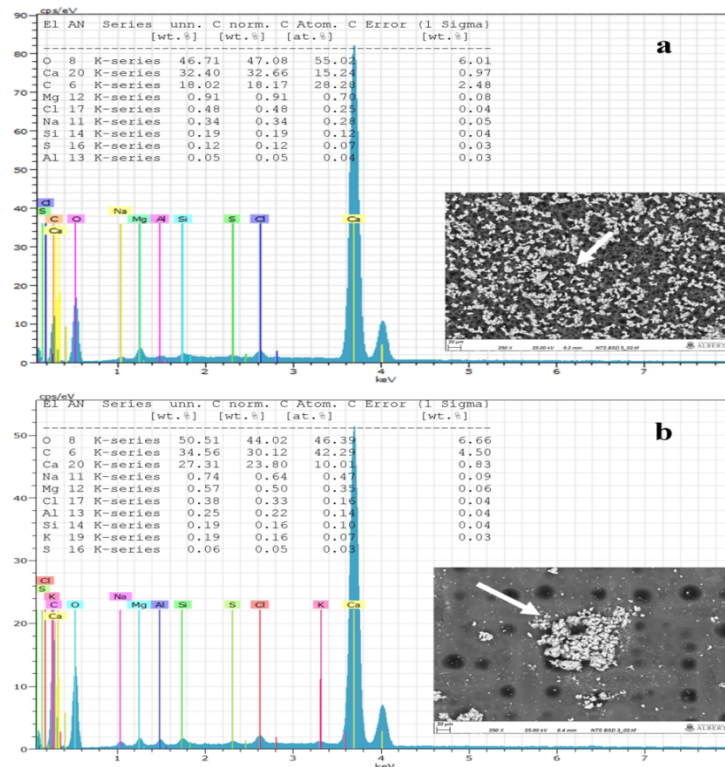


**Figure 2-9** EDS analysis of foulants found on the sides orienting OSPW. (a) active layer (FO mode); (b) support layer (PRO mode). In Figure 2-8 a, strong peaks of carbon, oxygen and

calcium (O 50.64%, Ca 25.61%, and C 21.96%) were detected on the tested foulants. In Figure 2-8 b, same elements were observed on the precipitations of the support layer. Same elements (O 48.14%, Ca 24.86%, and C 24.16%) still attributed to the major compositions, while other inorganic elements ranked as Cl 1.16% > Na 0.84% > Mg 0.53% > S 0.18% > K 0.12% > Si 0.02%.

### **2.3.3 Draw solute diffusion**

Due to the imperfection of FO membrane, bi-directional permeation of small draw/feed solutes can reduce the driving force and further affect the permeate flux. Therefore, the specific reverse TDS flux in both modes using DI water as the feed and BDW as the draw solution was primarily evaluated. The obtained values were 246.9 mg/L in FO mode and 297.6 mg/L in PRO mode, which were below the specific reverse solute flux (>600 mg/L) estimated by DI water and 10 to 15 g/L sea salt (0.17 to 0.27 M NaCl) (Cath, Hancock, Lundin, Hoppe-Jones, & Drewes, 2010). Because sodium and chloride were the most abundant ions in BDW, the diffusion of sodium and chloride were accounted for 70.0 and 76.5% of total TDS mass flux in FO and PRO, respectively, and those two ions were diffused at similar molar equivalent rate (FO mode: 3.0 and PRO mode: 4.0 meq/L). Compared to the previous findings, the diffusion of sodium and chloride were retarded, which was likely due to the diversified ion profiles in BDW, especially those multi-valence ions (i.e., magnesium). As suggested by Holloway et al. (Holloway, Maltos, Vanneste, & Cath, 2015), the presence of magnesium in NaCl majority draw solution can effectively reduce reverse salt flux caused by sodium and chloride.

In OSPW desalination, considering 480 mL and 423 mL water permeated to the draw solution in FO and PRO modes, the corresponding specific reverse TDS flux were 604 mg/L in FO mode and 632 mg/L in PRO mode, respectively. The results were similar to previous studies (400 to



500 mg/L) applying NaCl draw solutions (0 to 70 g/L) (Cath et al., 2010). Specific reverse solute fluxes were also measured for magnesium (7.84 mg/L in PRO mode, 5.94 mg/L in FO mode), calcium (0 mg/L in both modes, possibly due to its precipitation), and potassium (5.39 mg/L in PRO mode and 2.43 mg/L in FO mode). After 24-hr filtration, BDW were diluted approximately 1.5 times. The total dissolved solid were reduced from  $14739.2 \pm 86.2$  mg/L to  $7605 \pm 85.1$  mg/L in FO mode and  $7418.3 \pm 60.12$  mg/L in PRO mode, respectively. Some heavy metals exceeding the Canadian Environmental Quality Guidelines (CEQG) for fresh water were successfully diluted to the concentration under safety range. Ion composition of OSPW and BDW before and after desalination can be found in Appendices (Table 8-1). For instance, the concentration of chromium was  $9.9 \pm 0.2$   $\mu\text{g/L}$  in original BDW, after the process, it was reduced to  $4.7 \pm 0.2$   $\mu\text{g/L}$ , below the standard concentration of  $8.9$   $\mu\text{g/L}$ . However, some regulated metal ions like selenium and, copper were still above the regulated concentrations. It was expected that by optimizing the process, more regulated metal ions can be diluted to fulfill the requirement of recycle and reuse.

#### **2.3.4 Organic rejection**

The concentrations of TOC, COD and NAs before and after the treatment are shown in Fig. 2-9. As BDW diluted, COD concentrations in BDW were reduced from  $167.3 \pm 15.4$  to  $108 \pm 10.2$  and  $97.5 \pm 5.7$  mg/L and TOC concentration was reduced from  $12.9 \pm 0.5$  to  $6.13 \pm 1.9$  and  $5.8 \pm 0.1$  mg/L in FO and PRO mode, respectively.

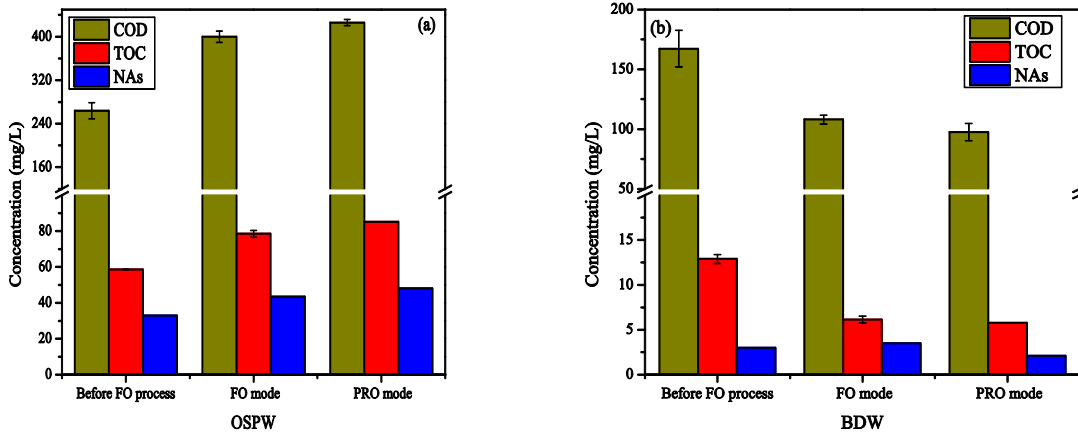


**Figure 2-10** The concentrations of COD, TOC and NA species before and after desalination (a) OSPW, (b) BDW. Error bar represents standard deviation from triplicate experiments.

NA concentrations, as one important contributor of TOC, were reduced from 3.0 to 2.1 mg/L in FO mode and it was kept at the similar level (3.2 mg/L) in PRO mode. The specified NA concentrations corresponding with the carbon and the deficiency of hydrogen atoms (Z) in BDW were presented (Fig. 2-10). The estimated rejection efficiencies of NAs in FO and PRO modes were 98.3% and 90.0%, respectively, which was higher than the NA rejection ratios reported in other processes (Alpatova et al., 2014). Consistent with other research (Hickenbottom et al., 2013), the imperfect rejection of NAs should be associated with the organic diffusion of smaller size compounds. The synchronous fluorescence spectroscopy (SFS) analysis conducted before and after desalination (Fig. 2-11) verified our assumption. The spectra showed that the intensity of lower ring compounds (1-3) slightly increased in the diluted BDW, while no signal was detected on those higher ring compounds (Alpatova et al., 2014). The rejection of NAs could be explained by the following: (1) Size exclusion: NA species with high carbon and Z number (usually means more rings and hydrophobic) intended to exhibit comparative larger size; (2) Retarded forward diffusion (Xie, Nghiem, Price, & Elimelech, 2012): the major draw solutes

(sodium and chloride) were small hydrated radii which could easily diffuse through the membrane pore and slower the diffusion of trace hydrophobic NA organic species.

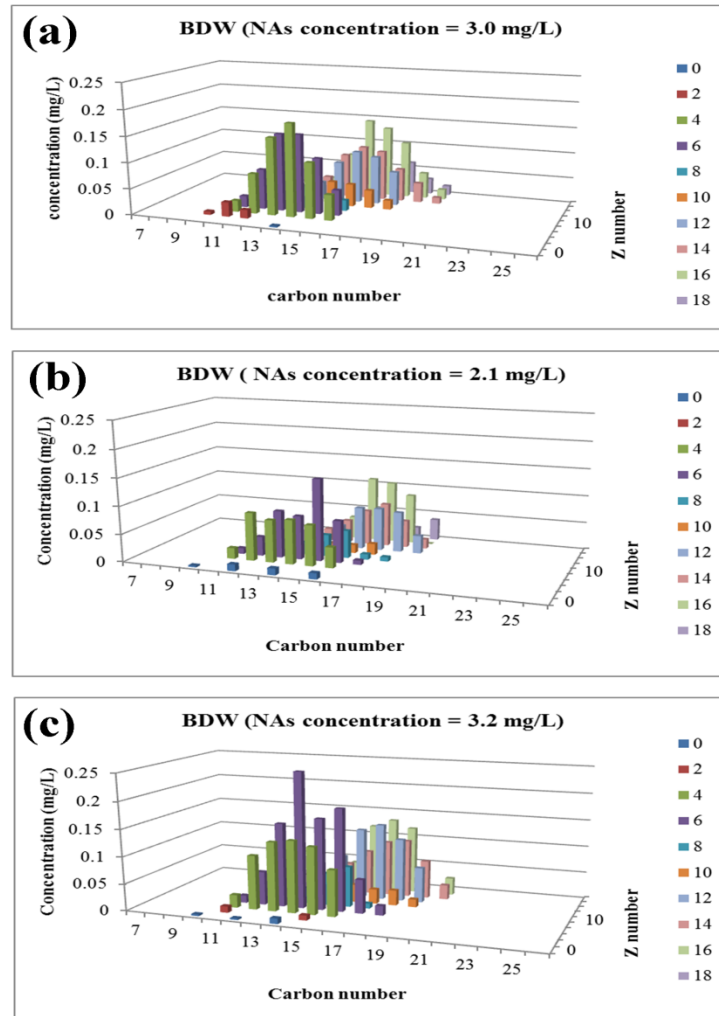


**Figure 2-11** The concentration of NA species in BDW with the corresponding carbon and Z numbers before and after desalination. Before desalination (a), after FO mode desalination (b), after PRO mode desalination (c).

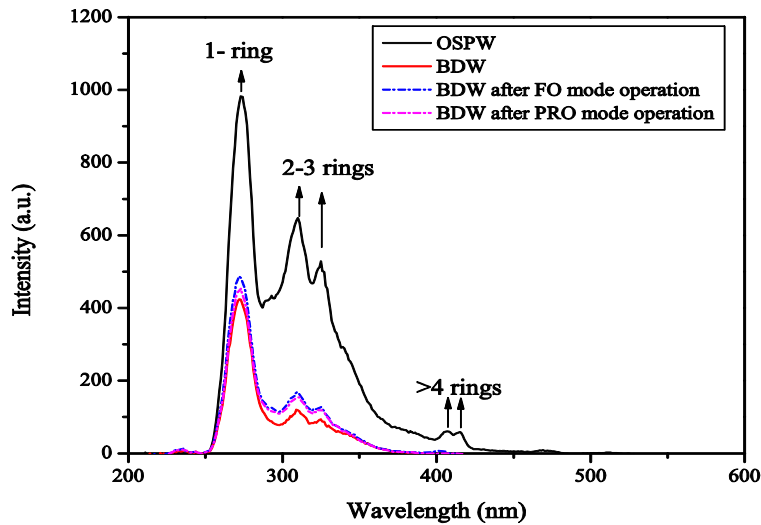


**Figure 2-12** The SFS of OSPW and BDW taken before and after desalination

#### 2.4 Sustainability of using FO to treat BDW and OSPW

In current oil sands industry, given the large amounts of process waters generated and retained on-site, there is an urgent need to seek for an appropriate water management method. In our study, FO was proposed to treat two types of process waters — OSPW and BDW in one membrane process in which OSPW concentration and BDW dilution could be achieved simultaneously. Using BDW as the draw solution to in FO process is comparative environmental-friendly and cost-effective because the draw solution does not require any extra expense and the diluted BDW could be directly recycled and reused in the industry after operation optimization.

The experimental results showed that the volume of 1L OSPW reduced more than 40% in an experimental period of 24-hour using 1L of BDW as draw solution. Applying the same experimental condition, the maximum reduced volume of OSPW was 53.4% and the corresponding water flux decline from 2.96 to 1.27 L/m<sup>2</sup> hr (57.1%) (Fig. 2-11) after 30 hours continuous running. By optimizing the operating condition, it was expected that OSPW/BDW

can be furtherly concentrated or diluted. In terms of the reduced volume of OSPW and rejection of organic and inorganic species, the current proposed process is promising. However, to apply it in practice, two main challenges need to be addressed: 1. Low driving force: BDW is less concentrated compared to other highly brackish water, thereby generating lower water flux. To increase water flux, larger membrane area (i.e., using hollow fiber FO membrane) is recommended. 2. Membrane fouling: Water flux decline due to membrane fouling was 30% without any pre-treatment. The impact of fouling can be diminished by carrying out pre-treatments (i.e., microfiltration, coagulation and flocculation) and optimizing operational condition (i.e., high crossflow velocity, using membrane spacer).

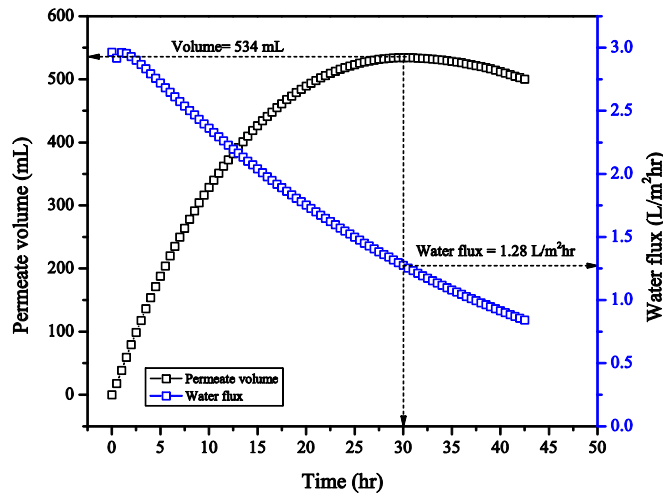


**Figure 2-13** Maximum capability of using BDW as the draw to desalinate OSPW. The experiment was conducted at the crossflow velocity of 14 cm/s in PRO mode. 1L of natural settled OSPW was used as the feed solution and 1L of BDW was used as the draw solution.

## 2.5 Conclusions

Considering the large quantities of stored oil sands tailing water, a water management approach is needed to alleviate its detrimental impact on environment. Therefore, FO was proposed as a

treatment method in the current investigation to reduce the volume of OSPW, meanwhile to dilute other brackish on-site wastewater — BDW, subsequently it could be recycle/reuse back to the industry. The overall objective of the study is to examine the feasibility of treating OSPW with BDW in FO process. Both short-term and long-term desalination experiments were performed. The results indicated that the accumulated permeate water volume were 2622.3 mL and 2800.6 mL in FO and PRO mode after long-term operating; suggesting 40% of OSPW volume can be reduced. Given the high rejection and reduced OSPW volume, the current process introduced an energy effective water management concept that not only aims to OSPW treatment but also the management of other process waters. However, the sustainability of process is limited likely due to the low water flux and membrane fouling. To unravel those obstacles, future works is required to optimize the operating condition and eliminate the impact of membrane fouling. In our future work, other types of concentrated wastewater, such as the wastewaters from electrodialysis (ED) process and the concentrated feeds solution from reverse osmosis (RO) process, would be screened, assessed and identified in OSPW desalination to increase the desalination efficiency and lower the operational cost further.

## **2.6 Reference**

- Allen, E. W. (2008a). Process water treatment in Canada's oil sands industry: I. Target pollutants and treatment objectives. *Journal of Environmental Engineering and Science*, 7(2), 123-138.
- Allen, E. W. (2008b). Process water treatment in Canada's oil sands industry: II. A review of emerging technologies. *Journal of Environmental Engineering and Science*, 7(5), 499-524. doi: Doi 10.1139/S08-020

- Alpatova, A., Kim, E. S., Dong, S. M., Sun, N., Chelme-Ayala, P., & El-Din, M. G. (2014). Treatment of oil sands process-affected water with ceramic ultrafiltration membrane: Effects of operating conditions on membrane performance. *Separation and Purification Technology*, 122, 170-182. doi: DOI 10.1016/j.seppur.2013.11.005
- Anderson, J. C., Wiseman, S. B., Wang, N., Moustafa, A., Perez-Estrada, L., El-Din, M. C., . . . Giesy, J. P. (2012). Effectiveness of Ozonation Treatment in Eliminating Toxicity of Oil Sands Process-Affected Water to *Chironomus dilutus*. *Environmental Science & Technology*, 46(1), 486-493. doi: Doi 10.1021/Es202415g
- Arkhangelsky, E., Lay, S. S., Wicaksana, F., Al-Rabiah, A. A., Al-Zahrani, S. M., & Wang, R. (2014). Impact of intrinsic properties of foulants on membrane performance in osmotic desalination applications. *Separation and Purification Technology*, 123, 87-95. doi: DOI 10.1016/j.seppur.2013.12.013
- Boo, C., Elimelech, M., & Hong, S. (2013). Fouling control in a forward osmosis process integrating seawater desalination and wastewater reclamation. *Journal of Membrane Science*, 444, 148-156. doi: 10.1016/j.memsci.2013.05.004
- Boo, C., Lee, S., Elimelech, M., Meng, Z. Y., & Hong, S. (2012). Colloidal fouling in forward osmosis: Role of reverse salt diffusion. *Journal of Membrane Science*, 390, 277-284. doi: 10.1016/j.memsci.2011.12.001
- Cath, T. Y., Childress, A. E., & Elimelech, M. (2006). Forward osmosis: Principles, applications, and recent developments. *Journal of Membrane Science*, 281(1-2), 70-87. doi: 10.1016/j.memsci.2006.05.048

- Cath, T. Y., Hancock, N. T., Lundin, C. D., Hoppe-Jones, C., & Drewes, J. E. (2010). A multi-barrier osmotic dilution process for simultaneous desalination and purification of impaired water. *Journal of Membrane Science*, 362(1-2), 417-426. doi: DOI 10.1016/j.memsci.2010.06.056
- Clesceri, L. S., Greenberg, A. E., Eaton, A. D., & American Public Health Association. (1998). *Standard methods for the examination of water and wastewater* /edited by Lenore S. Clesceri, Arnold E. Greenberg, Andrew D. Eaton (20th ed.). Washington, DC: American Public Health Association.
- Dong, S. M., Kim, E. S., Alpatova, A., Noguchi, H., Liu, Y., & El-Din, M. G. (2014). Treatment of oil sands process-affected water by submerged ceramic membrane microfiltration system. *Separation and Purification Technology*, 138, 198-209. doi: 10.1016/j.seppur.2014.10.017
- Frank, R. A., Kavanagh, R., Burnison, B. K., Arsenault, G., Headley, J. V., Peru, K. M., . . . Solomon, K. R. (2008). Toxicity assessment of collected fractions from an extracted naphthenic acid mixture. *Chemosphere*, 72(9), 1309-1314.
- Garcia-Garcia, E., Pun, J., Hodgkinson, J., Perez-Estrada, L. A., El-Din, M. G., Smith, D. W., . . . Belosevic, M. (2012). Commercial naphthenic acids and the organic fraction of oil sands process water induce different effects on pro-inflammatory gene expression and macrophage phagocytosis in mice. *Journal of Applied Toxicology*, 32(12), 968-979. doi: 10.1002/jat.1687



- Ge, Q. C., Ling, M. M., & Chung, T. S. (2013). Draw solutions for forward osmosis processes: Developments, challenges, and prospects for the future. *Journal of Membrane Science*, 442, 225-237. doi: 10.1016/j.memsci.2013.03.046
- Hickenbottom, K. L., Hancock, N. T., Hutchings, N. R., Appleton, E. W., Beaudry, E. G., Xu, P., & Cath, T. Y. (2013). Forward osmosis treatment of drilling mud and fracturing wastewater from oil and gas operations. *Desalination*, 312, 60-66. doi: 10.1016/j.desal.2012.05.037
- Holloway, R. W., Maltos, R., Vanneste, J., & Cath, T. Y. (2015). Mixed draw solutions for improved forward osmosis performance. *Journal of Membrane Science*, 491, 121-131. doi: 10.1016/j.memsci.2015.05.016
- Huang, C. K., Shi, Y. J., El-Din, M. G., & Liu, Y. (2015). Treatment of oil sands process-affected water (OSPW) using ozonation combined with integrated fixed-film activated sludge (IFAS). *Water Research*, 85, 167-176.
- Islam, M. S., Zhang, Y. Y., McPhedran, K. N., Liu, Y., & El-Din, M. G. (2015). Next-Generation Pyrosequencing Analysis of Microbial Biofilm Communities on Granular Activated Carbon in Treatment of Oil Sands Process-Affected Water. *Applied and Environmental Microbiology*, 81(12), 4037-4048.
- Kim, C., Lee, S., & Hong, S. (2012). Application of osmotic backwashing in forward osmosis: mechanisms and factors involved. *Desalination and Water Treatment*, 43(1-3), 314-322. doi: 10.1080/19443994.2012.672215

- Kim, E. S., Dong, S., Liu, Y., & Gamal El-Din, M. (2013). Desalination of oil sands process-affected water and basal depressurization water in Fort McMurray, Alberta, Canada: application of electrodialysis. [Research Support, Non-U.S. Gov't]. *Water Science and Technology*, 68(12), 2668-2675. doi: 10.2166/wst.2013.533
- Kim, E. S., Liu, Y., & El-Din, M. G. (2011). The effects of pretreatment on nanofiltration and reverse osmosis membrane filtration for desalination of oil sands process-affected water. *Separation and Purification Technology*, 81(3), 418-428. doi: DOI 10.1016/j.seppur.2011.08.016
- Kim, Y., Lee, S., Shon, H. K., & Hong, S. (2015). Organic fouling mechanisms in forward osmosis membrane process under elevated feed and draw solution temperatures. *Desalination*, 355, 169-177. doi: 10.1016/j.desal.2014.10.041
- Klamerth, N., Moreira, J., Li, C., Singh, A., McPhedran, K. N., Chelme-Ayala, P., . . . El-Din, M. G. (2015). Effect of ozonation on the naphthenic acids' speciation and toxicity of pH-dependent organic extracts of oil sands process-affected water. *Science of the Total Environment*, 506, 66-75. doi: 10.1016/j.scitotenv.2014.10.103
- Lee, J., Kim, B., & Hong, S. (2014). Fouling distribution in forward osmosis membrane process. *Journal of Environmental Sciences-China*, 26(6), 1348-1354. doi: Doi 10.1016/S1001-0742(13)60610-5
- Lee, S., Boo, C., Elimelech, M., & Hong, S. (2010). Comparison of fouling behavior in forward osmosis (FO) and reverse osmosis (RO). *Journal of Membrane Science*, 365(1-2), 34-39. doi: 10.1016/j.memsci.2010.08.036

- Liu, Y. L., & Mi, B. X. (2012). Combined fouling of forward osmosis membranes: Synergistic foulant interaction and direct observation of fouling layer formation. *Journal of Membrane Science*, 407, 136-144. doi: 10.1016/j.memsci.2012.03.028
- Lutchmiah, K., Verliefde, A. R. D., Roest, K., Rietveld, L. C., & Cornelissen, E. R. (2014). Forward osmosis for application in wastewater treatment: A review. *Water Research*, 58, 179-197. doi: 10.1016/j.watres.2014.03.045
- Mi, B., & Elimelech, M. (2008). Chemical and physical aspects of organic fouling of forward osmosis membranes. *Journal of Membrane Science*, 320(1-2), 292-302. doi: 10.1016/j.memsci.2008.04.036
- Mi, B. X., & Elimelech, M. (2010). Organic fouling of forward osmosis membranes: Fouling reversibility and cleaning without chemical reagents. *Journal of Membrane Science*, 348(1-2), 337-345. doi: 10.1016/j.memsci.2009.11.021
- Mohamed, M. H., Wilson, L. D., Peru, K. M., & Headley, J. V. (2013). Colloidal properties of single component naphthenic acids and complex naphthenic acid mixtures. *Journal of Colloid and Interface Science*, 395, 104-110. doi: 10.1016/j.jcis.2012.12.056
- Motsa, M. M., Mamba, B. B., D'Haese, A., Hoek, E. M. V., & Verliefde, A. R. D. (2014). Organic fouling in forward osmosis membranes: The role of feed solution chemistry and membrane structural properties. *Journal of Membrane Science*, 460, 99-109. doi: 10.1016/j.memsci.2014.02.035
- Moustafa, A. M. A., Kim, E. S., Alpatova, A., Sun, N., Smith, S., Kang, S., & El-Din, M. G. (2014). Impact of polymeric membrane filtration of oil sands process water on organic

- compounds quantification. *Water Science and Technology*, 70(5), 771-779. doi: 10.2166/wst.2014.282
- Qin, M. H., & He, Z. (2014). Self-Supplied Ammonium Bicarbonate Draw Solute for Achieving Wastewater Treatment and Recovery in a Microbial Electrolysis Cell-Forward Osmosis-Coupled System. *Environmental Science & Technology Letters*, 1(10), 437-441. doi: 10.1021/ez500280c
- Rastogi, N. K., & Nayak, C. A. (2011). Membranes for forward osmosis in industrial applications. *Advanced Membrane Science and Technology for Sustainable Energy and Environmental Applications*(25), 680-717. doi: Book\_DoI 10.1533/9780857093790
- Shaffer, D. L., Chavez, L. H. A., Ben-Sasson, M., Castrillon, S. R. V., Yip, N. Y., & Elimelech, M. (2013). Desalination and Reuse of High-Salinity Shale Gas Produced Water: Drivers, Technologies, and Future Directions. *Environmental Science & Technology*, 47(17), 9569-9583. doi: Doi 10.1021/Es401966e
- Tang, C. Y. Y., She, Q. H., Lay, W. C. L., Wang, R., & Fane, A. G. (2010). Coupled effects of internal concentration polarization and fouling on flux behavior of forward osmosis membranes during humic acid filtration. *Journal of Membrane Science*, 354(1-2), 123-133. doi: 10.1016/j.memsci.2010.02.059
- Wang, Y. N., Wicaksana, F., Tang, C. Y., & Fane, A. G. (2010). Direct Microscopic Observation of Forward Osmosis Membrane Fouling. *Environmental Science & Technology*, 44(18), 7102-7109. doi: 10.1021/es101966m

- Xie, M., Nghiem, L. D., Price, W. E., & Elimelech, M. (2012). Comparison of the removal of hydrophobic trace organic contaminants by forward osmosis and reverse osmosis. *Water Research*, 46(8), 2683-2692. doi: 10.1016/j.watres.2012.02.023
- Yashina, A., Meldrum, F., & deMello, A. (2012). Calcium carbonate polymorph control using droplet-based microfluidics. *Biomicrofluidics*, 6(2).
- Yeo, S. Y., Wang, Y., Chilcott, T., Antony, A., Coster, H., & Leslie, G. (2014). Characterising nanostructure functionality of a cellulose triacetate forward osmosis membrane using electrical impedance spectroscopy. *Journal of Membrane Science*, 467, 292-302. doi: 10.1016/j.memsci.2014.05.035
- Yip, N. Y., Tiraferri, A., Phillip, W. A., Schiffman, J. D., & Elimelech, M. (2010). High Performance Thin-Film Composite Forward Osmosis Membrane. *Environmental Science & Technology*, 44(10), 3812-3818. doi: 10.1021/es1002555
- Zhang, M. M., Hou, D. X., She, Q. H., & Tang, C. Y. Y. (2014). Gypsum scaling in pressure retarded osmosis: Experiments, mechanisms and implications. *Water Research*, 48, 387-395.
- Zhao, P., Gao, B. Y., Yue, Q. Y., Liu, S. C., & Shon, H. K. (2016). Effect of high salinity on the performance of forward osmosis: Water flux, membrane scaling and removal efficiency. *Desalination*, 378, 67-73.
- Zhao, P., Gao, B. Y., Yue, Q. Y., & Shon, H. K. (2015). The performance of forward osmosis process in treating the surfactant wastewater: The rejection of surfactant, water flux and

physical cleaning effectiveness. *Chemical Engineering Journal*, 281, 688-695. doi: 10.1016/j.cej.2015.07.003

Zhao, S. F., Zou, L., Tang, C. Y. Y., & Mulcahy, D. (2012). Recent developments in forward osmosis: Opportunities and challenges. *Journal of Membrane Science*, 396, 1-21. doi: 10.1016/j.memsci.2011.12.023

Zhou, X. S., Gingerich, D. B., & Mauter, M. S. (2015). Water Treatment Capacity of Forward-Osmosis Systems Utilizing Power-Plant Waste Heat. *Industrial & Engineering Chemistry Research*, 54(24), 6378-6389. doi: 10.1021/acs.iecr.5b00460

### 3 Chapter 3 Rejection of naphthenic acids by forward osmosis: Effect of pH value and draw solutes<sup>2</sup>

#### 3.1 Introduction

The Clark hot water extraction method is widely applied by the Canadian oil sands industry, in which large amounts of water are used to separate the bitumen from the oil sands. As a result, both organic and inorganic compounds are dissolved into the process water, creating oil sands process-affected water (OSPW). The organic contents of OSPW are made up of naphthenic acids (NAs), polycyclic aromatic hydrocarbons (PAHs), benzene, toluene, ethylbenzene, xylene (BTEX) and phenols (Allen, 2008a; Mikula et al., 1996). Nearly 50% of the extractable organic fraction in OSPW is NAs which are considered to be one of the primary sources of OSPW toxicity towards aquatic species (Kannel & Gan, 2012). NAs have an empirical structure formula of  $C_nH_{2n+Z}O_2$ , where n represents the number of carbon atoms and Z is the deficiency of hydrogen atoms (Frank et al., 2008). Typically, the NAs found in OSPW have n number varying from 7 to 30 and the Z number ranging from -12 to 0 (Hao et al., 2005; Kannel & Gan, 2012). The concentrations of these complex ringed compounds range from 40 to 120 mg/L in the tailing ponds, depending on the mining process and the pond age (Mohamed et al., 2013). Various treatment processes, including physical, chemical, and biological approaches have been evaluated on NA removal in OSPW. For membrane process, the reported rejection efficiency for NAs in OSPW varies from 12.4% to 95%, depending on the membrane types and pre-treatment methods (Allen, 2008b; Alpatova et al., 2014; Deriszadeh, Harding, & Husein, 2009).

---

<sup>2</sup> This chapter has been submitted to: Shu Zhu, Mingyu Li and Mohamed Gamal El-Din, 2017. Rejection of naphthenic acids by forward osmosis: Effect of pH value and draw solutes. Submitted to: *Journal of Membrane Science*

Forward osmosis (FO) is a membrane-based process that employs osmotic pressure difference between draw and feed solution as driving force (Cath et al., 2006). In FO process, ideally, only water molecules can be drawn from the less concentrated feed solution to the concentrated draw solution and those undesirable contaminants can be retained in the feed side. Along with high rejection efficiency, FO owns a few advantages over pressure-driven membrane process including less membrane fouling, reduced energy cost, and simplified operating system (Cath et al., 2006). Therefore, applying FO to treat oil and gas wastewater is attracting more research interests (Coday et al., 2015; Duong & Chung, 2014; Minier-Matar et al., 2015). FO has been incorporated in the reclamation of oil and gas drilling wastewater (Coday, Xu, et al., 2014; Hickenbottom et al., 2013), separation of emulsified oil-water (Duong & Chung, 2014), and recovery water from petroleum/water emulsions (S. Zhang et al., 2014), among others. Desirable organic rejections and high water recovery can be achieved with the help of FO process in the treatment of oil and gas wastewater (Coday et al., 2015; Hickenbottom et al., 2013).

Rejections of organic compounds can be affected by several factors including properties of target compounds, membrane characteristics, and feed/draw solution chemistry (McGovern, Mizerak, Zubair, & Lienhard, 2014). For instance, Jin et al. (Jin et al., 2012) investigated the rejection of pharmaceuticals including diclofenac, carbamazepine, ibuprofen, and naproxen by commercial cellulose triacetate (CTA) and thin film composite (TFC) FO membranes. The authors found that TFC exhibited a stable performance in terms of contaminant rejection under various pH conditions. They also suggested that, for CTA membranes, size and hydrophobicity of compounds were two important factors affecting the rejection of tested pharmaceuticals at low pH level. Moreover, Cui et al. (Cui et al., 2016) studied the removal of phenol, aniline, and nitrobenzene via laboratory fabricated FO membrane using feed/draw solutions with different



concentration level. It was reported that the rejection efficiencies of organic micro-pollutants were barely affected by the concentration of draw solution lower than 2000 ppm. The authors also observed that, increasing the draw solution concentration, in other words, increasing water flux can benefit the organic contaminant removal. Besides the influence of pH and membrane types, membrane fouling also needs to be mentioned in organic rejection. Linares et al. (Linares, Yangali-Quintanilla, Li, & Amy, 2011) evaluated the rejection of organic micro-pollutants using clean and fouled FO membranes. The experimental results illustrated that the hydrophilic ionic compounds showed a higher rejection in both clean and fouled membranes and the fouling layering improved the rejection of all the micro-pollutants due to the increased hydrophilicity and membrane surface charge.

In this study, the effects of feed solution pH and draw solutes were examined as two important factors affecting the NA rejection and OSPW filtration performance. The rejections of NA model compounds, including cyclohexane carboxylic acid (CHA), 1-adamantaneacetic acid (AAA) and the refined Merichem mixture of NAs, were evaluated at different pH conditions. Also, four draw solutions (i.e., NaCl, NH<sub>4</sub>Cl, CaCl<sub>2</sub> and Na<sub>2</sub>SO<sub>4</sub>) were studied in order to evaluate their influence on NA removal in terms of reverse salt diffusion and permeate water flux.

## **3.2 Materials and methods**

### **3.2.1 Bench-scale FO system**

A schematic experimental set-up is shown in Fig. 3-1. The cellulose triacetate (CTA) membrane was purchased from HTI (Hydration Technologies Innovations, Inc., Albany, OR, USA). The commercial CTA membrane was fabricated asymmetrically with a smooth active layer and an embedded polyester mesh support. Detailed membrane characteristics were described elsewhere (Arkhangelsky et al., 2014; C. Kim et al., 2012; Wang et al., 2010). The FO membrane was

placed in a SEPA FO membrane cell provided by Sterlitech Corporation (Kent, WA, USA) with the feed solution facing the active layer. The effective membrane surface was 140 cm<sup>2</sup>. The mean pore radius of CTA-FO membrane is 0.25–0.30 nm (Fang, Bian, Bi, Li, & Wang, 2014). No mesh spacer nor permeate carrier was employed during the system operation. Draw and feed solutions were recirculated counter-current on the two sides of the membrane by two speed-variable peristaltic pumps (Cole-Palmer, Vernon Hills, IL, USA). A digital balance (Scout Pro, Ohaus Corp., Parsippany, NJ, USA) was used for monitoring the weight change of the draw solution every 30 seconds. All the batch experiments were conducted at room temperature of 21±2 °C.

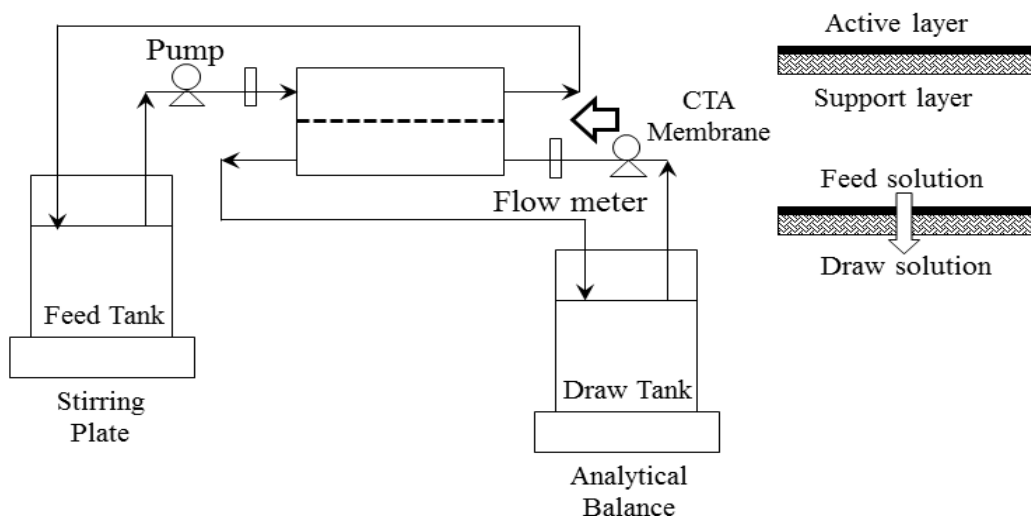


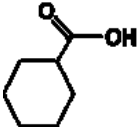
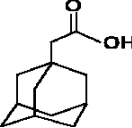
**Figure 3-1** Schematic of FO system set-up.

### 3.2.2 NA model compound rejection experiments

Three NA model compounds including: cyclohexane carboxylic acid (CHA), 1-adamantaneacetic acid (AAA) and the refined Merichem mixture of NAs were investigated. High purity CHA and AAA were purchased from Sigma–Aldrich (Oakville, ON, Canada) and the refined Merichem mixture of NAs was used as purchased from Merichem Company (Houston, TX, USA). Detailed characteristics of the model compounds are presented in Table 3-

1. The feed solutions were prepared by directly dissolving 100 mg CHA and AAA into 1L 0.01 M phosphate buffer solution and 100 mg Merichem NAs into 1L 0.05 M carbonate bicarbonate buffer solution, respectively. pH values of feed solutions were further adjusted to 3, 6 and 9 by 1M NaOH or HCl. The solubility of NA model compounds decreases with pH, therefore, AAA and CHA aqueous feed solutions with lower concentration (25 mg/L) were also prepared at pH 3 to exclude the impact of the organic precipitation. Merichem NAs was only prepared at the concentration of 100 mg/L at pH 6 and 9, because at pH 3, Merichem NA mixture has a lowest solubility.

**Table 3-1** Characteristics of NA model compounds

| Model compound                  | Cyclohexanecarboxylic acid (CHA)   | 1-adamantaneacetic acid (AAA)   | Merichem NA mixture (NAs)                       |
|---------------------------------|--|---|---|
| Chemical structure              |  |  | N/A   |
| Formula                         | C <sub>7</sub> H <sub>12</sub> O <sub>2</sub>                                      | C <sub>12</sub> H <sub>18</sub> O <sub>2</sub>                                      | N/A   |
| Molecular weight, g/mol         | 128  | 194   | N/A   |
| pK <sub>a</sub> <sup>a</sup>    | 4.91±0.1   | 5.00±0.1  | 5.5±0.1; 6.6±0.2; 7.8±0.1; 9.4±0.1 <sup>b</sup> |
| Log D <sup>a</sup> at pH 3      | 1.64   | 3.10  | N/A   |
| pH 6                            | 0.53   | 2.06  |   |
| pH 9                            | -1.94  | -0.46   |   |
| Solubility <sup>a</sup> at pH 3 | 7.9 g/L  | 0.099 g/L   | N/A   |
| pH 6                            | 100 g/L  | 1.1 g/L   |   |
| pH 9                            | 1000 g/L   | 0.099 g/L   |   |

a: Data source: SciFinder Scholar, calculated using Advanced Chemistry Development(ACD/Labs)

Software V11.02 (© 1994-2015 ACD/Labs)

b: (Moustafa et al., 2014)

N/A: not available

1M (58.4 g/L) NaCl with a corresponding osmotic pressure of 4.7 MPa was used as the draw solution for the rejection experiments for CHA, AAA, and Merichem NAs at a pH range between 3 and 9. Extra three inorganic salts including CaCl<sub>2</sub>, NH<sub>4</sub>Cl and Na<sub>2</sub>SO<sub>4</sub> were applied as draw solutes, respectively, to study the rejection of CHA at pH =9. To maintain the same osmotic pressure level, 0.6 M (71.2 g/L) CaCl<sub>2</sub>, 1 M (53.4 g/L) NH<sub>4</sub>Cl and 1M Na<sub>2</sub>SO<sub>4</sub> (142.8 g/L) were prepared with Milli-Q water. All the inorganic salts used for draw solution preparation were analytical grade chemicals purchased from Sigma–Aldrich, Oakville, ON, Canada.

The NA model compound rejection experiments were conducted continuously for 7 h with a constant crossflow velocity of 14 cm/s. Each experiment was conducted using a new membrane. The experiments started with 1L of feed solution and 1L of draw solution. Approximate 1mL water samples from both feed and draw solutions were taken every hour for liquid chromatography/mass spectrometer (LC/MS) and ion chromatography (IC) analysis. Baseline experiments using the buffer solution only as the feed solution were performed prior to exclude the decline of osmotic pressure caused by the continuous dilution of draw solution. All the presented water fluxes in the following discussions were baseline corrected.

To further compare the draw salt diffusion with or without the presence of NA model compounds, additional reverse salt diffusion experiments were conducted with the inorganic salt solutions (0.1, 0.2, 0.5, 1 M) as the draw and Milli-Q water as the feed following the same operating condition as rejection experiment.

Water flux was determined by the weight change of draw solution as follows

$$J_w = \frac{V_p}{A_m \times t} \quad (1)$$

Where  $J_w$  is the permeate flux,  $V_p$  is the permeate volume,  $A_m$  is the effective area of membrane surface, and  $t$  is the operating time.

The rejection of each model compound was determined through a mass balance by considering the dilution of draw solution. The dilution factor (DF) can be obtained using (Xie, Price, Nghiem, & Elimelech, 2013; Zheng et al., 2015).

$$DF = \frac{V_{d,t}}{V_{p,t}} \quad (2)$$

Where  $V_{d,t}$  and  $V_{p,t}$  are the volume of draw solution and permeate at time = t.

$$R (\%) = \left(1 - \frac{DF \times C_{d,t}}{C_{f,0}}\right) \times 100\% \quad (3)$$

Where DF is the dilution factor determined from Eq. (2),  $C_{d,t}$  is the concentration of organic compound in draw solution at time = t and  $C_{f,0}$  is the concentration of organic compound in feed solution at time = 0.

The reverse salt diffusion was evaluated by reverse salt flux:

$$J_{salt} = \frac{V_{f,t}C_{fs,t} - V_{f,0}C_{fs,0}}{A_m \times t} \quad (4)$$

Where  $C_{fs,0}$  and  $C_{fs,t}$  are the concentration of draw solute in feed solution at time = 0 and t, respectively.  $V_{f,t}$  and  $V_{f,0}$  are the volumes of feed solution at time = 0 and t, respectively. The specific  $J_{salt}$  was determined using reverse salt flux ( $J_{salt}$ ) divided by corresponding water flux ( $J_w$ ).

### 3.2.3 Analytical methods

The conductivity and pH value were measured with a pH /conductivity meter (Fisher Scientific, Ottawa, ON, Canada). The concentrations of CHA and AAA were determined by liquid chromatography - mass spectrometric (LC/MS) (500-MS LC Ion Trap. Varian, Inc., CA, USA) and the concentration of Merichem NAs were measured by an ultra-performance liquid chromatograph (UPLC) (Waters Corp., Milford, MA, USA) based on the method described elsewhere (Alpatova et al., 2014; Moustafa et al., 2014). The analysis of cation and anion

concentration was conducted by ion chromatography (ICS-2000 and 2500, Dionex, Sunnyvale, CA, USA). Scanning electron microscopy (SEM) (Tescan, Brno, Czech Republic) was used to observe the membrane surface morphology after the rejection experiment. The contact angle was measured by FTA-200 instrument (FOLIO Instrument Inc., Kitchener, ON, USA) using DI water.

### **3.3 Results and discussion**

#### **3.3.1 Effect of pH on NA model compound and OSPW NA rejection**

##### **3.3.1.1 Water flux**

Fig. 3-2 presents the baseline corrected water flux in the rejection experiments at various pH values using CHA, AAA and Merichem NAs as feed solution and 1M NaCl as draw solution, respectively. As a reference, water flux of pH adjusted OSPW (NA concentration = 48.13 mg/L) is also shown in Fig. 3-2 (d). No significant changes on water flux were observed with respect of pH when applying CHA and AAA aqueous solution as the feed. Decreasing the initial CHA and AAA concentrations from 100 to 25 mg/L did not affect the water flux behavior at pH = 3 neither. Rather than pH values, it appeared that water flux was more depended on the chemical structure of each model compound. When CHA solution was applied as the feed, the water flux slightly decreased from 6.8 L/m<sup>2</sup> hr to 6.2 L/m<sup>2</sup> hr in the first 100 mL permeate and leveled off after that. On the contrary, a continuous flux decline was found when the feed was switched to AAA solution (Fig. 3-2 (b)), the water flux was reduced successively from 7.5 L/m<sup>2</sup> hr to 6.5 L/m<sup>2</sup>. Interestingly, different water flux profiles were found using Merichem NAs feed solution at two pH values: at pH 9, water flux experienced a sharp decline (~20%), and then remained stable at 5.5 L/m<sup>2</sup> hr; at pH 6, a consistently decreasing trend from 7.5 to 6 L/m<sup>2</sup> hr was shown. For real OSPW (Fig. 3-2 (d)), the effect of pH on water flux was more distinctive because of its impact on the NA solubility. As discussed in Headley et al.'s (Headley, Peru, McMartin, &

Winkler, 2002) paper, the total solubility of NAs increases with pH values (pH = 3 to 9). Hence, at lower pH level, NAs will precipitate, thereby forming large size foulants. The authors also pointed out that at lower pH level, only noncyclic NAs were dissolved and as pH increasing, cyclic NAs and other NA components became soluble. The observed flux fluctuation might be associated with membrane fouling phenomenon and changed membrane surface characteristics.

To avoid the interference of model compound solubility, the SEM images (Fig. 3-3) were taken and contact angle analyses were conducted before and after the experiment at pH 9 only. Fig. 3-3 showed no surface fouling for CHA and AAA filtered membranes. However, some surface accumulations were found after the membrane exposure to Merichem NAs, which agrees with the flux profile in Fig.3-2 (c). Furthermore, the contact angle of membrane active layer after Merichem NA rejection experiment increased from  $66.6 \pm 2.4^\circ$  to  $77.9 \pm 0.4^\circ$  (Fig. 3-4) while those values decreased after CHA and AAA rejection experiment. This phenomenon might due to the adsorbed model compound at the membrane surface. Because the solubility of the tested model compound ranked as  $CHA > AAA > Merichem \text{ NAs}$  at pH 9 and the contact angle of used membranes followed the same order.

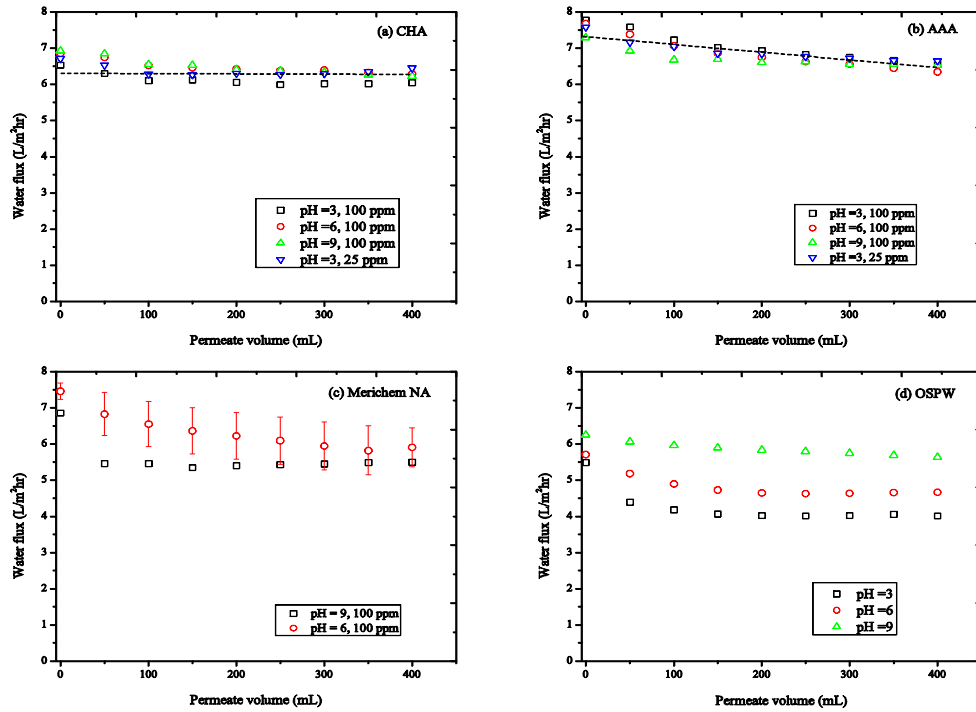


**Figure 3-2** Water flux at various pH values as a function of permeate volume. (a) CHA (b) AAA (c) Merichem NAs, and (d) OSPW (NA concentration = 25.4 mg/L) as the feed solution. 1M NaCl was the draw solution. The presented water flux was baseline corrected. The baseline experiments were conducted using corresponding buffer solution only as the feed solution and 1M NaCl solution as the draw.



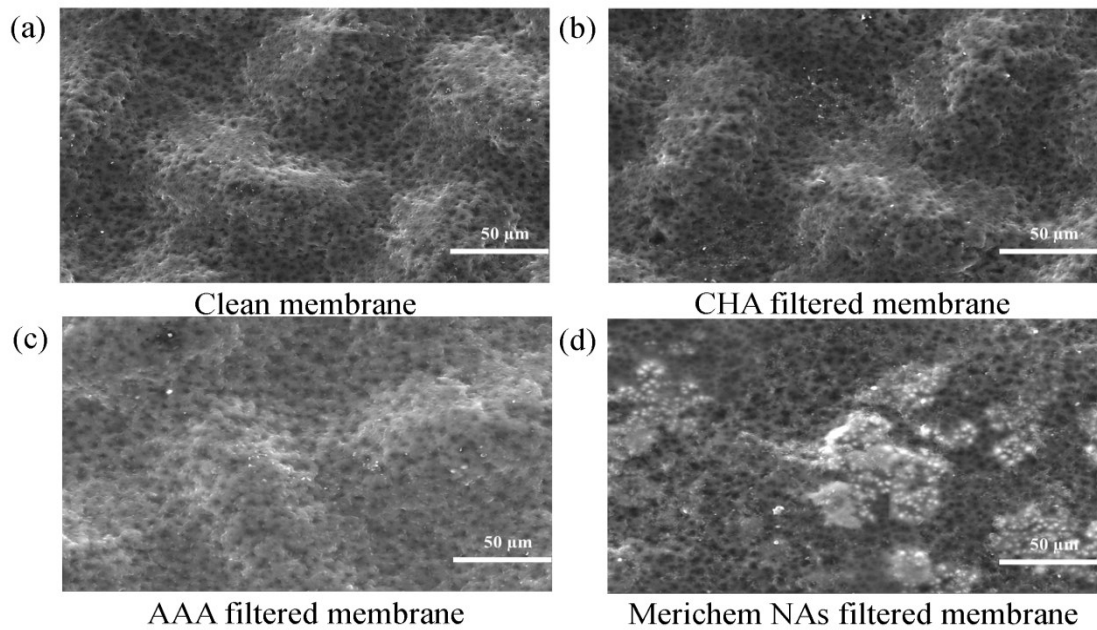


**Figure 3-3** SEM images taken before and after the rejection experiment for each NA model compound (100 ppm at pH = 9)

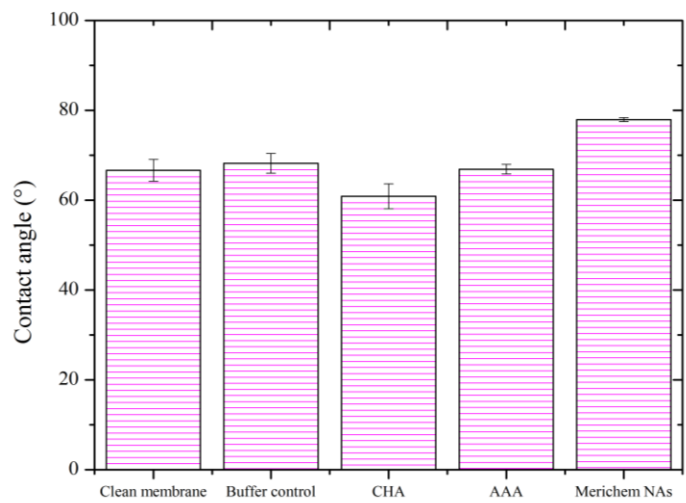


**Figure 3-4** Contact angle analysis before and after the rejection experiment for each NA model compound (100 mg/L at pH = 9)

### 3.3.2 Specific reverse salt diffusion

The specific reverse salt diffusion of NaCl for different NA model compounds and different pH values is shown in Fig. 3-5. When applying Merichem NAs as feed solution at pH = 6 and 9, the specific reverse salt flux was maintained around 12 mmol/L. With the presence of 100 mg/L CHA, as pH increased from 3 to 9, the specific reverse flux was slightly increased from  $15.9 \pm 2.2$  mmol/L to  $22.4 \pm 3.8$  mmol/L, while that of AAA was relatively consistent in Fig. 3-5 (b). By measuring the contact angle after CHA experiment, we also found that membrane surface became more hydrophobic ( $71.6 \pm 1.6^\circ$ ) at pH=3.

As suggested from previous studies (Phillip, Yong, & Elimelech, 2010), the specific reverse salt diffusion can only be affected by the membrane own characteristics. The exposure of organic compound might change the membrane structure, water permeability, and salt permeability (Coday et al., 2016), thereby slightly increasing specific reverse flux. Our observation arise the possibility that the specific reverse flux can be affected by membrane surface hydrophobicity. At pH 9, the contact angle of the fouled membrane showed the same trend with the specific flux. The contact angle of Merichem NAs fouled membrane was the highest ( $77.9 \pm 0.42^\circ$ ). Meanwhile, the specific reverse flux ( $13.5 \pm 5.6$  mmol/L) through NAs filtered membrane was lower than those values of CHA and AAA filtered membranes under the same experiment condition. However, due the research limitation of current study, no conclusion can be drawn and further investigation regarding the membrane properties after the rejection experiment is needed.

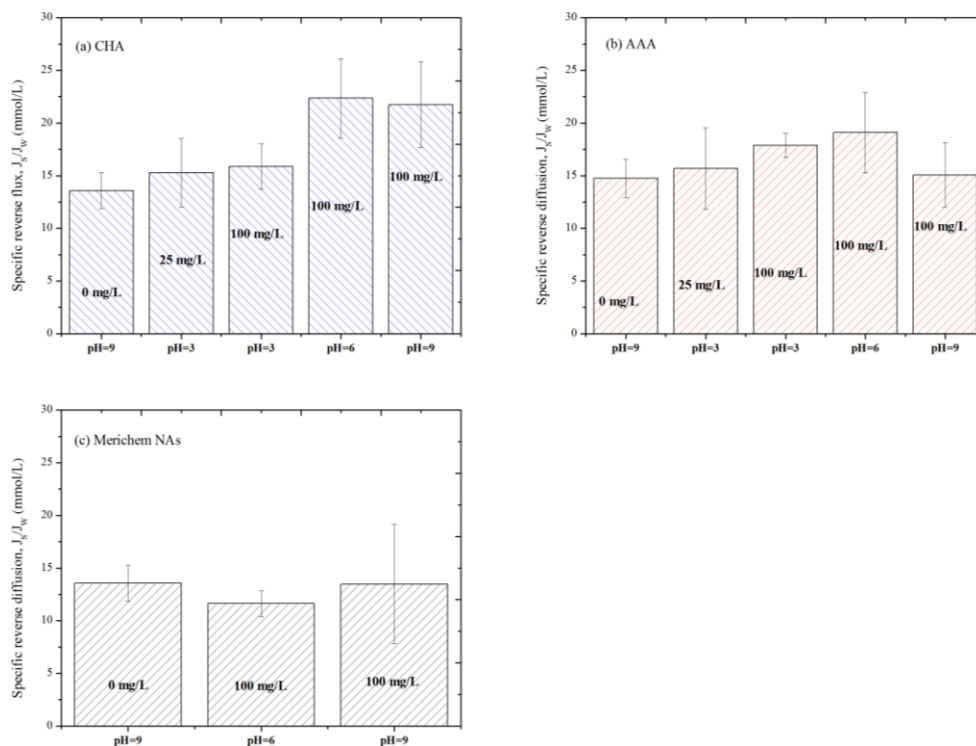


**Figure 3-5** Specific reverse salt flux of NaCl at different pH values with presence of NA model compound. Experimental condition: Draw solution = 1M NaCl, initial feed solutions (a) 100 mg/L of CHA at pH = 3, 6, 9; 25 mg/L of CHA at pH = 3 (b) 100 mg/L of AAA at pH = 3, 6, 9; 25 mg/L of AAA at pH = 3 (c) 100 mg/L of Merichem NAs at pH = 6, 9. The specific reverse diffusion of 1M NaCl as draw solution and corresponding buffer solution only as the feed solution was also plotted as a reference.

### 3.3.3 NA model compound rejection

The rejection of CHA and AAA feed solution at pH = 3, 6, 9 are presented in Fig. 3-6 as a function of time. It is worth noting that the pH value significantly affected the rejection of CHA and AAA. When pH increased from 3 to 9, the rejection rate of CHA elevated from  $23.7 \pm 2.5\%$  to  $97.1 \pm 0.3\%$  and the rejection rate of AAA increased from  $80.5 \pm 4.0\%$  to  $95.7 \pm 0.69\%$ . The pKa values of CHA and AAA are  $4.91 \pm 0.1$  and  $5.00 \pm 0.1$  (Table 3-1), indicating both compounds

were negatively charged at pH 9. The active layer of CTA membrane used in our experiment was also negatively charged and its zeta potential decreased with the increasing pH (Jin et al., 2012; Xie, Nghiem, Price, & Elimelech, 2013). Therefore, the increase in rejection can be attributed to the enhanced electrostatic repulsive force between membrane and the model compounds. This was in good agreement with previous finding by Jin et al. (Jin et al., 2012) in which the author concluded that the rejection increase of two negatively charged organic compounds (ibuprofen and naproxen) with increasing pH was due to the electrostatic repulsion.

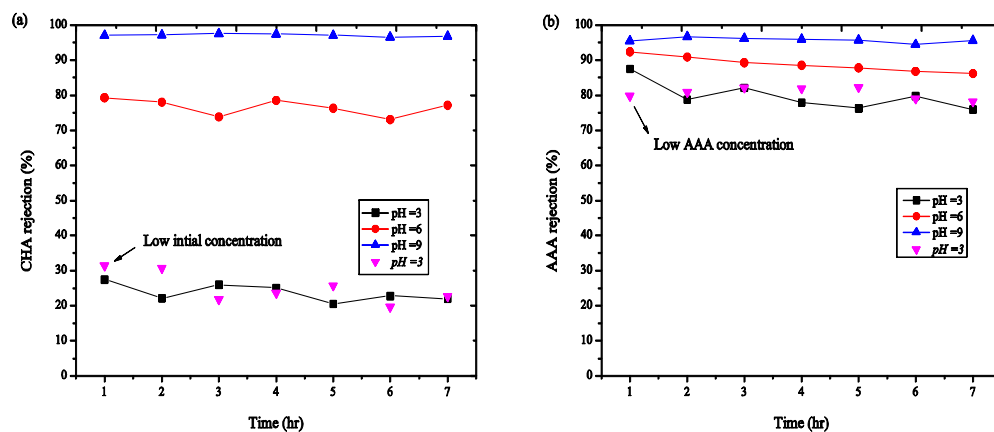


**Figure 3-6** Rejection of CHA (a) and AAA (b) as a function of time. The experimental conditions were as follows: the initial concentrations of CHA and AAA were  $100 \pm 3.2$  ppm and  $25 \pm 1.3$  ppm, draw solution was 1M NaCl.

As reported by several researchers, hydrophobicity of organic compounds was as another important factor affecting rejection (Coday, Yaffe, Xu, & Cath, 2014). They observed that in short-term experiment, the trace organic compounds with higher hydrophobicity demonstrated higher rejection efficiency because the hydrophobic interaction between organic compound and membrane surface enhanced the adsorption, and thus delayed the diffusion process. As shown in Table 3-1, log D values of CHA and AAA indicated that the hydrophobicity of these two

compounds increases with the decrease of pH. Hence, at lower pH, more AAA would be adsorbed and the rejection efficiency would decrease with time due to the diffusion of the adsorbed organics. However, the rejection efficiencies of both compounds remained comparatively stable at three pH values throughout the 7 hr experiment, which can be explained by the less adsorbed membrane surface and the small molecular size of CHA and AAA. The water solubility of those two compounds decreases with the decrease of pH. To exclude the influence of possible precipitation at pH 3, the rejections of CHA and AAA with initial concentrations of 25 mg/L were evaluated as well and the results showed that their rejections were kept at the similar level ( $80.5\pm 1.6\%$  for AAA and  $25.5\pm 4.5\%$  for CHA). Interestingly, it was found the overall rejection of AAA was higher than CHA at all test pH values and this different rejection behavior might be attributed to the molecular size difference between CHA and AAA.

Merichem NAs are a commercial mixture of NAs and they might behave differently from CHA and AAA. To better understand its rejection in terms of different carbon number ( $n$ ) and hydrogen efficiency ( $-Z$ ) at pH = 6 and 9, the rejection efficiencies were plotted with corresponding  $Z$  and  $n$  numbers, respectively (Fig. 3-7). The overall rejections of Merichem NAs were  $95.6\pm 1.3\%$  at pH = 6 and  $95.4\pm 2.1\%$  at pH = 9, showing that pH influence over 6 to 9 was insignificant. The reported pKa value of NAs in natural water was 5 to 6 (J. Xue, Zhang, Liu, & Gamal El-Din, 2016); therefore, at the pH range of interest, the electrostatic repulsive force triggered by the deprotonation of some NA species can be one explanation of the high rejection. In addition, size exclusion still influenced its rejection. NAs with higher  $n$  and  $-Z$  numbers demonstrated higher molecular weight. In Fig. 3-7 (a), the rejection efficiencies were stably around 95% from  $-Z$  number = 0 to 4, as  $-Z$  number increased above 6, the rejection increased to

100%. In Fig. 3-7 (b), when  $n$  increased from 9 to 16, the rejection increased from 95% to 100%. NA species with higher carbon number ( $n$ ) or lower hydrogen deficiency ( $-Z$ ) are reported to be more hydrophobic (J. Xue et al., 2016); however, our results did not demonstrate any rejection trends regarding hydrophobicity.

In Fig. 3-7 (c) and (d), the 3D-images of Merichem-NA removal are also presented at pH = 6 and pH = 9, respectively. In general, the difference on Merichem-NA rejection between pH = 6 and 9 was insignificant because those two pH values were higher than its pKa. In addition, as a reference, the rejection efficiency of OSPW-NAs was introduced in Fig. 3-8. Consistent with the result observed in Fig. 3-8 (a), it showed that the OSPW-NA rejection increased as  $-Z$  number increased. In Fig. 3-8 (b), no specific trend on rejection efficiency was found through carbon number range from 9 to 23. Compared to the Merichem NAs, OSPW-NAs showed a complicate matrix (Fig. 3-9). The rejections of OSPW-NA species varied from 31% to 100% (Fig. 3-8 (c)). Interestingly, we found that the lower rejected OSPW-NA species lay in the category of  $-Z=0$ . However, TOF-MS analysis results (Fig. 3-9) indicated that limited OSPW-NA species were detected at  $-Z=0$ , leaving the results statically unconvincing.

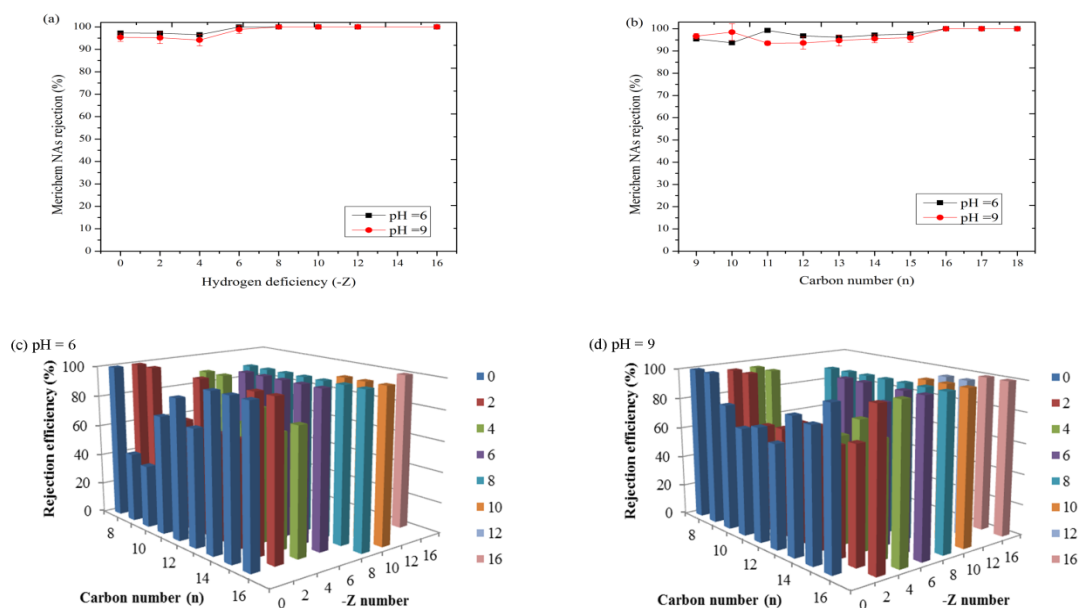


**Figure 3-7** Rejection of Merichem NAs as a function of hydrogen deficiency (-Z) (a) and carbon number (n) (b). 3D-rejection image along with corresponding carbon number and -Z number at pH =6 (c) and pH =9 (d), respectively. The experimental conditions were as follows: the initial concentrations of were 93.7 and 96.2 mg/L, respectively. Draw solution was 1M NaCl.

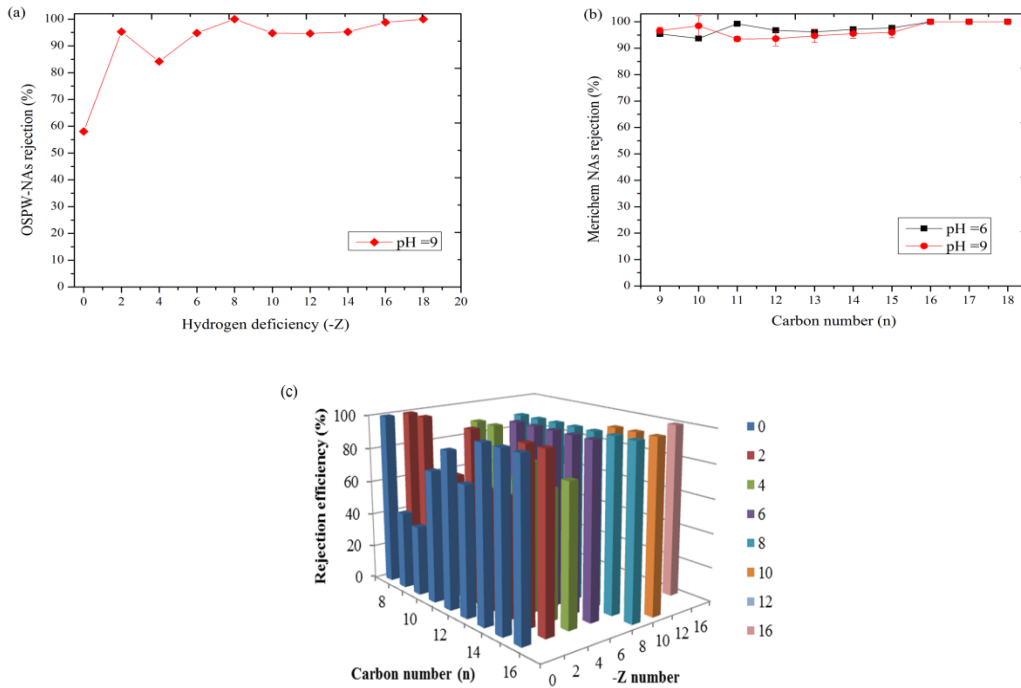


**Figure 3-8** Rejection of OSPW NAs as a function of (a) hydrogen deficiency (-Z) and (b) carbon number (n). 3D-rejection image (c) along with corresponding carbon number and -Z number at pH =6, respectively. The experimental conditions were as follows: the initial concentrations of OSPW NAs were 25.4 mg/L and draw solution was 1M NaCl.

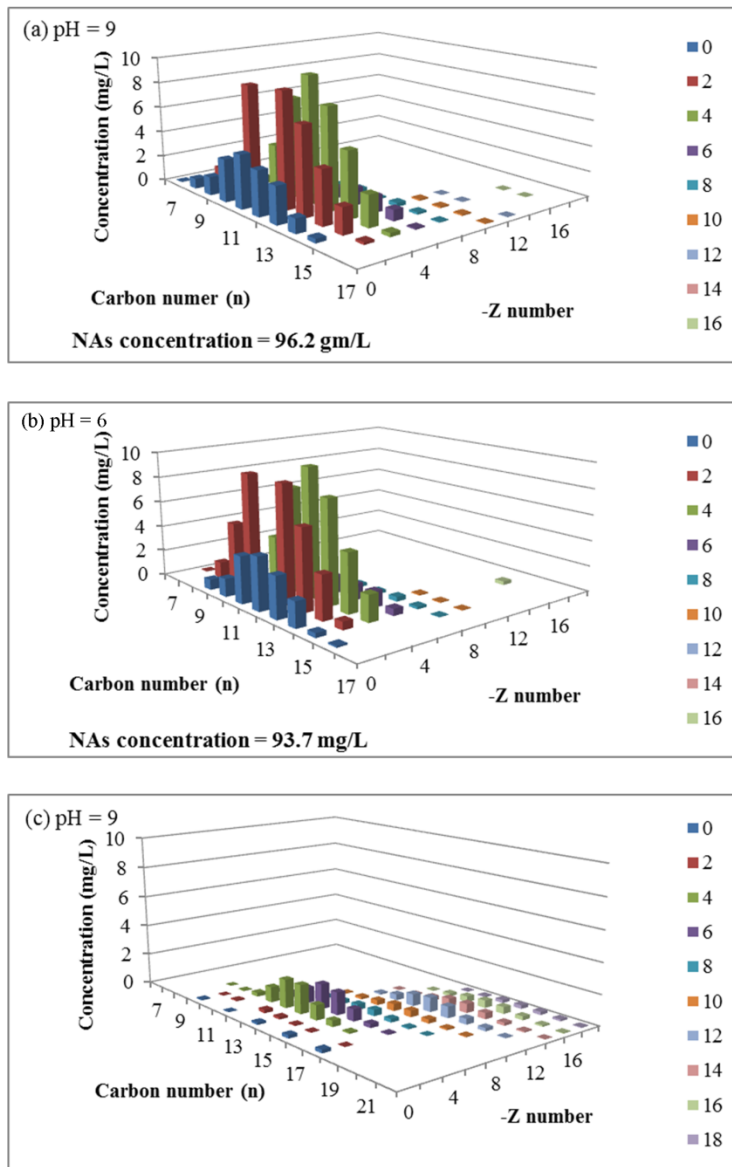


**Figure 3-9** Concentration of NAs in Merichem NA aqueous solution (a) pH = 9, (b) pH = 6 and (c) in oil sands process-affected water (OSPW) at pH = 9.



### 3.3.4 Effect of draw solute on NA model compound rejection

#### 3.3.4.1 Water flux

To obtain the similar driving force, the osmotic pressure was maintained at the same level using approximately 1M NaCl, NH<sub>4</sub>Cl, Na<sub>2</sub>SO<sub>4</sub> and 0.6 M CaCl<sub>2</sub> as the draw solution (Achilli, Cath, & Childress, 2010). The normalized flux (baseline corrected) versus permeate volume is presented Fig. 3-10. To collect 400 mL permeate water, the flux decline followed the order of CaCl<sub>2</sub> (15%) > NaCl (6%) > NH<sub>4</sub>Cl (5%) > Na<sub>2</sub>SO<sub>4</sub> (2%). The significant flux loss found on CaCl<sub>2</sub> might associate with the fouling due to the interaction of CHA and reverse diffused Ca<sup>2+</sup>. As discussed in previous literatures (She, Jin, Li, & Tang, 2012; M. Xie, L. D. Nghiem, et al., 2013), Ca<sup>2+</sup> can enhance the membrane fouling caused by carboxylic group-rich organic compound (i.e., alginate and humic acids). Further discussion on CaCl<sub>2</sub> used as draw solution is presented in below section.

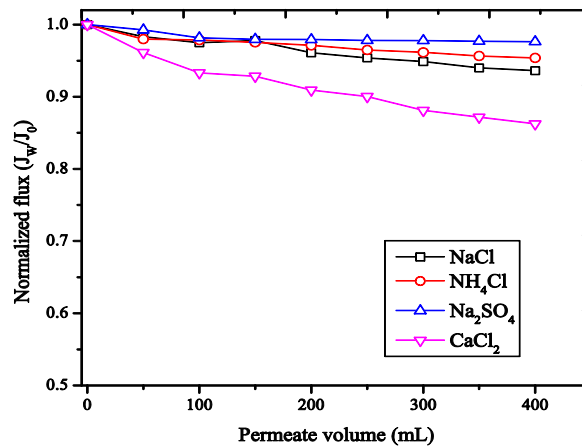


**Figure 3-10** Normalized flux (baseline corrected) as a function of permeate volume using 1M NaCl, NH<sub>4</sub>Cl, Na<sub>2</sub>SO<sub>4</sub>, and 0.6 M CaCl<sub>2</sub> as the draw solution. The initial flux generated by these draw solutions was around 7.3±0.2 L/m<sup>2</sup> hr. Experimental condition: initial CHA concentration =92.6±3.7 mg/L, pH =9. Baseline experiments were conducted using the corresponding

concentrations of inorganic salt solutions as the draw solutions and clean DI water as the feed at the same operating condition.

### 3.3.4.2 Specific reverse solute flux

To better compare the specific reverse salt diffusion with and without the presence of CHA, the reverse draw solute flux was investigated prior using all inorganic salt solutions with concentrations up to 1 M as the draw solution and clean DI water as the feed solution. The reverse salt flux is shown in Fig. 3-10 (a) as a function of water flux, along with the specific salt flux calculated by reverse salt flux divided by the corresponding water flux. An approximate linear relation was found between reverse salt flux and water flux, implying the specific salt flux was almost a constant for each specific draw solute. This result was in good agreement with other literatures (Phillip et al., 2010; Yong, Phillip, & Elimelech, 2012) describing the specific salt flux only associates with the membrane characteristics (i.e., water permeability and salt permeability). The calculated specific salt flux for the tested inorganic salts ranked as  $\text{NH}_4\text{Cl} > \text{NaCl} > \text{CaCl}_2 > \text{Na}_2\text{SO}_4$ . The estimated specific salt flux indicated that to obtain the same volume of permeate, highest amount of  $\text{NH}_4\text{Cl}$  will diffuse through the membrane, compared to other three tested inorganic draw solutes. As reported where else (S. A. F. Zhao & Zou, 2011), the hydrated radiuses of the studied cations rank as  $\text{Ca}^{2+} > \text{Na}^+ > \text{NH}_4^+$  and the trend in the anions radius is:  $\text{SO}_4^{2-} > \text{Cl}^-$ . Therefore,  $\text{NH}_4\text{Cl}$  composing of two smallest ions showed a comparatively high specific reverse salt diffusion, which agreed with the results reported by previous studies (Achilli et al., 2010). According to the specific reverse salt flux presented in Fig. 3-11 (a),  $9.7 \pm 0.8$  mmol  $\text{CaCl}_2$  should diffuse to the feed solution (DI water) as per liter of permeate. The specific reverse fluxes of  $\text{NH}_4\text{Cl}$  ( $24.9 \pm 2.6$  mmol/L) and  $\text{NaCl}$  ( $17.9 \pm 2.2$  mmol/L) were slightly increased, which was likely due to the increased hydrophilicity of membrane surface. The

specific reverse flux of  $\text{Na}_2\text{SO}_4$  ( $3.1 \pm 0.2$  mmol/L) was not influenced by the exposure to CHA (Fig. 3-11 (b)). However, when present with CHA at a concentration of 100 ppm, the specific reverse salt flux of  $\text{CaCl}_2$  was reduced to  $1.2 \pm 0.5$  mmol/L.

The reverse salt flux reduction of  $\text{CaCl}_2$  was further studied by the corresponding reverse anion and cation flux. The IC analysis results showed that the average reverse flux of  $\text{Ca}^{2+}$  and  $\text{Cl}^-$  was  $0.43 \pm 0.1$  and  $7.8 \pm 0.3$  mmol/m<sup>2</sup> hr, respectively. To obtain the electro-neutrality of the solution, although  $\text{Cl}^-$  diffused faster than  $\text{Ca}^{2+}$ , equivalent of  $\text{Ca}^{2+}$  was expected to diffuse to the feed solution. The decrease of reverse  $\text{Ca}^{2+}$  flux was likely due to membrane fouling and cake-enhanced concentration polarization (CECP) (S. Lee et al., 2010). The reverse  $\text{Ca}^{2+}$  can bind with CHA to form the fouling layer on the membrane surface, thereby hindering the forward transportation of salt ions from feed to draw. This phenomenon resulted in enhanced concentration polarization on the feed side and hence, possibly led to the precipitation of calcium combined CHA. The reduced specific reverse  $\text{Cl}^-$  flux might be explained by the electrostatic repulsive force between the fouled membrane and  $\text{Cl}^-$ . As reported by Xie et al. (M. Xie, L. D. Nghiem, et al., 2013), the negatively charged fouling layer resulted in a hindrance of reverse  $\text{Cl}^-$  flux.

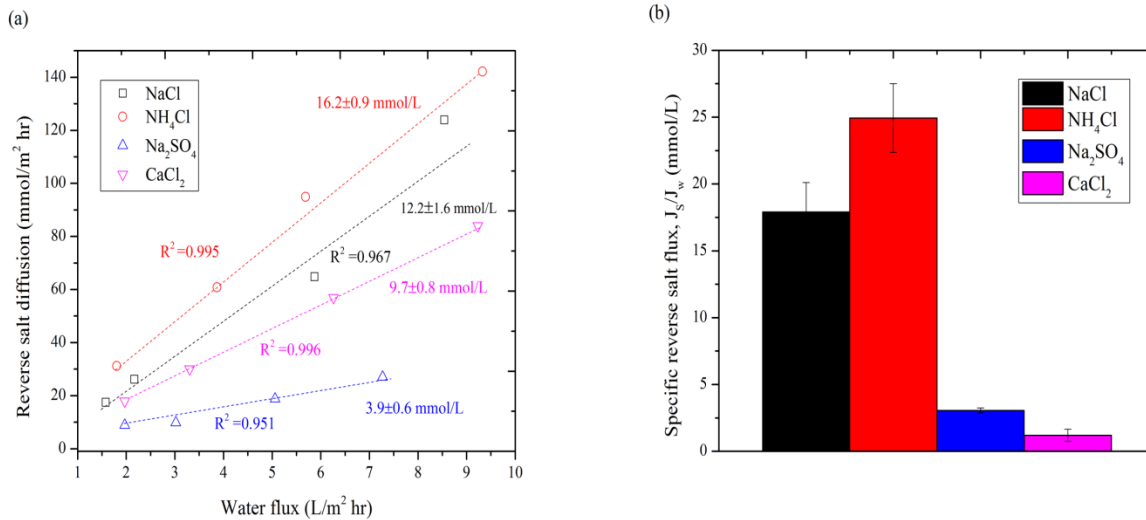


**Figure 3-11** (a) Reverse salt flux as a function of water flux. Experimental conditions: using 0.1, 0.2, 0.5 and 1 M inorganic salt solutions (NaCl, NH<sub>4</sub>Cl, Na<sub>2</sub>SO<sub>4</sub>, and CaCl<sub>2</sub>) as draw and DI water as the feed (b) Specific reverse draw solute flux for NaCl, NH<sub>4</sub>Cl, Na<sub>2</sub>SO<sub>4</sub>, and CaCl<sub>2</sub>. Experimental condition: initial feed solution with CHA concentration = 92.6 ± 3.7 mg/L, pH = 9.

### 3.3.4.3 CHA rejection

The rejections of CHA for each draw solutions are presented in Fig. 3-12 as a function of time. In general, when CaCl<sub>2</sub> was used as the draw solution, the rejection of CHA was the highest (98.6 ± 0.2%) compared to NaCl (97.1 ± 0.3%), NH<sub>4</sub>Cl (96.2 ± 0.8%), Na<sub>2</sub>SO<sub>4</sub> (97.3 ± 0.3%). As we discussed in the previous section, at pH 9, the governing rejection mechanism was electrostatic repulsive force, therefore, no significant difference was found between those four draw solutes. A slightly elevated rejection found on CaCl<sub>2</sub> was due to the membrane surface fouling caused by the reversely diffused Ca<sup>2+</sup>. The 2 to 3% incomplete rejection suggested that small amount of CHA can still diffuse into the draw solution through the fouled or un-fouled membrane. “Retarded forward diffusion” was one of the important phenomena reported by many researchers

(Cui et al., 2016; Xie et al., 2012) to explain the high rejection of organic compound in FO process. The author concluded that the reverse diffusion of draw solute could slower the transport of organic compound and thus, increasing the rejection efficiency. Therefore, increasing the draw solution concentration or selecting easily diffusive draw solute can benefit the rejection. Cui et al. (Cui et al., 2016) observed that when a draw solution (NaCl) increased from 0.5 to 2 M, the rejections of phenol, nitrobenzene and aniline were all increased in different levels. The authors pointed out that although elevating the draw solution concentration can promote the water flux, it also slowed down the organic solute diffusion. Therefore, the increased organic rejection was mainly due to the retarded diffusion from feed to the draw solution. In our experiment, no distinction had been seen on CHA rejection comparing  $\text{NH}_4\text{Cl}$  and  $\text{Na}_2\text{SO}_4$  (the highest and the lowest solute diffusion) as the draw solutes because the rejections under both draw solutes were comparatively high. However, our results still cannot exclude the impact of draw solute diffusion on CHA rejection. To further investigate the effect of draw solution diffusion on CHA, higher CHA and draw solute concentration are recommended to employ.

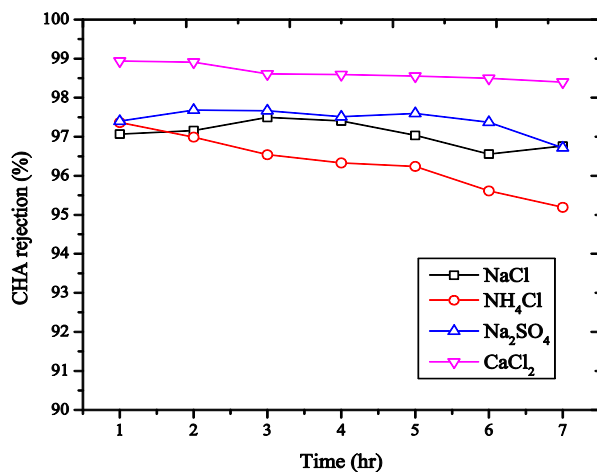


**Figure 3-12** Rejection of CHA as a function of time using 1M NaCl,  $\text{NH}_4\text{Cl}$ ,  $\text{Na}_2\text{SO}_4$ , and 0.6 M  $\text{CaCl}_2$  as the draw solution. The initial water flux was maintained at  $7.46 \pm 0.32 \text{ L/m}^2 \text{ hr}$ .

### 3.4 Conclusions

The current study presented the effect of pH and four draw solutes – NaCl, NH<sub>4</sub>Cl, Na<sub>2</sub>SO<sub>4</sub> and CaCl<sub>2</sub> – on the rejection of selected NA model compounds including CHA, AAA and Merichem NAs in 7 hours. The results indicated that from pH 3 to 9, electrostatic repulsion mechanism dominated CHA and AAA rejection. From pH 6 to 9, the rejection of Merichem NAs was stable (> 92%) likely due to its larger size and electrostatic repulsion force. At pH 9, the overall rejection of three NA model compounds was above 95% when using 100 mg/L model compound aqueous solution as feed and 1M NaCl as the draw solution. The water flux observed during the rejection experiment was comparatively pH-independent, however, more severe flux decline was found when using AAA and Merichem NA aqueous solution. The rejection study with respect to various inorganic draw solutes suggested that the tested draw solutes did not significantly affect the rejection of CHA at pH 9 and the corresponding water flux was maintained at a similar level, except for CaCl<sub>2</sub>. Using 0.6 M CaCl<sub>2</sub> as draw solution led to a more rapid flux decline and a reduced reverse salt diffusion, showing the propensity of membrane fouling caused by reverse Ca<sup>2+</sup> and CHA. The specific reverse salt flux of NaCl revealed that exposure to three aqueous NA model compounds solutions might alternate the membrane characteristics which need to be further investigated.

### 3.5 Reference

Achilli, A., Cath, T. Y., & Childress, A. E. (2010). Selection of inorganic-based draw solutions for forward osmosis applications. *Journal of Membrane Science*, 364(1-2), 233-241. doi: 10.1016/j.memsci.2010.08.010

- Allen, E. W. (2008a). Process water treatment in Canada's oil sands industry: I. Target pollutants and treatment objectives. *Journal of Environmental Engineering and Science*, 7(2), 123-138.
- Allen, E. W. (2008b). Process water treatment in Canada's oil sands industry: II. A review of emerging technologies. *Journal of Environmental Engineering and Science*, 7(5), 499-524. doi: Doi 10.1139/S08-020
- Alpatova, A., Kim, E. S., Dong, S. M., Sun, N., Chelme-Ayala, P., & El-Din, M. G. (2014). Treatment of oil sands process-affected water with ceramic ultrafiltration membrane: Effects of operating conditions on membrane performance. *Separation and Purification Technology*, 122, 170-182. doi: DOI 10.1016/j.seppur.2013.11.005
- Arkhangelsky, E., Lay, S. S., Wicaksana, F., Al-Rabiah, A. A., Al-Zahrani, S. M., & Wang, R. (2014). Impact of intrinsic properties of foulants on membrane performance in osmotic desalination applications. *Separation and Purification Technology*, 123, 87-95. doi: DOI 10.1016/j.seppur.2013.12.013
- Cath, T. Y., Childress, A. E., & Elimelech, M. (2006). Forward osmosis: Principles, applications, and recent developments. *Journal of Membrane Science*, 281(1-2), 70-87. doi: 10.1016/j.memsci.2006.05.048
- Coday, B. D., Almaraz, N., & Cath, T. Y. (2015). Forward osmosis desalination of oil and gas wastewater: Impacts of membrane selection and operating conditions on process performance. *Journal of Membrane Science*, 488, 40-55. doi: 10.1016/j.memsci.2015.03.059
- Coday, B. D., Hoppe-Jones, C., Wandera, D., Shethji, J., Herron, J., Lampi, K., Cath, T. Y. (2016). Evaluation of the transport parameters and physiochemical properties of forward

- osmosis membranes after treatment of produced water. *Journal of Membrane Science*, 499, 491-502.
- Coday, B. D., Xu, P., Beaudry, E. G., Herron, J., Lampi, K., Hancock, N. T., & Cath, T. Y. (2014). The sweet spot of forward osmosis: Treatment of produced water, drilling wastewater, and other complex and difficult liquid streams. *Desalination*, 333(1), 23-35. doi: 10.1016/j.desal.2013.11.014
- Coday, B. D., Yaffe, B. G. M., Xu, P., & Cath, T. Y. (2014). Rejection of Trace Organic Compounds by Forward Osmosis Membranes: A Literature Review. *Environmental Science & Technology*, 48(7), 3612-3624. doi: 10.1021/es4038676
- Cui, Y., Liu, X. Y., Chung, T. S., Weber, M., Staudt, C., & Maletzko, C. (2016). Removal of organic micro-pollutants (phenol, aniline and nitrobenzene) via forward osmosis (FO) process: Evaluation of FO as an alternative method to reverse osmosis (RO). *Water Research*, 91, 104-114. doi: 10.1016/j.watres.2016.01.001
- Deriszadeh, A., Harding, T. G., & Husein, M. M. (2009). Improved MEUF removal of naphthenic acids from produced water. *Journal of Membrane Science*, 326(1), 161-167.
- Duong, P. H. H., & Chung, T. S. (2014). Application of thin film composite membranes with forward osmosis technology for the separation of emulsified oil-water. *Journal of Membrane Science*, 452, 117-126. doi: 10.1016/j.memsci.2013.10.030
- Fang, Y. Y., Bian, L. X., Bi, Q. Y., Li, Q., & Wang, X. L. (2014). Evaluation of the pore size distribution of a forward osmosis membrane in three different ways. *Journal of Membrane Science*, 454, 390-397. doi: DOI 10.1016/j.memsci.2013.12.046



- Frank, R. A., Kavanagh, R., Burnison, B. K., Arsenault, G., Headley, J. V., Peru, K. M., . . . Solomon, K. R. (2008). Toxicity assessment of collected fractions from an extracted naphthenic acid mixture. *Chemosphere*, 72(9), 1309-1314.
- Hao, C. Y., Headley, J. V., Peru, K. A., Frank, R., Yang, P., & Solomon, K. R. (2005). Characterization and pattern recognition of oil-sand naphthenic acids using comprehensive two-dimensional gas chromatography/time-of-flight mass spectrometry. *Journal of Chromatography A*, 1067(1-2), 277-284. doi: 10.1016/j.chroma.2005.01.041
- Headley, J. V., Peru, K. M., McMartin, D. W., & Winkler, M. (2002). Determination of dissolved naphthenic acids in natural waters by using negative-ion electrospray mass spectrometry. *Journal of Aoac International*, 85(1), 182-187.
- Hickenbottom, K. L., Hancock, N. T., Hutchings, N. R., Appleton, E. W., Beaudry, E. G., Xu, P., & Cath, T. Y. (2013). Forward osmosis treatment of drilling mud and fracturing wastewater from oil and gas operations. *Desalination*, 312, 60-66. doi: 10.1016/j.desal.2012.05.037
- Jin, X., Shan, J. H., Wang, C., Wei, J., & Tang, C. Y. Y. (2012). Rejection of pharmaceuticals by forward osmosis membranes. *Journal of Hazardous Materials*, 227, 55-61. doi: 10.1016/j.jhazmat.2012.04.077
- Kannel, P. R., & Gan, T. Y. (2012). Naphthenic acids degradation and toxicity mitigation in tailings wastewater systems and aquatic environments: A review. *Journal of Environmental Science and Health Part a-Toxic/Hazardous Substances & Environmental Engineering*, 47(1), 1-21. doi: 10.1080/10934529.2012.629574

- Kim, C., Lee, S., & Hong, S. (2012). Application of osmotic backwashing in forward osmosis: mechanisms and factors involved. *Desalination and Water Treatment*, 43(1-3), 314-322. doi: 10.1080/19443994.2012.672215
- Lee, S., Boo, C., Elimelech, M., & Hong, S. (2010). Comparison of fouling behavior in forward osmosis (FO) and reverse osmosis (RO). *Journal of Membrane Science*, 365(1-2), 34-39. doi: 10.1016/j.memsci.2010.08.036
- Linares, R. V., Yangali-Quintanilla, V., Li, Z. Y., & Amy, G. (2011). Rejection of micropollutants by clean and fouled forward osmosis membrane. *Water Research*, 45(20), 6737-6744. doi: 10.1016/j.watres.2011.10.037
- McGovern, R. K., Mizerak, J. P., Zubair, S. M., & Lienhard, J. H. (2014). Three dimensionless parameters influencing the optimal membrane orientation for forward osmosis. *Journal of Membrane Science*, 458, 104-110. doi: 10.1016/j.memsci.2014.01.061
- Mikula, R. J., Kasperski, K. L., Burns, R. D., & MacKinnon, M. D. (1996). Nature and fate of oil sands fine tailings. *Suspensions: Fundamentals and Applications in the Petroleum Industry*, 251, 677-723.
- Minier-Matar, J., Hussain, A., Janson, A., Wang, R., Fane, A. G., & Adham, S. (2015). Application of forward osmosis for reducing volume of produced/Process water from oil and gas operations. *Desalination*, 376, 1-8.
- Mohamed, M. H., Wilson, L. D., Peru, K. M., & Headley, J. V. (2013). Colloidal properties of single component naphthenic acids and complex naphthenic acid mixtures. *Journal of Colloid and Interface Science*, 395, 104-110. doi: 10.1016/j.jcis.2012.12.056
- Moustafa, A. M. A., Kim, E. S., Alpatova, A., Sun, N., Smith, S., Kang, S., & El-Din, M. G. (2014). Impact of polymeric membrane filtration of oil sands process water on organic

- compounds quantification. *Water Science and Technology*, 70(5), 771-779. doi: 10.2166/wst.2014.282
- Phillip, W. A., Yong, J. S., & Elimelech, M. (2010). Reverse Draw Solute Permeation in Forward Osmosis: Modeling and Experiments. *Environmental Science & Technology*, 44(13), 5170-5176. doi: 10.1021/es100901n
- She, Q. H., Jin, X., Li, Q. H., & Tang, C. Y. Y. (2012). Relating reverse and forward solute diffusion to membrane fouling in osmotically driven membrane processes. *Water Research*, 46(7), 2478-2486. doi: DOI 10.1016/j.watres.2012.02.024
- Wang, Y. N., Wicaksana, F., Tang, C. Y., & Fane, A. G. (2010). Direct Microscopic Observation of Forward Osmosis Membrane Fouling. *Environmental Science & Technology*, 44(18), 7102-7109. doi: 10.1021/es101966m
- Xie, M., Nghiem, L. D., Price, W. E., & Elimelech, M. (2012). Comparison of the removal of hydrophobic trace organic contaminants by forward osmosis and reverse osmosis. *Water Research*, 46(8), 2683-2692. doi: 10.1016/j.watres.2012.02.023
- Xie, M., Nghiem, L. D., Price, W. E., & Elimelech, M. (2013). Impact of humic acid fouling on membrane performance and transport of pharmaceutically active compounds in forward osmosis. *Water Research*, 47(13), 4567-4575. doi: 10.1016/j.watres.2013.05.013
- Xie, M., Price, W. E., Nghiem, L. D., & Elimelech, M. (2013). Effects of feed and draw solution temperature and transmembrane temperature difference on the rejection of trace organic contaminants by forward osmosis. *Journal of Membrane Science*, 438, 57-64. doi: 10.1016/j.memsci.2013.03.031
- Xue, J., Zhang, Y., Liu, Y., & Gamal El-Din, M. (2016). Treatment of raw and ozonated oil sands process-affected water under decoupled denitrifying anoxic and nitrifying aerobic

conditions: a comparative study. *Biodegradation*, 27(4-6), 247-264. doi: 10.1007/s10532-016-9770-9

Yong, J. S., Phillip, W. A., & Elimelech, M. (2012). Coupled reverse draw solute permeation and water flux in forward osmosis with neutral draw solutes. *Journal of Membrane Science*, 392, 9-17. doi: 10.1016/j.memsci.2011.11.020

Zhang, S., Wang, P., Fu, X. Z., & Chung, T. S. (2014). Sustainable water recovery from oily wastewater via forward osmosis-membrane distillation (FO-MD). *Water Research*, 52, 112-121. doi: 10.1016/j.watres.2013.12.044

Zhao, S. A. F., & Zou, L. D. (2011). Relating solution physicochemical properties to internal concentration polarization in forward osmosis. *Journal of Membrane Science*, 379(1-2), 459-467. doi: 10.1016/j.memsci.2011.06.021

Zheng, Y., Huang, M. H., Chen, L., Zheng, W., Xie, P. K., & Xu, Q. (2015). Comparison of tetracycline rejection in reclaimed water by three kinds of forward osmosis membranes. *Desalination*, 359, 113-122. doi: 10.1016/j.desal.2014.12.009

## **4 Chapter 4 Forward osmosis desalination of oil sands produced water: comparison between cellulose triacetate-based and aquaporin-based membranes<sup>3</sup>**

### **4.1 Introduction**

The oil sands industry in northern Alberta, Canada uses large amounts of water to separate the bitumen from the oil sands, generating oil sands process-affected water (OSPW) (E. S. Kim, Liu, & El-Din, 2012). Similar to the produced water in unconventional oil and gas, OSPW contains both organic and inorganic species: organic species are made up of naphthenic acids (NAs), polycyclic aromatic hydrocarbons (PAHs), benzene, toluene, ethylbenzene, xylene (BTEX) and phenols, while the inorganic species contain dissolved salts, heavy metals, carbonates and suspended solids (clay, silts, etc.) (Allen, 2008a). Because of the complicate organic and inorganic compounds in OSPW, it is stored in tailing ponds and cannot be directly discharged into the environment. Other brackish water stream — basal depressurization water (BDW) is also produced in the oil sands mining process to control surface runoff and seepage water accumulation (E. S. Kim et al., 2013). Compared to OSPW, BDW contains more inorganic ions and less organic compounds. Although it was reported that 80 to 85% of OSPW can be recycled and reused in the extraction process, the large volumes of stored OSPW and onsite BDW remain an environmental concern (Allen, 2008a). Till now, to manage the oil sands produced water, physical, chemical and biological methods such as advanced oxidation, membrane technology,

---

<sup>3</sup> This chapter has been submitted to: Shu Zhu, Mingyu Li and Mohamed Gamal El-Din, 2017. Forward osmosis desalination of oil sands produced water: comparison between cellulose triacetate-based and aquaporin-based membranes. Submitted to: *Science of the Total Environment*

and adsorption were all investigated to alleviate its environmental impact (Allen, 2008b; Alpatova et al., 2014; Y. J. Shi, Huang, Rocha, El-Din, & Liu, 2015; J. K. Xue, Zhang, Liu, & El-Din, 2016).

Recently, an osmotic driven membrane process — forward osmosis (FO) springs up as a promising treatment of oil and gas produced waters. The driving force of FO is the chemical potential difference between the high concentrated draw solution and the less concentrated feed solution (Cath et al., 2006). Therefore, compared to pressure-driven process, FO shows less fouling propensity. To date, its applications on wastewater treatment and brackish water desalination were investigated in several studies (Linares et al., 2014; Lutchmiah et al., 2014). Also, FO is reported as a potential reclamation method for oil and gas wastewater as well as for OSPW (Coday, Xu, et al., 2014; Nasr & Sewilam, 2015). However, current studies were limited to cellulose triacetate (CTA) and thin film composite (TFC) membrane manufactured by Hydration Technology Innovations (HTI). Jiang et al. (Jiang et al., 2016) investigated the OSPW desalination applying CTA membrane in FO process and using 2M  $\text{NH}_4\text{HCO}_3$ , 4M  $\text{NH}_4\text{HCO}_3$ , and 4M urea as draw solutions and OSPW as the feed solution. The authors found that by employing 4M  $\text{NH}_4\text{HCO}_3$  as the draw solution, 85% water recovery rate and 80 to 100% metals and ions rejection were achieved. Hickenbottom et al. (Hickenbottom et al., 2013) studied the treatment of drilling mud and fracturing wastewater from oil and gas industry using FO by CTA membrane. The results demonstrated that 80% of the volume of drilling wastewater was recovered and high inorganic and organic rejection was observed as well. Moreover, Coday et al. (Coday et al., 2016) studied the effect of FO membrane types (CTA and polyamide-based TFC membranes) and operating conditions on oil and gas wastewater. The results indicated that compared to the clear effect of initial water flux and crossflow velocity, membrane types had

little impact on membrane fouling. The difference between CTA and TFC membranes was spotted on chemical cleaning applying two foulants (EDTA and KL7330). TFC membranes exhibited water recoveries above 90%, while CTA membrane only recovered around 75%. Moreover, CTA and TFC membranes performed distinctively on pharmaceutical rejection (Jin et al., 2012). Compared to CHA membranes, TFC showed steadier rejections (>95%) and permeate fluxes when treating carbamazepine, diclofenac, ibuprofen and naproxen at various pH values. In addition to CTA and TFC membranes, Porifera Inc. and Aquaporin A/S are newly manufactured commercial available FO membranes. The comparison between CTA, TFC and two Porifera membranes have been done by Blandin et al. (Blandin et al., 2016) on aspects of membrane fouling and cleaning. The researchers reported that although two Porifera membranes showed higher water permeability than CTA and TFC; however, they suffered more severe fouling. Nowadays, as a new membrane material, aquaporin (AQPs) is gaining increasing research interests. AQPs is a type of water channel protein obtained from living organism (Shen, Saboe, Sines, Erbakan, & Kumar, 2014). Due to the incorporation of AQPs, this type of membranes could deliver high water permeability and solute rejection efficiency (W. Y. Xie et al., 2013). However, the investigations of AQP membrane are mainly focusing on membrane fabrication rather than its implication on water or wastewater treatment. As summarised in Qi et al.'s study (Qi et al., 2016), three types of biomimetic AQP membranes had already been synthesized so far including: (1) bilayer membrane with incorporated AQP; (2) polymer layer membrane with immobilized AQP; and (3) thin film composite AQP membrane fabricated by interfacial polymerization. The authors also mentioned that although AQP membrane showed several advantages on water flux and rejection, its weak mechanical strength may cast a shadow over its practical application. Li et al. (Li et al., 2015) fabricated hollow fiber composite RO membrane

with AQP and the authors reported that AQP-based membrane improved both water flux and salt rejection. Meanwhile, the fabricated AQP membrane exhibited a stable “anti-fouling” property using strong organic foulants. Unfortunately, the performance of AQP membrane in FO process regarding membrane fouling, salt diffusion, and organic rejection, among other parameters, is yet to be investigated on wastewater treatment, especially in the area of oil and gas produced water.

The main objective of current investigation was to compare the performance of two FO membranes (CTA and aquaporin <sup>inside</sup>) on the treatment of oil sands produced water (i.e. OSPW and BDW). To accomplish this goal, membrane fouling, organic and inorganic rejections were evaluated, as well as the adsorption of NA model compounds. The specific objectives of current study are as follow: 1) to examine the membrane properties of CTA and AQP-FO membrane; 2) to investigate the organic removal and adsorption on these two membranes using NA model compounds; and 3) to evaluate the membrane performance on OSPW and BDW treatment in terms of water flux, membrane fouling, and organic and inorganic rejections.

## **4.2 Materials and methods**

### **4.2.1 NA model compounds**

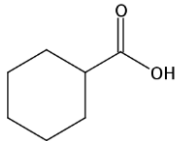
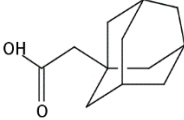
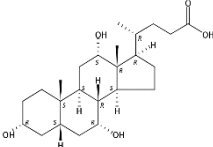
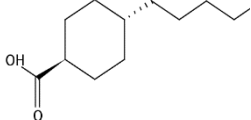
Four NA model compounds were investigated, including: cyclohexane carboxylic acid (CHA), 1-adamantaneacetic acid (AAA), cholic acid (CA), and trans-4-Pentylcyclohexanecarboxylic acid (TPCA). High purity NA model compounds were purchased from Sigma–Aldrich (Oakville, ON, Canada). The organic feed solutions were prepared by directly dissolving 50 mg model compound into 1 L 0.1 M carbonate bicarbonate buffer solutions. 1M HCl or NaOH solution was used to adjust the solution to pH = 9. Detailed characteristics of the model compounds are presented in Table 4-1.



#### 4.2.2 Oil sands produce water

Two types of oil sands produce waters (OSPW and BDW) were collected from Fort McMurray, Alberta, Canada. The process waters were stored under 4°C and warmed up to room temperature (20°C) before experimental use. To better understand the impact of particulates on membrane fouling, water samples filtered through 0.45-µm membrane were also prepared. The characteristics of OSPW and BDW are shown in Table 4-2. Sodium chloride (NaCl ≥ 99%) purchased from Fisher Scientific (ON, Canada) was used to prepare the draw solution.

**Table 4-1** Characteristics of NA model compounds at pH = 9

| Model compound          | cyclohexanecarboxylic acid (CHA)  | 1-adamantaneacetic acid (AAA)   | cholic acid (CA)   | trans-4-pentylcyclohexanecarboxylic acid (TPCA)                                       |
|-------------------------|---|---|--|---|
| Molecular weight, g/mol | 128.17  | 180.24  | 408.57   | 198.3   |
| Log D                   | -1.94   | -1.01   | -0.75  | 0.65  |
| pKa                     | 4.91±0.10   | 4.86±0.20   | 4.76±0.10  | 4.94±0.10   |
| Solubility, g/L         | 1000  | 354   | 110  | 666   |
| Chemical structure      |  |  |  |  |

**Data source:** SciFinder Scholar calculated using Advanced Chemistry

#### 4.2.3 Membrane properties and FO operating system

Two commercial FO membranes (CTA-FO, AQP-FO) made by cellulose triacetate and aquaporin were provided by Hydration Technologies, Inc. (Albany, OR) and Aquaporin A/S (Kongens Lyngby, Denmark), respectively. Before the rejection, adsorption, and fouling tests,

all the membranes were soaked in clean deionized water for 24 hours. Membrane properties provided by manufacturers are presented in Table 4-3.

The test FO system was a bench-scale crossflow system similar to that used in our previous study (Zhu, Li, & Gamal El-Din, 2017). The FO membrane was placed in a SEPA FO membrane cell provided by Sterlitech Corporation (Kent, WA, USA) with the feed solution facing the active layer. The effective membrane surface was 140 cm<sup>2</sup>. No mesh spacer nor permeate carrier was employed for the current study. Draw and feed solutions were recirculated counter-current by two speed-variable peristaltic pumps (Cole-Palmer, Vernon Hills, IL, USA). A digital balance (Scout Pro, Ohaus Corp., Parsippany, NJ, USA) was used for monitoring the weight change of the draw solution to obtain permeate water flux.

**Table 4-2** Characteristics of OSPW and BDW

| <b>Parameters</b>                             | <b>OSPW</b>  | <b>OSPW<br/>(0.45 µm<br/>filtered)</b> | <b>BDW<br/>(0.45 µm filtered)</b> |
|---|--------------|--|-----------------------------------|
| <b>pH value</b>                               | 8.5          | 8.5                                    | 9.1                               |
| <b>Turbidity, NTU</b>                         | 6.1±0.1      | 2.6±0.0                                | 0.7±0.1                           |
| <b>Conductivity, mS/cm</b>                    | 2.5±0.00     | 2.4±0.02                               | 19.0±0.01                         |
| <b>Total dissolved solids (TDS),<br/>mg/L</b> | 1490±7.09    | 1432±0.0                               | 11540±12                          |
| <b>Total organic carbon (TOC),<br/>mg/L</b>   | 54.88±4.19   | 44.68±2.97                             | 11.30±0.30                        |
| <b>NAs, mg/L</b>                              | 25.04        |  | 3.00                              |
| <b>Lithium, mg/L</b>                          | 0.24±0.00    |  | 1.62±0.03                         |
| <b>Sodium, mg/L</b>                           | 557.88±23.97 |  | 4299.18±56.71                     |
| <b>Potassium, mg/L</b>                        | 26.81±1.19   |  | 45.36±0.86                        |
| <b>Magnesium, mg/L</b>                        | 25.24±1.05   |  | 141.19±2.38                       |
| <b>Calcium, mg/L</b>                          | 38.38±1.64   |  | 6.99±0.23                         |
| <b>Fluoride, mg/L</b>                         | 1.69±0.05    |  | N.A.                              |
| <b>Chloride, mg/L</b>                         | 387.67±2.31  |  | 7072.7±65.00                      |
| <b>Nitrate, mg/L</b>                          | 5.96±0.24    |  | 30.01±0.72                        |
| <b>Sulfate, mg/L</b>                          | 146.17±1.04  |  | N.A.                              |

**Table 4-3** Membrane properties

| Membrane type | Polymer                    | Rejection (%)     | pH range |
|---------------|----------------------------|-------------------|----------|
| CTA-FO        | Cellulose triacetate (CTA) | >95% <sup>a</sup> | 3-8      |
| AQP-FO        | Polyethersulfone (PES)     | 99.4 <sup>b</sup> | 2-11     |

**Notes:**

a. the rejection of arsenic

b. the rejection of sodium chloride

**4.2.4 Determination of membrane characteristics**

The water permeability (A) and solute permeability (B) were measured using a dead-end nanofiltration (NF) system with an effective membrane area of 21.23 cm<sup>2</sup>. DI water was applied as the feed solutions under pressures of 5.4 bar and 2.9 bar for CTA-FO and AQP-FO membrane, respectively. Water flux was calculated using:

$$J_w = \frac{V_p}{A_m t} \quad (1)$$

Where  $J_w$  is the permeate flux,  $V_p$  is the permeate volume,  $A_m$  is the effective area of membrane surface, and  $t$  is the operating time.

The salt rejection (R) was determined by the salt concentrations in feed solution ( $C_f$ ) and permeate ( $C_p$ ) ( $R = 1 - \frac{C_p}{C_f}$ ). R was measure by using 2000 mg/L NaCl as feed solution in the

NF system. A and B were obtained from the following equations:

$$A = \frac{J_w}{\Delta P} \quad (2)$$

$$B = \left(\frac{1-R}{R}\right) \times A \times (\Delta P - \Delta\pi) \quad (3)$$

Where  $\Delta\pi$  and  $\Delta P$  were osmotic pressure difference and the transmembrane pressure, respectively.

Structural parameter (S) was calculated from:

$$S = \frac{D}{J_w} \ln \frac{B+A\pi_{draw}}{B+J_w} \quad (4)$$

Where D is the salt diffusion coefficient,  $\pi_{draw}$  is the osmotic pressure in the draw solution. A, B values were previously determined by the NF experiment.

In FO performance evaluation, NaCl with a concentration ranging from 0.2 to 3 M was used as the draw solution facing the support side and DI water was used as the feed facing the active layer to calculate the specific reverse flux of draw solutes. Water flux and NaCl rejection were measured using 1M NaCl as the draw solution and DI water as the feed solution. As recommended by the membrane manufacturer, the crossflow velocity for AQP-FO membrane should keep as low as possible. Therefore, the applied crossflow velocities were 14 cm/s and 2.3 cm/s for CTA-FO and AQP-FO, respectively.

#### **4.2.5 NA model compound adsorption and rejection experiment protocol**

The NA model compound aqueous stock solutions were prepared by dissolving 50 mg of the model compound into 1 L 0.05 M carbonate bicarbonate buffer solutions and 1M HCl/NaOH were used to adjust the pH level of the stock solutions to 9. The CTA and AQP membranes were cut into 2 cm × 2 cm section and placed into 50 mL glass volumetric flask with glass caps. The flasks with the membrane and 20 mL stock solution were placed on a stirrer with a speed of 200 rpm. The control experiments were also carried out to ensure the results were not affected by other factors. The adsorption experiment lasted for 7 hrs and 0.2 mL of samples were taken every hour for liquid chromatography/mass spectrometry (LC-MS) analysis. The experiments were conducted in three times for each NA model compound.

The NA model compound rejection experiments were conducted continuously for 7 hr with a constant crossflow velocity of 2.3 cm/s. Each experiment was carried out using a new membrane. The experiments started with 1 L of feed solution and 1 L of 1 M NaCl solution. Approximate 1 mL water samples from both feed and draw solutions were taken every hour for LC/MS and ion chromatography (IC) analysis.

The rejection efficiency was calculated by considering dilution factor (DF):

The dilution factor (DF) can be obtained using (M. Xie, W. E. Price, et al., 2013; Zheng et al., 2015)

$$DF = \frac{V_{d,t}}{V_{p,t}} \quad (4)$$

Where  $V_{d,t}$  and  $V_{p,t}$  are the volumes of draw solution and permeate at time = t.

$$R (\%) = \left( 1 - \frac{DF \times C_{d,t}}{C_{f,0}} \right) \times 100\% \quad (5)$$

Where DF is the dilution factor determined from Eq. (2),  $C_{d,t}$  is the concentration of organic compound in the draw solution at time = t and  $C_{f,0}$  is the concentration of organic compound in the feed solution at t = 0.

#### 4.2.6 OSPW/BDW fouling experiment

Baseline experiments were conducted primarily to track the flux decline due to draw solution dilution. 0.01 M and 0.23 M NaCl were used as the feed solution to mimic the osmotic pressure of OSPW and BDW, respectively. The baseline tests were performed for each membrane applying active layer facing the feed solution and the crossflow velocity was maintained in 2.3 cm/s. The results of baseline experiments were plotted along with the results of the fouling test. Although the two tested membranes had asymmetric structure, only the active layer facing the feed solution was evaluated.

A 7-hour fouling experiment using OSPW, 0.45  $\mu\text{m}$  filtered OSPW, and 0.45  $\mu\text{m}$  BDW as the feed and BDW as the draw solution was conducted at fixed crossflow velocity of 2.3 cm/s after the baseline experiment. The weight changes of draw solution were taken every 30 s and water samples were collected after the experiment for further analyses.

#### **4.2.7 Analytical methods**

##### **4.2.7.1 Membrane characterization**

Scanning electron microscopy (SEM) (Tescan, Brno, Czech Republic) was used to observe the membrane surface morphology. The contact angle was measured by FTA-200 instrument (FOLIO Instrument Inc., Kitchener, ON, USA) using DI water. X-ray photoelectron spectroscopy (XPS) was used to obtain the chemical composition of membrane surface. Attenuated total reflectance (ATR)-Fourier Transform Infrared (FT-IR) Spectroscopy (Nicolet 8700, FT-IR with ATR, Thermo Electron Corp., West Palm Beach, FL, USA) was used to elucidate the surface functional groups of the membranes. The surface roughness of membrane was measured by atomic force microscopy (Asylum MFP-3D AFM, Asylum Research, CA, USA).

##### **4.2.7.2 Water chemistry analysis**

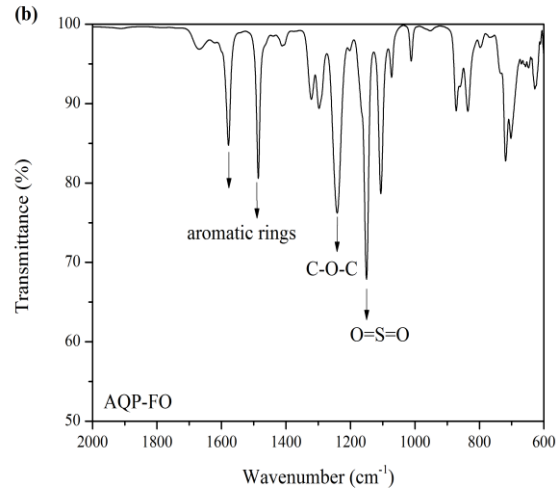
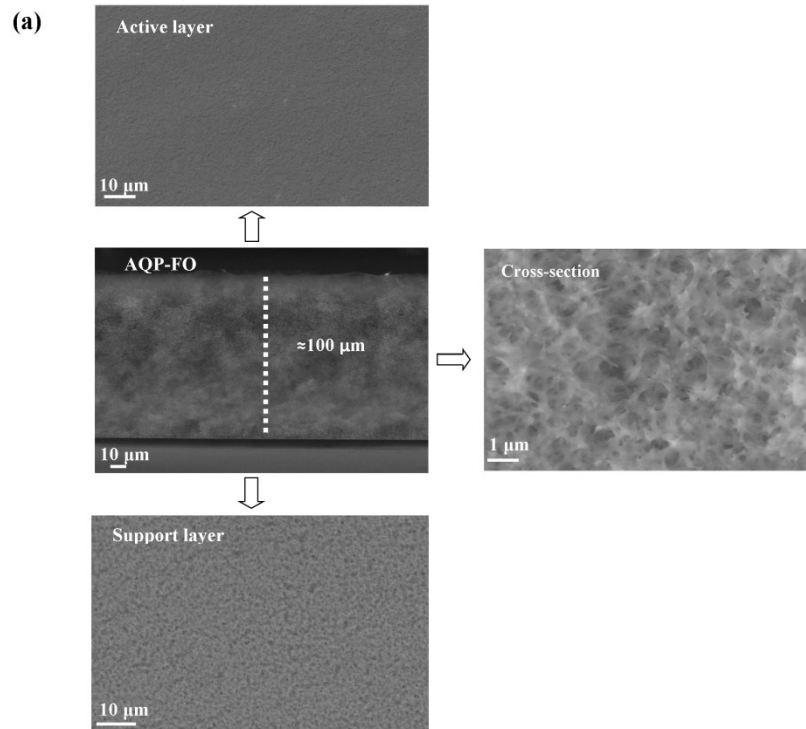
The conductivity and pH value were measured with a pH /conductivity meter (Fisher Scientific, Ottawa, ON, Canada). The concentrations of NA model compound were determined by a LC/MS (500-MS LC Ion Trap. Varian, Inc., CA, USA). NA concentrations in oil sands produced waters were measured by an ultra-performance liquid chromatography time-of-flight mass spectrometry (UPLC-TOFMS) (Waters Corp., Milford, MA, USA) based on the method described elsewhere (Alpatova et al., 2014; Moustafa et al., 2014). The analysis of cation and anion concentrations was conducted by ion chromatography (ICS-2000 and 2500, Dionex, Sunnyvale, CA, USA). The

concentrations of trace elements were quantified by inductively coupled plasma mass spectrometry (ICP-MS, Elan 6000 ICP mass spectrometer, PerkinElmer, Waltham, MA, USA). The total organic carbon (TOC) concentration was determined by Apollo 9000 TOC combustion analyzer (FOLIO Instrument Inc., Kitchener, ON, Canada). The turbidity was measured using Orbeco-Hellige 965 Digital Nephelometric Turbidimeter (Orbeco Analytical System Inc., Sarasota, FL, USA). Each analysis was conducted in triplicate and presented with the standard deviation.

## **4.3 Results and discussion**

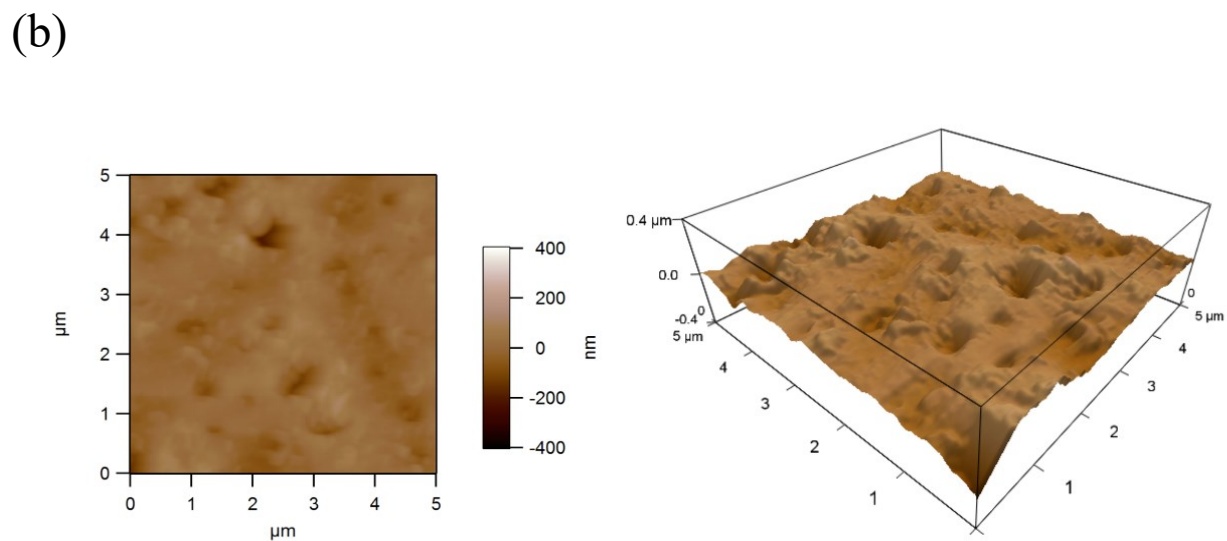
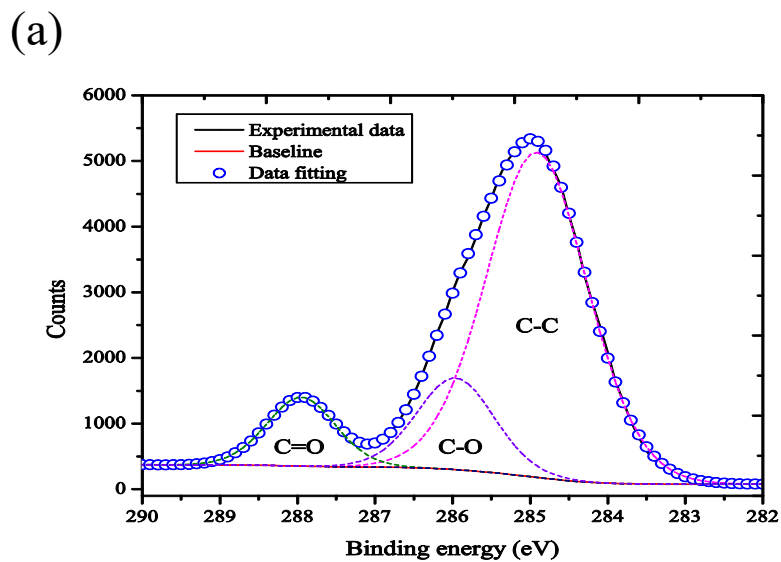
### **4.3.1 Membrane characterization**

Fig. 4-1 shows the morphology of the AQP-FO membrane along with the ATR-FTIR image of the active layer. The corresponding information of CTA-FO membrane can be found elsewhere (Mazlan et al., 2016). Unlike CTA-FO membrane, the AQP-FO membrane has a thin-film structure without mesh support. The AQP-FO membrane still has an asymmetric structure in which the active layer is smoother than its support layer. The total thickness of AQP-FO is approximately 100  $\mu\text{m}$  which is comparable to that of the CTA-FO membrane (Wei, Qiu, Tang, Wang, & Fane, 2011). In ATR-FTIR spectra (Fig. 4-1 (b)), two aromatic-ring adsorption bands were shown at frequencies of 1470  $\text{cm}^{-1}$  and 1575  $\text{cm}^{-1}$ , the adsorption at 1160  $\text{cm}^{-1}$  was attributed to O=S=O stretch vibration and the peak at 1250  $\text{cm}^{-1}$  was associated to C-O-C stretch vibration. These peaks were found as evidences of PES substrate (Arkhangelsky, Kuzmenko, & Gitis, 2007) for the AQP-FO membrane. On the active layer of CTA-FO membrane, -C=O, -C-C-O- and -C-O as typical functional groups of CTA were all observed (Parida & Ng, 2013). XPS and surface roughness analysis of AQP-FO membrane can be found in Fig. 4-2.



**Figure 4-1** (a) SEM images of AQP-FO membrane and (b) ATR-FTIR image of AQP-FO membrane active layer.





**Figure 4-2** (a) XPS results and (b) AFM images of AQP-FO membrane surface. The roughness of AQP-FO membrane was  $36.30 \pm 0.34$  nm.

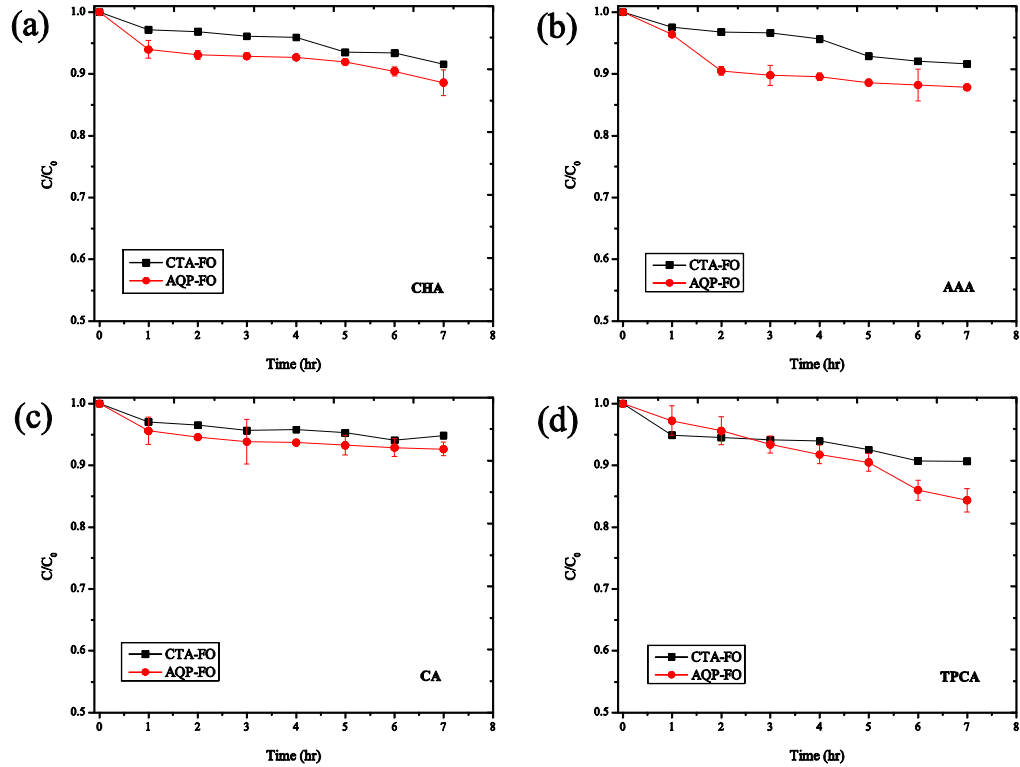


**Figure 4-3** Comparison of CTA-FO and AQP-FO membranes on NA model compounds adsorption (a) CHA, (b) AAA, (c) CA, and (d) TPCA. Experimental conditions: the initial concentration of each compound was 50 mg/L. Effective area was 4 cm<sup>2</sup> and the adsorption experiment lasted for 7 hours.

### 4.3.2 Membrane performance

The membrane performance of both FO and NF are summarized in Table 4-4. The water flux, specific reverse solute diffusion, and NaCl rejection were tested in FO system. As recommended by the AQP-FO membrane manufacturer, the crossflow velocity for AQP membrane was maintained at 2.3 cm/s, meanwhile the crossflow velocity for CTA-FO membrane was kept around 14 cm/s to reduce the impact of external concentration polarization (ECP). Although the crossflow velocity of the CTA-FO membrane was much higher than that of AQP-FO membrane, the water flux generated by the CTA membrane did not significant win over AQP membrane.

The two FO membranes showed similar specific reverse solute flux and NaCl rejection. The calculated water permeability of AQP-FO membrane was 4.92 L/m<sup>2</sup> hr per bar, which is 8 times higher than the permeability of CTA membrane. Compared to the solute permeability (B) obtained from crossflow test cell, operating under dead-end cell might overestimate the solute permeability because of the impact of concentration polarization on the feed side (Boo et al., 2013). Although the AQP-FO membrane displayed high water permeability, it also accompanied with high solute permeability. Hence, combined with A and B, the structure parameter S value of AQP-FO membrane (1221±204 μm) was slightly above of that of the CTA membrane (874±64 μm).

**Table 4-4** FO and NF performances of CTA and AQP membranes

| Membrane | Water flux <sup>a</sup><br>(L m <sup>-2</sup> hr <sup>-1</sup> ) | Specific<br>reverse solute<br>flux <sup>a</sup> (mol/L) | NaCl<br>rejection <sup>a</sup><br>(%) | Water<br>permeability <sup>b</sup><br>(A, L m <sup>-2</sup> hr <sup>-1</sup><br>bar <sup>-1</sup> ) | Solute<br>permeability <sup>b</sup><br>(B, L m <sup>-2</sup> hr <sup>-1</sup> ) | Structure<br>parameter <sup>b</sup><br>(S, μm) |
|----------|--|---|---------------------------------------|---|---|--|
| CTA-FO   | 7.71±0.75  | 0.06±0.01   | 99.2                                  | 0.65±0.05   | 0.63±0.07   | 874±64   |
| AQP-FO   | 6.07±0.57  | 0.051±0.01  | 99.0                                  | 4.92±0.37   | 1.58±0.11   | 1221±204                                       |

Notes:

- a. FO performance.
- b. NF performance.

### 4.3.3 NA model compounds adsorption and rejection experiment

The results of NA model compounds adsorption experiment at pH = 9 are shown in Fig. 4-4 as concentration (C) divided by initial concentration (C<sub>0</sub>). In 7-hour experiment, less than 15% of model compounds were adsorbed regardless of the types of model compounds and tested FO

membrane. The low adsorption can be explained by the electrostatic-force between model compounds and the membrane. Because at pH = 9, CTA-FO and AQP-FO membrane were negatively charged (Mazlan et al., 2016) and the pKa values (< 5) of these model compounds indicated that de-protonation occurred. Although the contact angle of AQP-FO ( $46.1\pm 2.6^\circ$ ) and CTA-FO ( $65.9\pm 0.8^\circ$ ) membrane indicated that AQP-FO was less hydrophobic than the CTA-FO membrane, the impact of hydrophobic-hydrophobic interaction did not significantly affect the adsorption for CTA membrane. At pH = 9, the log D values of model compounds ranked as  $CHA > AAA > CA > TPCA$ , demonstrating that CHA was the most hydrophilic model compound and TPCA was the most hydrophobic one. Theoretically, more TPCA should be adsorbed rather than CHA if their adsorption onto the membranes was driven by hydrophobic-hydrophobic interaction and CTA-FO membrane should adsorb more TPCA than AQP-FO membrane. However, after the adsorption experiment, 12% of CHA was adsorbed into AQP membrane and correspondingly, 10% of CHA was adsorbed into CTA membrane. In addition, for TPCA, the most hydrophobic compound, the CTA membrane did not show a relatively high adsorption capability (10%) compared to AQP membrane (16%). All NA model compounds carry one negative charge at pH 9 and two FO membranes with PES and CTA as substrates, respectively, have the similar negative zeta potential range (Huang et al., 2015; Nguyen, Yun, Kim, & Kwon, 2013) at current pH value. Therefore, it was concluded that at current pH, the charge repulsive force was governing the adsorption phenomenon of CTA- and AQP-FO membrane rather than the hydrophobic interaction between the compound and membrane surface and neither CTA- nor AQP-based membrane exhibited high adsorption capacity.

The comparison between CTA and AQP membrane at pH = 9 on NA model compound rejection efficiency is shown in Fig. 4-4. The rejection experiment was conducted in FO system with a

crossflow of 2.3 cm/s. Firstly, the rejection efficiency for the two FO membranes was above 90% for all the NA model compounds. The high rejection was mainly because of electro-repulsive force, which was consistently with the results found in adsorption test. It was also observed that the model compound rejection of the AQP-FO membrane was slightly below that of CTA membrane and the rejection efficiency was more intended to be affected by time. This result was consistent with the slightly higher adsorption on AQP-FO membrane. AQP-FO membrane demonstrated higher water permeability (A) than CTA-FO, which was also in good agreement with the higher permeate water flux obtained in the current experiment (Fig. 4-5). As reported by Zhang et al. (S. Zhang et al., 2014) and Geise et al. (Geise, Paul, & Freeman, 2014), permeate flux can promote the transport of organic solutes. Even though it was concluded previously that electrostatic force played a dominant role in the model compound rejection, the promoted NA model compound diffusion might also positively affect the adsorption process on the AQP membrane, thereby decreasing the rejection efficiency. Additionally, the molecular size of CHA and AAA were comparative small, which might also benefit their forward diffusion from the feed solution to the draw solution, resulting in a lower rejection.

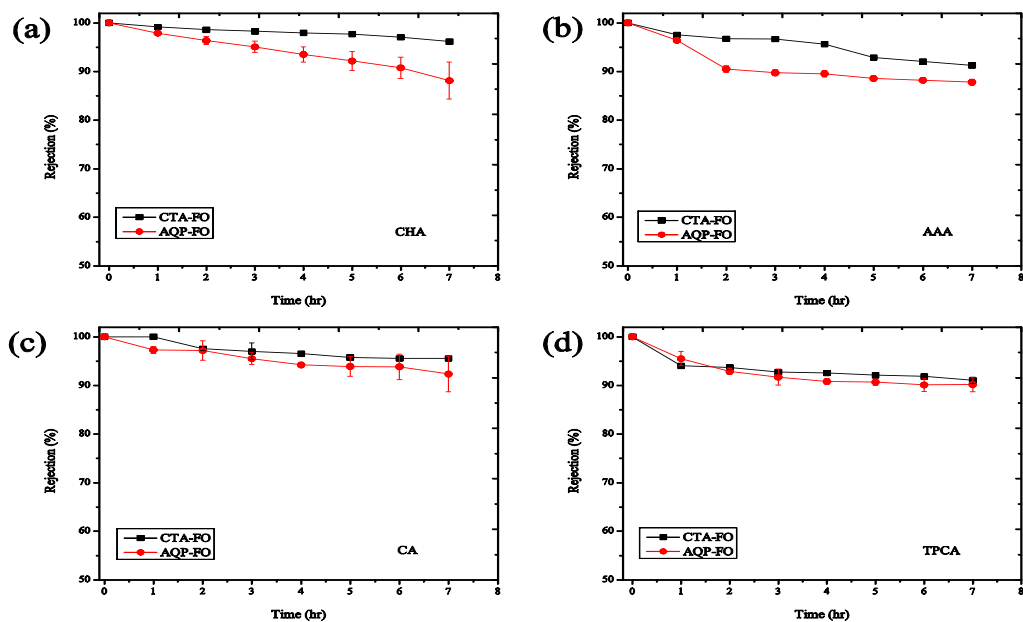


**Figure 4-4** Comparison between CTA-FO and AQP-FO membranes on NA model compounds rejection efficiency (a) CHA, (b) AAA, (c) CA, and (d) TPCA. Experimental condition: Initial concentration of each model compound was 50 mg/L. Cross-flow velocity = 2.3 cm/s, the experiment lasted for 7 hours.

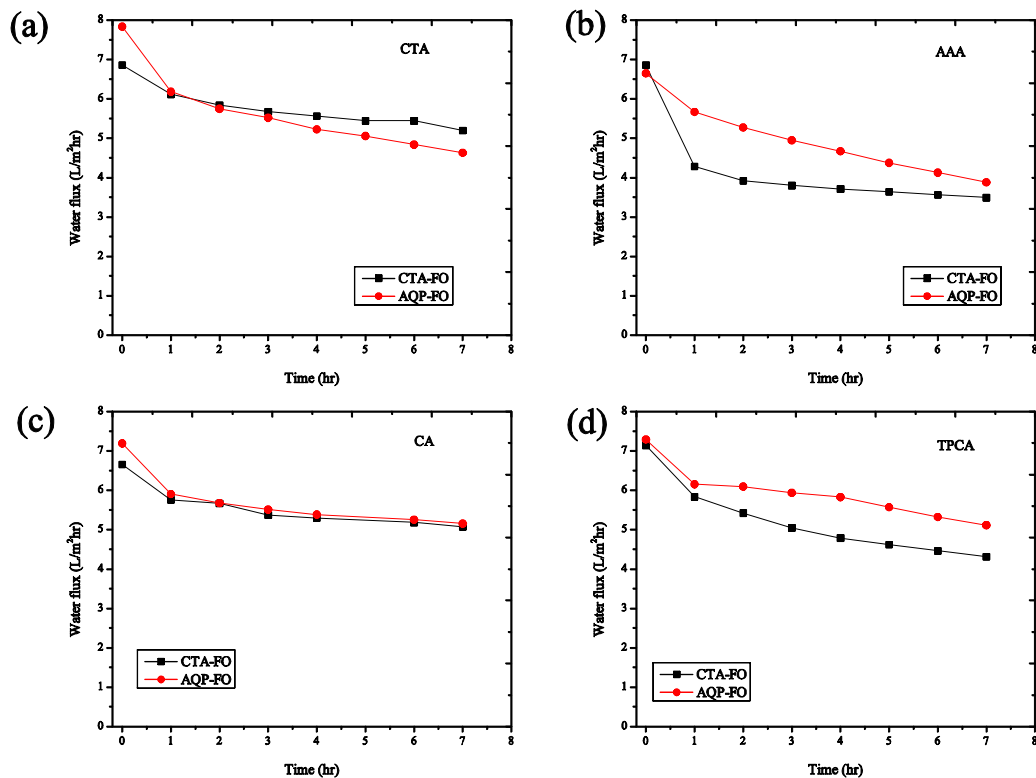


**Figure 4-5** The comparison between CTA and AQP-FO membranes on water flux applying NA model compound solutions. (a) CHA, (b) AAA, (c) CA, and (d) TPCA. Experimental condition: Initial concentration of each model compound was 50 mg/L. Cross-flow velocity = 2.3 cm/s, the experiments lasted for 7 hours.

#### 4.3.4 FO performance treating oil sands produced water

##### 4.3.4.1 Water flux

In Fig. 4-6, the two membranes were compared in terms of water flux on the treatment of OSPW and BDW. OSPW and BDW represented two types of oil sand produced water – the former has high organic concentration and the latter contains high salt concentration. As can be seen from Table 4-2, the TOC of OSPW was approximately four times higher than that of BDW and the TDS concentration of BDW was much higher than that of OSPW. Fig. 4-6 (a) presents the baseline performance of AQP-FO and CTA-FO membranes when 1M NaCl was applied as the

draw solution and 0.01 M NaCl and 0.23 M NaCl were applied to mimic the osmotic pressure level in the OSPW and BDW, respectively. Interesting, it was found that when 0.01 M NaCl was applied as synthetic OSPW, no significant difference was found on the two membranes. However, when the feed solution switched to the synthetic BDW (0.23 M NaCl), the AQP-FO membrane displayed a significant higher water flux than the CTA membrane. This can be explained by the impact of internal concentration polarization (ICP). Because of the asymmetric structure of the CTA-FO membrane, it may have a relative low porosity and tortuosity, leading to a more severe ICP (D. T. Qin, Liu, Sun, Song, & Bai, 2015).

The water flux profiles seen in Fig. 4-6 (b), (c) and (d) were baseline corrected using the water flux result shown in Fig. 4-6 (a). The baseline correction process can be found in other literature (B. Mi & Elimelech, 2008). In Fig. 4-6 (b), the water flux generated by raw OSPW were reduced from 6.42 L/m<sup>2</sup> hr to 5.71 L/m<sup>2</sup> hr for CTA-FO membrane and from 6.42 L/m<sup>2</sup> hr to 5.23 L/m<sup>2</sup> for AQP-FO, respectively, showing similar water flux profile. When applying CTA-FO membrane, 0.45 μm filtered OSPW as feed solution did not elevate the water flux. In contrast, the water flux of AQP-FO membrane was slightly increased to 5.47 L/m<sup>2</sup> hr after 700 mL permeate was collected. Overall, it was worth noting that regardless of OSPW types, the water flux through the CTA-FO membrane was slightly above that of AQP-FO membrane. The results suggested: (1) the AQP-FO membrane was more likely to be affected by particles and natural organic matters (size > 0.45 μm); and (2) the CTA-FO membrane showed a comparative high anti-fouling propensity compared to AQP-FO membrane. Interestingly, the water flux generated by BDW (Fig. 4-6 (d)) showed that, at the beginning of experiment, AQP-FO exhibited a better performance. Unlike the water flux observed in the baseline experiment, the AQP-FO membrane did not demonstrate a continuously superior performance along the whole experiment. The



unexpected water flux might be explained by the complex water matrix of BDW. As shown in Table 4-1, BDW had a high concentration of  $Mg^{2+}$ . Holloway et al. (Holloway et al., 2015) reported that the presence of  $Mg^{2+}$  can slow the reverse diffusions of mixed draw solution, especially NaCl dominant draw solution. In FO process, the salt ion can be transported both from draw to feed side and feed to draw side. The hindrance of small radii solute can occur on feed solution as feed solution as well. Hence, in our experiment, the presence of  $Mg^{2+}$  may hinder the transport of other solute in BDW, thereby incrementing the ICP on feed site and leaving no distinctive difference between two membranes. Overall, considering the water flux, CTA demonstrated a less fouling propensity. In our experiment, the FO operating system was operated under a low crossflow velocity. Increasing the hydraulic force should help with increasing the water flux.

The SEM and EDX images were taken after raw and 0.45  $\mu m$  filtered OSPW fouling experiments (Fig. 4-7). The surface morphology of the used membranes did not clearly show the difference between these two membranes in terms of membrane fouling or scaling. No particular fouling pattern was observed on the active layer on both membranes. Several studies had concluded that  $Ca^{2+}$  can be bonded with carboxylic rich organic compound (i.e., humic acids) to form foulant layer on the membrane surface (B. Mi & Elimelech, 2008; Parida & Ng, 2013). EDX analysis exhibited that the foulants were associated with the presence of  $Ca^{2+}$  in OSPW, which was in good agreement with previous findings.

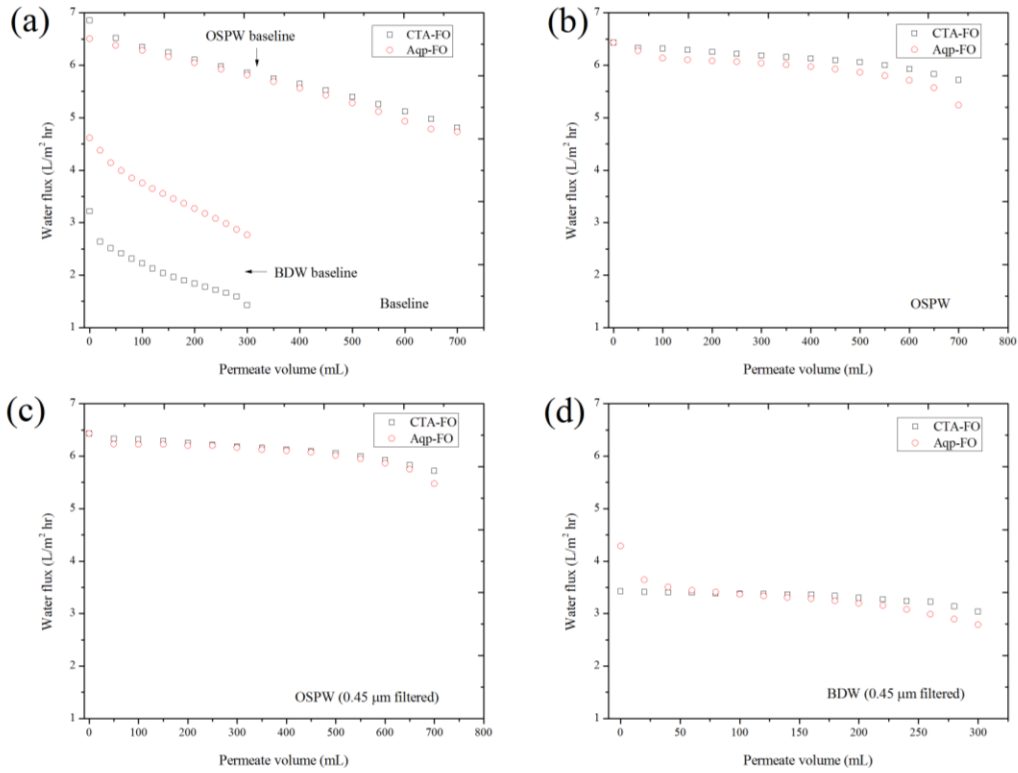


**Figure 4-6** The comparison of CTA-FO and AQP-FO membranes on water flux when using (b) OSPW, (c) OSPW (0.45 μm filtered), and (d) BDW (0.45 μm filtered) as feed solution. Experimental condition: FO membrane was operated in active layer facing the feed solution. Crossflow velocity = 2.3 cm/s, draw solution: 1 M NaCl. Baseline experiment (a) was conducted using 0.23 M and 0.01 M NaCl to mimic the osmotic pressure level of BDW and OSPW, respectively. 1M NaCl was used as the draw solution.

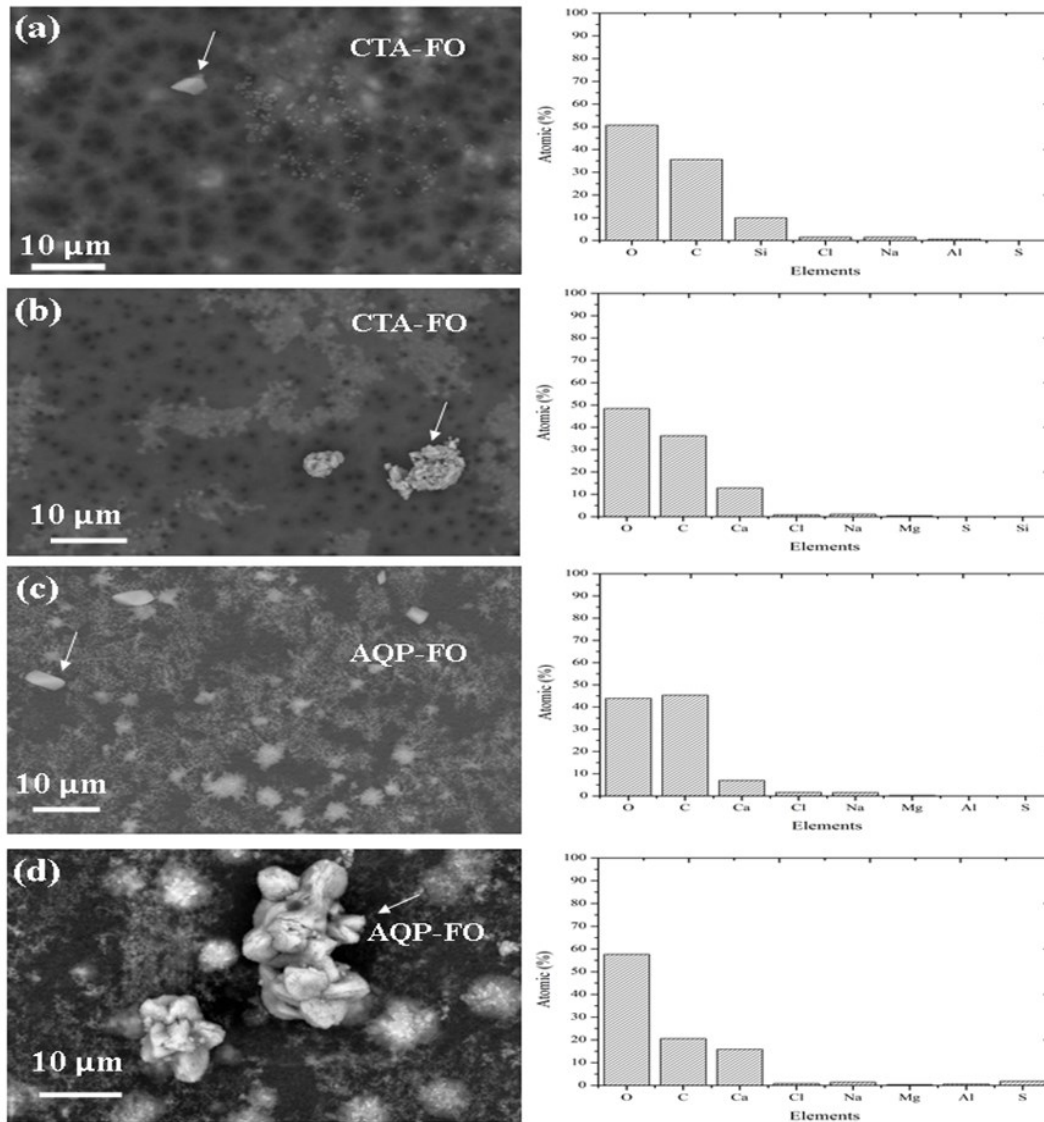


**Figure 4-7** SEM and EDX images taken after the FO performance experiment: (a), (c) raw OSPW and (b), (d) 0.45 μm filtered OSPW.

#### 4.3.4.2 Organic and inorganic rejections

NA rejection efficiency was only evaluated after using OSPW and 0.45 μm OSPW as the feed solution. The NA concentration of OSPW was 25.4 mg/L and 3-D concentration matrix can be found in Fig. 4-8. The comparison between AQP and CTA-FO membrane on NA-OSPW

removal is shown in Fig. 4-9. Both FO membranes presented good performance in terms of NA rejection. The rejection efficiencies of OSPW-NAs in 0.45  $\mu\text{m}$  filtered OSPW were 92.4% and 90.9% for CTA-FO and AQP-FO membrane, respectively. The rejection efficiencies of NAs in raw OSPW were found to be 94.0% and 93.8% for CTA-FO and AQP-FO membrane, respectively. The increased rejection efficiency observed in unfiltered OSPW was likely because of colloid particles. As reported by Xie et al. (Xie, Nghiem, Price, & Elimelech, 2014), the organic rejection was promoted by the loose foulant layer created by colloidal particles and lower initial water flux. No particle trend was observed with respect to carbon number (n) or hydrogen deficiency (-Z).

The comparison between CTA and AQP membranes on inorganic rejection is shown in Fig. 4-10. In addition to OSPW, the inorganic rejection in BDW was also evaluated. Unfortunately, the transported anion solute from feed to draw was unable to be determined due to the detection limitation. Therefore, only the rejection efficiency of cation was evaluated in 0.45  $\mu\text{m}$  filtered OPSW and BDW, respectively. Compared to the CTA membrane, the AQP membrane showed a better inorganic rejection regardless of the produced water type. Complete rejections were observed on Cr, Ni, Cu, As, and Mo in OSPW and BDW. This phenomenon was more likely to be associated with their ion size and charge number. Comparative low rejection was seen in  $\text{Ca}^{2+}$  dissolved in OSPW regardless of the membrane type. As observed in SEM image,  $\text{Ca}^{2+}$  was found on fouling layers of both membranes, which might be considered as the evidence of cake enhanced concentration polarization (CP) (S. Lee et al., 2010). On the other hand, the presence of cake enhanced CP might promote the diffusion of  $\text{Ca}^{2+}$  (Codday et al., 2015), thereby decreasing its rejection efficiency. Compared to the high inorganic rejection of the selected elements in OSPW, relative low rejection efficiency was seen in BDW. The lower rejection can be explained

by the enhanced CP caused by BDW. Due to the relative high TDS in BDW, membrane might suffer a more severe CP which subsequently promoted the transportation of feed solutes, especially under current low crossflow velocity. It was reported that the hydraulic radii and valence state of the ions were two governing factors controlling its diffusion (Hancock & Cath, 2009). However, a relative high diffuse rate of Al was seen using CTA membrane when treating both OSPW and BDW. This undesirable rejection efficiency might suggest that the rejection of CTA membrane was more relied on size exclusion rather than electrostatic force. As Madsen et al. (Madsen, Bajraktari, Helix-Nielsen, Van der Bruggen, & Sogaard, 2015) reported, the rejection mechanism of CTA membrane on trace organics was mainly due to steric hindrance, in another words, size exclusion. Moreover, the author also suggested that the high rejection of AQP membrane was likely attributed to diffusion process.

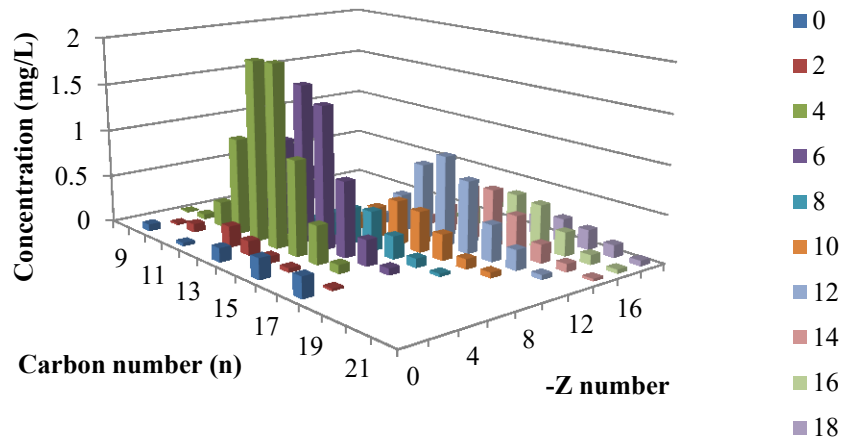


**Figure 4-8** 3-D matrix of NA concentration in OSPW (0.45 µm filtered). The concentration of NA was 25.4 mg/L.

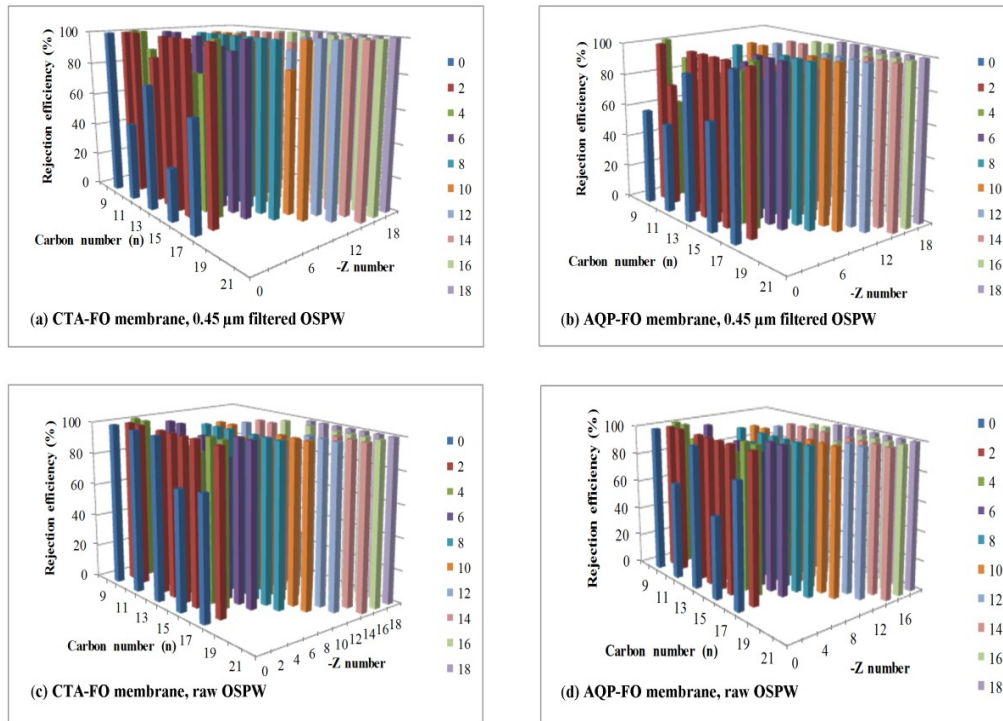


**Figure 4-9** The comparison between CTA and AQP-FO membranes on OSPW-NA rejection efficiency

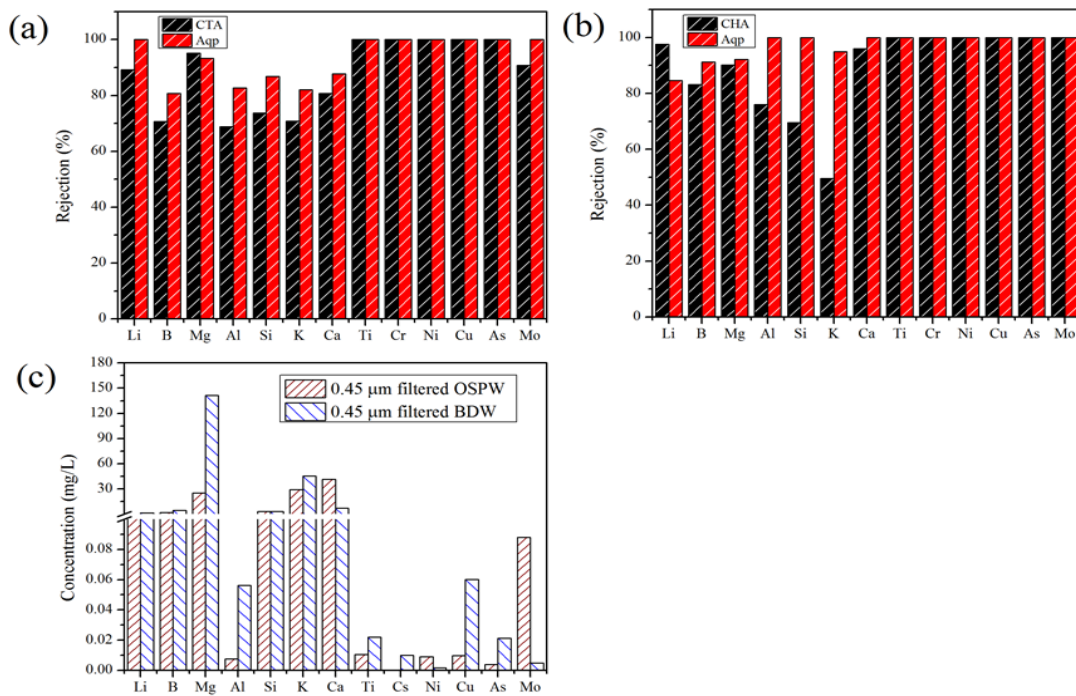


**Figure 4-10** The comparison between CTA and AQP membranes on rejection of inorganic ions in (a) 0.45  $\mu\text{m}$  filtered OSPW (b) 0.45  $\mu\text{m}$  filtered BDW (c) concentration of each ion in 0.45  $\mu\text{m}$  filtered OSPW and BDW, respectively.

#### 4.4 Conclusions

In the current study, CTA-FO and AQP-FO membranes were compared in terms of membrane characteristics, NA model compound adsorption and rejection, as well as performance of treating OSPW and BDW. The results indicated that the AQP membrane demonstrated higher water permeability than the CTA membrane. In terms of NaCl rejection, solute permeability and structure parameter, the two membranes showed no significant difference. At  $\text{pH} = 9$ , low adsorption of NA model compounds was observed on each of the membranes due to the electrostatic repulsive force. Moreover, the rejection efficiency for the two FO membranes was above 90% and that of AQP was slight below CTA because of the promoted compound diffusion by water flux. Our study also indicated less water flux decline were found on CTA membrane in treatment of OSPW, showing that the CTA membrane was more anti-fouling under low crossflow velocity. SEM image and EDX analysis confirmed the occurrence of membrane fouling and the presence of  $\text{Ca}^{2+}$  in the fouling layer on both membranes. Furthermore, high NAs and salt rejection were both observed. AQP showed a slight advantage on inorganic salt rejection. However, compared to membrane selection, the rejection of NAs and salt was more related to pretreatment methods and produced water type.

#### 4.5 Reference

Allen, E. W. (2008a). Process water treatment in Canada's oil sands industry: I. Target pollutants and treatment objectives. *Journal of Environmental Engineering and Science*, 7(2), 123-138.

- Allen, E. W. (2008b). Process water treatment in Canada's oil sands industry: II. A review of emerging technologies. *Journal of Environmental Engineering and Science*, 7(5), 499-524. doi: Doi 10.1139/S08-020
- Alpatova, A., Kim, E. S., Dong, S. M., Sun, N., Chelme-Ayala, P., & El-Din, M. G. (2014). Treatment of oil sands process-affected water with ceramic ultrafiltration membrane: Effects of operating conditions on membrane performance. *Separation and Purification Technology*, 122, 170-182. doi: DOI 10.1016/j.seppur.2013.11.005
- Arkhangelsky, E., Kuzmenko, D., & Gitis, V. (2007). Impact of chemical cleaning on properties and functioning of polyethersulfone membranes. *Journal of Membrane Science*, 305(1-2), 176-184.
- Blandin, G., Vervoort, H., Le-Clech, P., & Verliefde, A. R. D. (2016). Fouling and cleaning of high permeability forward osmosis membranes. *Journal of Water Process Engineering*, 9, 161-169. doi: <http://dx.doi.org/10.1016/j.jwpe.2015.12.007>
- Boo, C., Elimelech, M., & Hong, S. (2013). Fouling control in a forward osmosis process integrating seawater desalination and wastewater reclamation. *Journal of Membrane Science*, 444, 148-156. doi: 10.1016/j.memsci.2013.05.004
- Cath, T. Y., Childress, A. E., & Elimelech, M. (2006). Forward osmosis: Principles, applications, and recent developments. *Journal of Membrane Science*, 281(1-2), 70-87. doi: 10.1016/j.memsci.2006.05.048
- Coday, B. D., Almaraz, N., & Cath, T. Y. (2015). Forward osmosis desalination of oil and gas wastewater: Impacts of membrane selection and operating conditions on process performance. *Journal of Membrane Science*, 488, 40-55. doi: 10.1016/j.memsci.2015.03.059



- Coday, B. D., Hoppe-Jones, C., Wandera, D., Shethji, J., Herron, J., Lampi, K., . . . Cath, T. Y. (2016). Evaluation of the transport parameters and physiochemical properties of forward osmosis membranes after treatment of produced water. *Journal of Membrane Science*, 499, 491-502.
- Coday, B. D., Xu, P., Beaudry, E. G., Herron, J., Lampi, K., Hancock, N. T., & Cath, T. Y. (2014). The sweet spot of forward osmosis: Treatment of produced water, drilling wastewater, and other complex and difficult liquid streams. *Desalination*, 333(1), 23-35. doi: 10.1016/j.desal.2013.11.014
- Geise, G. M., Paul, D. R., & Freeman, B. D. (2014). Fundamental water and salt transport properties of polymeric materials. *Progress in Polymer Science*, 39(1), 1-42. doi: DOI 10.1016/j.progpolymsci.2013.07.001
- Hancock, N. T., & Cath, T. Y. (2009). Solute Coupled Diffusion in Osmotically Driven Membrane Processes. *Environmental Science & Technology*, 43(17), 6769-6775. doi: Doi 10.1021/Es901132x
- Hickenbottom, K. L., Hancock, N. T., Hutchings, N. R., Appleton, E. W., Beaudry, E. G., Xu, P., & Cath, T. Y. (2013). Forward osmosis treatment of drilling mud and fracturing wastewater from oil and gas operations. *Desalination*, 312, 60-66. doi: 10.1016/j.desal.2012.05.037
- Holloway, R. W., Maltos, R., Vanneste, J., & Cath, T. Y. (2015). Mixed draw solutions for improved forward osmosis performance. *Journal of Membrane Science*, 491, 121-131. doi: 10.1016/j.memsci.2015.05.016

- Huang, C. K., Shi, Y. J., El-Din, M. G., & Liu, Y. (2015). Treatment of oil sands process-affected water (OSPW) using ozonation combined with integrated fixed-film activated sludge (IFAS). *Water Research*, 85, 167-176.
- Jiang, Y., Liang, J., & Liu, Y. (2016). Application of forward osmosis membrane technology for oil sands process-affected water desalination. *Water Science and Technology*, 73(7), 1-8. doi: 10.2166/wst.2016.014
- Jin, X., Shan, J. H., Wang, C., Wei, J., & Tang, C. Y. Y. (2012). Rejection of pharmaceuticals by forward osmosis membranes. *Journal of Hazardous Materials*, 227, 55-61. doi: 10.1016/j.jhazmat.2012.04.077
- Kim, E. S., Dong, S., Liu, Y., & Gamal El-Din, M. (2013). Desalination of oil sands process-affected water and basal depressurization water in Fort McMurray, Alberta, Canada: application of electrodialysis. [Research Support, Non-U.S. Gov't]. *Water Science and Technology*, 68(12), 2668-2675. doi: 10.2166/wst.2013.533
- Kim, E. S., Liu, Y., & El-Din, M. G. (2012). Evaluation of Membrane Fouling for In-Line Filtration of Oil Sands Process-Affected Water: The Effects of Pretreatment Conditions. *Environmental Science & Technology*, 46(5), 2877-2884. doi: Doi 10.1021/Es2038135
- Lee, S., Boo, C., Elimelech, M., & Hong, S. (2010). Comparison of fouling behavior in forward osmosis (FO) and reverse osmosis (RO). *Journal of Membrane Science*, 365(1-2), 34-39. doi: 10.1016/j.memsci.2010.08.036
- Li, X. S., Chou, S. R., Wang, R., Shi, L., Fang, W. X., Chaitra, G., . . . Fane, A. G. (2015). Nature gives the best solution for desalination: Aquaporin-based hollow fiber composite membrane with superior performance. *Journal of Membrane Science*, 494, 68-77.

- Linares, R. V., Li, Z., Sarp, S., Bucs, S. S., Amy, G., & Vrouwenvelder, J. S. (2014). Forward osmosis niches in seawater desalination and wastewater reuse. *Water Research*, *66*, 122-139. doi: 10.1016/j.watres.2014.08.021
- Lutchmiah, K., Verliefde, A. R. D., Roest, K., Rietveld, L. C., & Cornelissen, E. R. (2014). Forward osmosis for application in wastewater treatment: A review. *Water Research*, *58*, 179-197. doi: 10.1016/j.watres.2014.03.045
- Madsen, H. T., Bajraktari, N., Helix-Nielsen, C., Van der Bruggen, B., & Sogaard, E. G. (2015). Use of biomimetic forward osmosis membrane for trace organics removal. *Journal of Membrane Science*, *476*, 469-474. doi: 10.1016/j.memsci.2014.11.055
- Mazlan, N. M., Marchetti, P., Maples, H. A., Gu, B., Karan, S., Bismarck, A., & Livingston, A. G. (2016). Organic fouling behaviour of structurally and chemically different forward osmosis membranes - A study of cellulose triacetate and thin film composite membranes. *Journal of Membrane Science*, *520*, 247-261.
- Mi, B., & Elimelech, M. (2008). Chemical and physical aspects of organic fouling of forward osmosis membranes. *Journal of Membrane Science*, *320*(1-2), 292-302. doi: 10.1016/j.memsci.2008.04.036
- Moustafa, A. M. A., Kim, E. S., Alpatova, A., Sun, N., Smith, S., Kang, S., & El-Din, M. G. (2014). Impact of polymeric membrane filtration of oil sands process water on organic compounds quantification. *Water Science and Technology*, *70*(5), 771-779. doi: 10.2166/wst.2014.282
- Nasr, P., & Sewilam, H. (2015). Forward osmosis: an alternative sustainable technology and potential applications in water industry. *Clean Technologies and Environmental Policy*, *17*(7), 2079-2090.

- Nguyen, T. P. N., Yun, E. T., Kim, I. C., & Kwon, Y. N. (2013). Preparation of cellulose triacetate/cellulose acetate (CTA/CA)-based membranes for forward osmosis. *Journal of Membrane Science*, 433, 49-59. doi: DOI 10.1016/j.memsci.2013.01.027
- Parida, V., & Ng, H. Y. (2013). Forward osmosis organic fouling: Effects of organic loading, calcium and membrane orientation. *Desalination*, 312, 88-98. doi: 10.1016/j.desal.2012.04.029
- Qi, S. R., Wang, R., Chaitra, G. K. M., Torres, J., Hu, X., & Fane, A. G. (2016). Aquaporin-based biomimetic reverse osmosis membranes: Stability and long term performance. *Journal of Membrane Science*, 508, 94-103.
- Qin, D. T., Liu, Z. Y., Sun, D. R. D. L., Song, X. X., & Bai, H. W. (2015). A new nanocomposite forward osmosis membrane custom-designed for treating shale gas wastewater. *Scientific Reports*, 5. doi: Artn 1453010.1038/Srep14530
- Shen, Y. X., Saboe, P. O., Sines, I. T., Erbakan, M., & Kumar, M. (2014). Biomimetic membranes: A review. *Journal of Membrane Science*, 454, 359-381.
- Shi, Y. J., Huang, C. K., Rocha, K. C., El-Din, M. G., & Liu, Y. (2015). Treatment of oil sands process-affected water using moving bed biofilm reactors: With and without ozone pretreatment. *Bioresource Technology*, 192, 219-227.
- Wei, J., Qiu, C. Q., Tang, C. Y. Y., Wang, R., & Fane, A. G. (2011). Synthesis and characterization of flat-sheet thin film composite forward osmosis membranes. *Journal of Membrane Science*, 372(1-2), 292-302. doi: 10.1016/j.memsci.2011.02.013
- Xie, M., Nghiem, L. D., Price, W. E., & Elimelech, M. (2014). Impact of organic and colloidal fouling on trace organic contaminant rejection by forward osmosis: Role of initial permeate flux. *Desalination*, 336, 146-152. doi: 10.1016/j.desal.2013.12.037

- Xie, M., Price, W. E., Nghiem, L. D., & Elimelech, M. (2013). Effects of feed and draw solution temperature and transmembrane temperature difference on the rejection of trace organic contaminants by forward osmosis. *Journal of Membrane Science*, 438, 57-64. doi: 10.1016/j.memsci.2013.03.031
- Xie, W. Y., He, F., Wang, B. F., Chung, T. S., Jeyaseelan, K., Armugam, A., & Tong, Y. W. (2013). An aquaporin-based vesicle-embedded polymeric membrane for low energy water filtration. *Journal of Materials Chemistry A*, 1(26), 7592-7600. doi: Doi 10.1039/C3ta10731k
- Xue, J. K., Zhang, Y. Y., Liu, Y., & El-Din, M. G. (2016). Treatment of oil sands process-affected water (OSPW) using a membrane bioreactor with a submerged flat-sheet ceramic microfiltration membrane. *Water Research*, 88, 1-11.
- Zhang, S., Wang, P., Fu, X. Z., & Chung, T. S. (2014). Sustainable water recovery from oily wastewater via forward osmosis-membrane distillation (FO-MD). *Water Research*, 52, 112-121. doi: 10.1016/j.watres.2013.12.044
- Zheng, Y., Huang, M. H., Chen, L., Zheng, W., Xie, P. K., & Xu, Q. (2015). Comparison of tetracycline rejection in reclaimed water by three kinds of forward osmosis membranes. *Desalination*, 359, 113-122. doi: 10.1016/j.desal.2014.12.009
- Zhu, S., Li, M., & Gamal El-Din, M. (2017). Forward osmosis as an approach to manage oil sands tailings water and on-site basal depressurization water. *Journal of Hazardous Materials*, 327, 18-27. doi: <http://dx.doi.org/10.1016/j.jhazmat.2016.12.025>

## **5 Chapter 5 Probing oil sands process-affected water fouling mechanism of forward osmosis membrane: impact of membrane materials and functional groups in naphthenic acids<sup>4</sup>**

### **5.1 Introduction**

The increasing volume of oil sands process-affect water (OSPW) in tailing pond places a demand on efficient water management approaches. To date, chemical, physical, biological processes (Allen, 2008a; E. S. Kim et al., 2011, 2012; J. Xue et al., 2016) have been investigated as potential treatment solutions, among which membrane process —forward osmosis (FO) starts to attract significant amount of research interests. The principle of FO is employing the osmotic pressure difference to transport water molecular from less concentrated solution to concentrated solution through a semi-permeable membrane (Cath et al., 2006). Because no or little hydraulic pressure is involved in FO process, it has advantages over pressure-driven membrane process on membrane fouling, energy consumption and water recovery (Gormly, 2014). Promising FO application has been already investigated on oil and gas wastewater management. Hickenbottom et al. (Hickenbottom et al., 2013) reported that FO process performed efficiently on treating drilling wastewater; a 50% water recovery with approximately 99% organic rejection was observed. Moreover, high heavy metal rejection (80~100%) and water recovery (85%) were also reported in Jiang's study treating OSPW by FO process (Jiang et al., 2016).

---

<sup>4</sup> This chapter will be submitted to: Xiang Li, Shu Zhu, Mingyu Li, Hongbo Zeng, and Mohamed Gamal El-Din 2017. Probing oil sand process-affected water fouling mechanism of forward osmosis membrane: impact of membrane materials and functional groups in naphthenic acids. Will be submitted to: *Environmental Science & Technology* in June, 2017

Although FO shows less fouling propensity, fouling is still the major concern hindering its practical application, especially for wastewaters with high organic concentration. Several studies have been conducted to investigate the fouling mechanism on FO process. Mi et al. (B. X. Mi & Elimelech, 2010) examined the anti-fouling property of FO membrane in aspects of membrane materials and hydraulic pressure involvement. The author found that comparing to cellulose acetate (CA-FO) membrane; thin-film polyamide (TFC-FO) membrane was more intended to be fouled. Same research group also evaluated the impact of physical and chemical interaction on organic fouling of FO process (B. Mi & Elimelech, 2008). It was suggested that generally, calcium binding, permeation drag and hydrodynamic force can all attribute to the formation of fouling layer. However, for each organic compound, the dominant mechanism may vary. As oil sands produced water, OSPW has a complex water matrix with both organic and inorganic compounds. For the organic part, naphthenic acids (NAs) contribute to majority of organic constituents and it was suggested that NAs was associated with membrane surface fouling in pressure-driven process (E. S. Kim et al., 2011).

Currently, limited FO membranes are commercial available: for example, asymmetric cellulose triacetate (CTA) membrane (Hydration Technology Innovation, USA) and flat sheet aquaporin (AQP) inside membrane (Aquaporin A/S, DK). However, these two FO membrane have their own drawbacks. CTA membrane suffers a high fouling propensity and low water flux because of its membrane materials and structure (D. T. Qin et al., 2015). Although AQP membranes showed high water flux and contaminant rejection efficiency, the mechanical strength was comparatively weak, thereby leaving its stability an important concern. As discussed in Mi et al's study (B. X. Mi & Elimelech, 2010), membrane material was a critical factor affecting fouling behavior, which needs to be systematically investigated, especially, the effect of membrane materials on

organic fouling. Atomic force microscopy (AFM) was one of the methods that quantify the intermolecular adhesion forces between the organic foulants and FO membrane (Castrillon, Lu, Shaffer, & Elimelech, 2014; Lu, Castrillon, Shaffer, Ma, & Elimelech, 2013; B. Mi & Elimelech, 2008). However, limited research has been conducted so far to compare the membrane materials in terms of NA fouling and the mechanism of organic fouling of FO is barely known in OSPW treatment.

This study investigated the organic fouling behavior of FO membrane in aspect of NAs fouling. To achieve the ultimate goal, surface force apparatus (SFA), along with atomic force microscopy (AFM) analysis, was used to elucidate the force between NA functional groups and membrane surface to evaluate the importance of materials on NA fouling behavior. To be more specific, the interaction between two most abundant functional groups in OSPW-NAs including hydroxyl (-OH), carboxyl (-COOH) (Moustafa et al., 2014) as well as the hydrophobic functional group (-CH<sub>3</sub>(CH<sub>2</sub>)<sub>17</sub>) and three membranes including two FO membranes and one RO membrane were studied and compared in terms of adhesive and repulsive force.

## **5.2 Materials and methods**

### **5.2.1 FO membrane and sample preparation**

Three commercial available membranes were investigated in current study. Two FO membranes (CTA-FO, AQP-FO) made by cellulose triacetate and aquaporin were provided by Hydration Technologies, Inc. (Albany, OR, USA) and Aquaporin A/S (Kongens Lyngby, Denmark), respectively. The substrate for CTA-FO and AQP-FO membrane is CTA and polyethersulfone (PES), respectively. The commercial RO membrane (PA-RO) with polyamide as substrate was purchased from TriSep™ (Goleta, CA, USA). The FT-IR spectra of three membranes are shown in Figure 5-1. Dimethylformamide (DMF, ACS reagent, purity ≥ 99.8%) obtained from Sigma-



Aldrich (Oakville, Ontario, CA) was used to prepare membrane polymer solution. To prepare the membranes polymer solution, membranes were cut into 6 cm × 6 cm and dissolved in 20 mL DMF overnight. AQP-FO membrane was completely dissolved while CTA-FO and PA-RO was partially dissolved due to the membrane support designed for the enhancement of mechanical strength. Therefore, the membrane polymer solutions were filtered using 0.2 μm filter before being spin-coated.

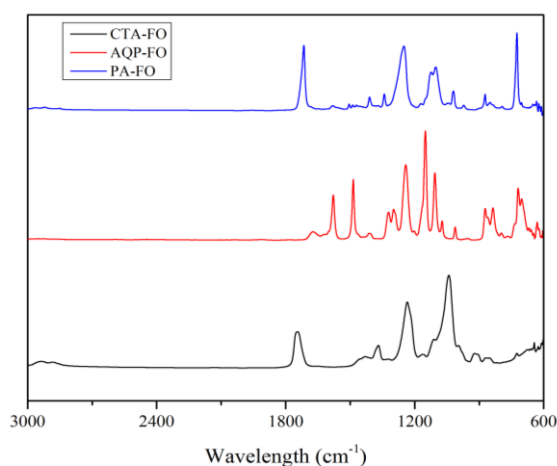


**Figure 5-1** FT-IR spectra of the three tested membranes.

### 5.2.2 SFA interaction force measurements and AFM imaging

An SFA (Surforce LLC, Santa Barbara, CA, USA) was used to measure the intermolecular interaction forces between membrane polymer surface and different NA functional groups in aqueous environment with pH = 9 (the typical pH of OSPW). The desirable aqueous solution was synthesized by Milli-Q water and 0.1 M NaOH. Three membrane films were prepared by spin-coating 6 drops of membrane DMF solutions on the freshly cleaved, back-silvered mica sheets that have already been glued on silica disks with radius R= 2 cm, respectively. The spin-coated membrane surfaces were vacuum-dried overnight to remove the residual solvent to

maintain the uniform thickness of the film. The preparation of functionalized mica sheets glued on silica disks were briefly described as follows: the mica surface with hydroxyl group was obtained by treating cleaved mica sheet with H<sub>2</sub>O-plasma for 15 mins; the hydrophobization of mica surface was conducted under octadecyltrichlorosilane (OTS, ACROS Organics) vapor in an evaporation chamber for 24 h. For the preparation of carboxyl-terminated (-COOH) surface, mica surface was first pretreated under (3-Aminopropyl) triethoxysilane ( $\geq 99.9\%$ , Sigma-Aldrich) vapor in an evaporation chamber for 3 h. And then, succinic anhydride (SA,  $\geq 99.9\%$ , Sigma-Aldrich) was used across-linker molecule to form carboxyl-terminated (-COOH) surface through subsequent reaction. The detailed functionalization process of mica surface can be found in other publications (Murib et al., 2016; C. Shi, Chan, Liu, & Zeng, 2014).

In the current study, the asymmetric configuration was used to investigate the interactions between a membrane polymer film and a functionalized mica surface. A detailed setup of SFA experiment can be found elsewhere (J. Israelachvili et al., 2010; J. N. Israelachvili & Adams, 1978). Briefly, one prepared membrane film coated silica disk and one functional group coated silica disk were mount to the SFA chamber in crossed-cylinder geometry which was locally equivalent to a sphere of radius  $R$  approaching a flat surface when the separation distance  $D$  was much smaller than  $R$  ( $R$  is the radius of the cylindrical silica disk). 50  $\mu\text{L}$  solution at pH =9 was injected between two mica surfaces and allowed to equilibrate for 30 min before force measurement. The normal forces  $F$  between the curved surfaces were measured as a function of surface separation distance  $D$  with force sensitivity and absolute separation distance accuracy down to  $<10$  nN and 0.1 nm, respectively. The absolute surface separation distance can be obtained in real time and *in situ* by employing fringes of equal chromatic order (FECO) which based on the multiple beam interferometry (MBI) optical technique and the surface forces were

derived through Hooke's law by multiplying the spring constant with the spring deformation (H. Zeng, Tian, Anderson, Tirrell, & Israelachvili, 2008; H. B. Zeng, Maeda, Chen, Tirrell, & Israelachvili, 2006). The reference distance ( $D = 0$ ) was determined between two bare mica surfaces contacted in air. The thickness of the membrane films and functional group films were measured by contacting these films with bare mica in air, respectively. During approaching, the surface energy ( $W$ ) between two flat surfaces is equal to the force  $F/R$  between two spheres of radius  $2R$  or a sphere of radius  $R$  near a flat surface by using  $W = F/2\pi R$  based on the Derjaguin approximation (J. N. Israelachvili, 2011). The measured normalized pull-off force  $F/R$  is corresponded to the adhesion energy per unit area by  $W_{ad} = 2F_{ad}/3\pi R$  based on the Johnson-Kendall-Roberts (JKR) model for soft materials with large deformations. Each measurement was repeated at least three times under each experimental condition to confirm their reproducibility.

The surface roughness and topography of the polymer coated mica sheet was examined by AFM (Agilent Technologies 5500, Agilent, Santa Barbara, CA, USA). The contact angle of the membrane polymer coated mica was measured by Rame-Hart contact goniometer (Rame-hart instrument co, Succasunna, NJ, USA) using Milli-Q water sessile drop and the images were taken by a CCA camera. Same morphology analysis was conducted on functionalized mica sheets as well before the force measurement.

### **5.2.3 OSPW**

The raw OSPW used in this study was obtained from Fort McMurray, AB, Canada. The collected samples were stored in a polyvinyl chloride barrel at 4 °C. Raw OSPW was filtered through a 0.45  $\mu\text{m}$  filter to reduce its high turbidity. The characteristics of 0.45  $\mu\text{m}$  filtered

OSPW are shown in Table 5-1. 3D-images showing NAs ( $C_nH_{2n+Z}O_2$ ) with its corresponding carbon number (n) and hydrogen deficiency (-Z) can be found in Figure 5-2.

**Table 5-1** Water matrices of 0.45  $\mu\text{m}$  filtered OSPW

| Parameters                            | OSPW<br>(0.45 $\mu\text{m}$ filtered) |
|---------------------------------------|---------------------------------------|
| pH value                              | 8.5                                   |
| Turbidity, NTU                        | 2.6 $\pm$ 0.0                         |
| Conductivity, mS/cm                   | 2.4 $\pm$ 0.02                        |
| Total dissolved solids<br>(TDS), mg/L | 1432 $\pm$ 0.0                        |
| Total organic carbon<br>(TOC), mg/L   | 44.68 $\pm$ 2.97                      |
| NAs, mg/L                             | 25.04                                 |

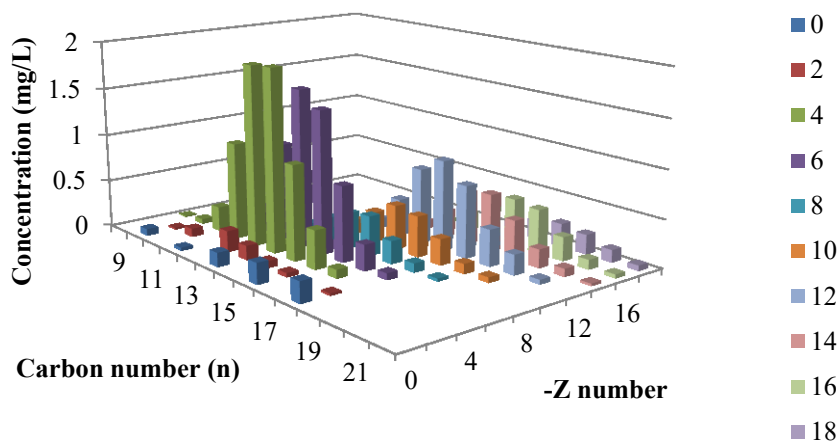


**Figure 5-2** NA concentration in OSPW at corresponding n and -Z number.

#### 5.2.4 NA model compound adsorption experiment

In current experiment, cyclohexanecarboxylic acid (CHA) and cholic acid (CA) were selected as NA model compounds. Chemical characteristics of each model compound can be found in the Appendix. The stock solutions were prepared by directly dissolving 50 mg CHA and CA into 1 L

0.05 M carbonate bicarbonate buffer solution, respectively. 1M HCl/NaOH were used to adjust the pH level of the stock solutions to 9. CTA, AQP and PA-based membranes were cut into 6 cm × 6 cm section and placed into 50 mL glass conical flask with glass caps. The flasks with membranes and 20 mL stock solution were placed on a stirrer with a speed of 200 rpm. Control experiments were also carried out to monitor the experimental quality. 1 mL of sample was taken after 24 hours for liquid chromatography/mass spectrometry (LC-MS) analysis. The experiments were conducted in three times for each model compound.

### **5.2.5 Membrane performance in OSPW fouling experiment**

The test FO system is a bench-scale crossflow system used our previous study (Zhu et al., 2017). Only active layer facing to feed solution was evaluated. A 20-hour experiment using 0.45 μm filtered OSPW as the feed and 1 M NaCl as the draw was performed at fixed crossflow velocity of 2.3 cm/s. The crossflow was kept as low as possible, as suggested by the AQP-FO membrane manufacturer. The weight changes of draw solution were monitored to obtain the water flux ( $J_w$ ).

$$J_w = \frac{V_p}{A_m t} \quad (1)$$

Where  $J_w$  is the permeate flux,  $V_p$  is the permeate volume, and  $A_m$  (140 cm<sup>2</sup>) is the effective area of membrane surface, and  $t$  is the operating time.

Baseline experiments using were conducted primarily using 0.01 M NaCl was as the feed solution and 1 M NaCl as the feed solution to eliminate the impact of draw solution dilution. Same operating conditions were maintained as the fouling test.

## 5.3 Results and discussion

### 5.3.1 Morphology of membrane polymer coated and functionalized micas

AFM images of spin-coated membrane polymer film are shown in Fig. 5-3 (a) to (c). The root-mean-square roughness (RMS) of membrane polymer film was 1.23 nm, 0.54 nm, and 1.32 nm for AQP-FO film, PA-RO film and CTA-FO film, respectively. The low roughness suggesting the results of force measurement would not be affected by surface roughness.

The corresponding contact angle for each membrane polymer film was also evaluated. The contact angle ranked as AQP-FO ( $77^\circ$ ) > PA-RO ( $65^\circ$ ) > CTA-FO ( $62^\circ$ ), indicating AQP-FO film was the most hydrophobic compared to the other two polymer surfaces. This result was contradictory with the contact angle directly measured from the commercial membranes. For the commercial membranes, the contact angle ranked as CTA-FO ( $69.9 \pm 0.8^\circ$ ) > AQP-FO ( $46.6 \pm 2.8^\circ$ ) > PA ( $46.1 \pm 2.6$ ). The difference of contact angle between the mica film and commercial membrane was attributed to the impact of surface roughness. The surface roughness (RMS) membrane polymer coated mica film was approximately 1 nm; however, the RMS for the commercial membrane was significantly higher than mica surface, and for instance, the measured RMS for the commercial CTA-FO membrane was 36 nm. Fig. 5-3 (e) and (d) showed the surface morphology of functionalized mica surfaces. The contact angles for hydrophobic, carboxylated and hydroxylated mica surface were  $90^\circ$ ,  $37^\circ$  and  $0^\circ$ , respectively.

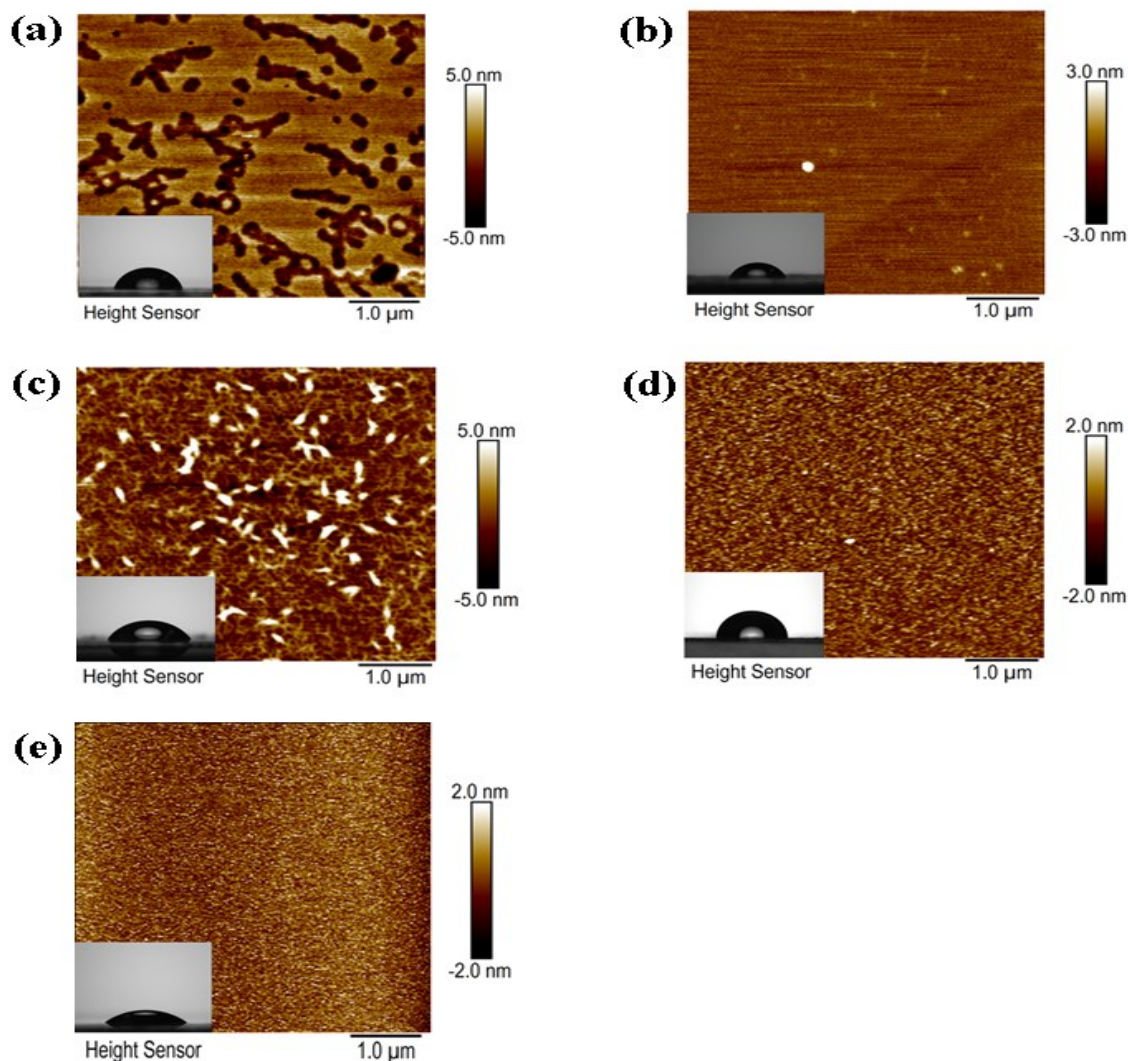


**Figure 5-3** AFM images of membrane polymer films: (a) AQP-FO (b) PA-RO (c) CTA-FO and AFM images of functionalized mica: (d) hydrophobalized and (e) carboxylated surface.

### 5.3.2 Interaction between polymeric membrane surface and functional groups

To better understand the organic fouling mechanism of FO membrane with respect to NA fouling, the effect of different functional groups in NAs should be considered. Therefore, the interaction between membrane surfaces and three main functional groups was investigated. The force measurement between membrane surface and functional groups (asymmetric configuration) at pH = 9 aqueous condition was carried out by using SFA. Figure 5-4 (a) to (i) presented the

normalized force-distance profile of CTA-FO, AQP-FO and PA-RO membrane between -OH, -COOH and -CH<sub>3</sub> modified surfaces (hydrophobic functional end), separately. In addition, all the typical approach force-distance curves were fitted by Derjaguin-Landau-Verwey-Overbeek (DLVO) model and hydration model or Alexander-de Gennes (AdG) scaling model as shown in Appendix. As at pH 9, -OH and -COOH groups as well as membrane polymer surfaces were all negatively charged (Hurwitz, Guillen, & Hoek, 2010; Nguyen et al., 2013; Salgin, Salgin, & Soyer, 2013). During approaching and separation of two mica surfaces, the repulsive forces were observed between -OH modified surface and all three membrane surfaces as well as the case of -COOH modified surface, which was likely due to the impact of repulsive electrostatic interaction and steric interaction of two surfaces in the current pH condition. During approaching, repulsive forces were also detected between -CH<sub>3</sub> modified surface and all three membrane surfaces, which was mainly attributed to the steric interaction between the hydrophobic surface and all membrane surfaces. However, when the two surfaces separated, adhesion interaction ( $F_{ad}/R$ )  $\sim 2$ ,  $\sim 2.1$ ,  $\sim 5.7$  mN/m were observed between -CH<sub>3</sub> modified group and PA, CTA, AQP membrane surface, respectively. The adhesion force during separation was probably due to the hydrophobic interaction, since the hydrophobic parts of the membrane films rearranged their conformation to be exposed to the -CH<sub>3</sub> modified surface, leading to a proper orientation for adhesion. As observed in previous contact angle test, the tested membrane polymer surfaces were comparatively hydrophobic and the AQP-FO demonstrated the highest contact angle. In a good agreement, AQP-FO membrane surface exhibited the strongest attractive force compared to other two membranes. The results of force measurement, along with observations in the contact angle, indicated that the hydrophobic-hydrophobic interaction was the dominating mechanism which resulted in the attraction between membrane polymer and hydrophobic functional group. Overall,



it was found that in the current experimental condition: 1) introducing only -OH and -COOH functional group would not cause adhesive force; 2) hydrophobic-hydrophobic interaction was the dominant mechanism for membrane fouling; and 3) compared to CTA-FO and PA-RO membrane, AQP-membrane was more intended to foul.

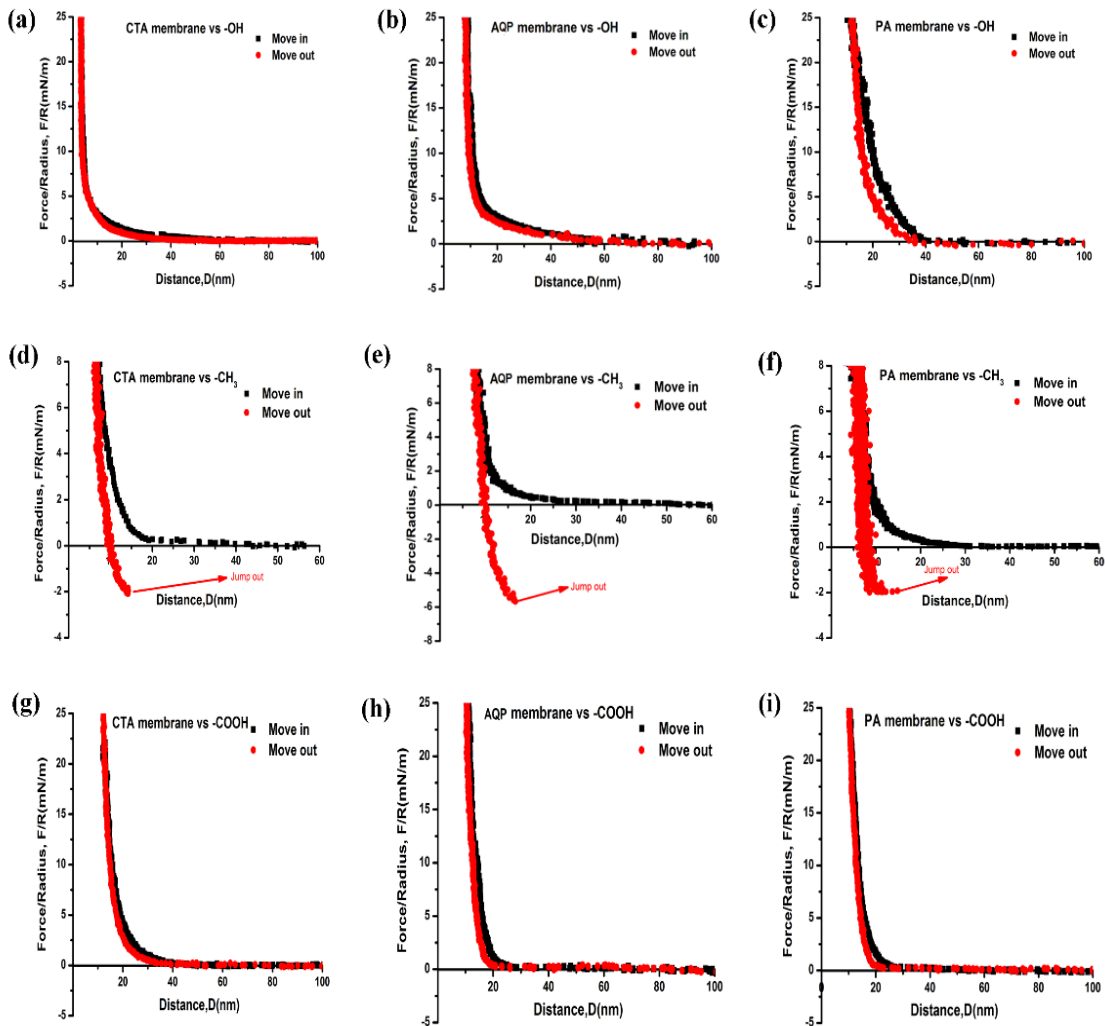


**Figure 5-4** The results of direct force measurement between three membrane polymer films and functional groups. (a) to (c) -OH, (d) to (f) -COOH and (g) to (i) -CH<sub>3</sub>.

### 5.3.3 NA model compound adsorption experiment

The comparison between three membranes on adsorption of CHA and CA is shown in Fig. 5-5.  $C$  and  $C_0$  represented the concentration of NA model compound in liquid solution before and after 24 hr adsorption experiment. The given results illustrated that the only 8% to 11% of model compound were adsorbed regardless of membrane substrate materials. This phenomenon was likely attributed to the electro-repulsive forces between negatively charged membrane surface and model compound. pKa values of CHA and CA were less than 5, indicating these two NA model compounds were negatively charged at pH 9 because of deprotonation. For CTA-FO, AQP-FO and PA-RO membrane, the similar adsorption amount was observed for both CHA and CA. As indicated by previous contact angle measurement, AQP-FO membrane film showed the highest hydrophobicity. Furthermore, the log  $D$  value of CA (0.65) was higher than that of CHA (-1.94), suggesting CA is more hydrophobic than CHA. Therefore, it was expected that more CA should be adsorbed on AQP-FO membrane due to the hydrophobic-hydrophobic interaction between membrane surface and CA. However, our experimental results did not show enough evidence to support the hydrophobic-hydrophobic interaction, which reversely revealed the importance of electro-repulsive force to the reduction of NA adsorption or membrane fouling.

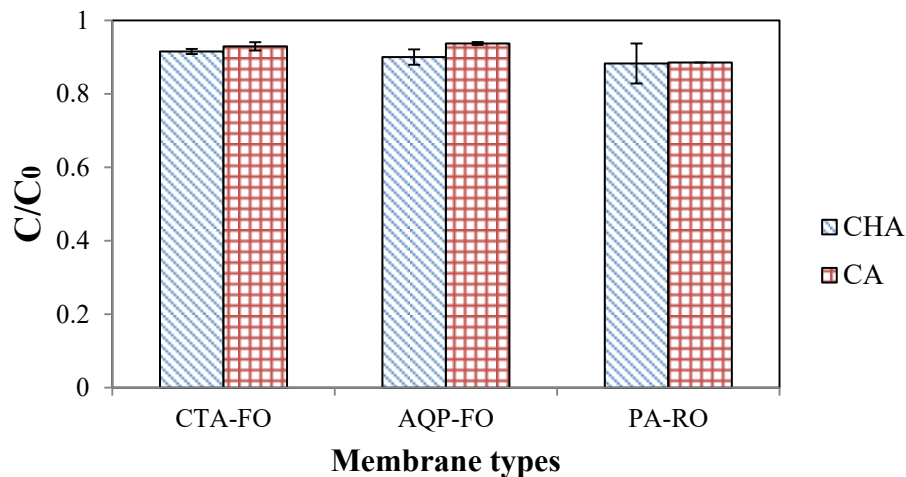


**Figure 5-5** The comparison between CTA-FO, AQP-FO and PA-RO on NA model compound adsorption. The concentrations of initial NA model compound were 49.6 mg/L and 46.8 mg/L for both CHA and CA.

#### **5.3.4 Membrane fouling experiment using OSPW as the feed solution**

To further compare the fouling performance of three membranes and organic fouling in OSPW, the FO fouling test was conducted using 0.45  $\mu\text{m}$  OSPW as the feed solution and 1 M NaCl as the draw solution. The whole experiment lasted for 20 hrs at the crossflow of 2.3 cm/s. By the end of the experiment, the permeate volumes obtained by CTA-FO, AQP-FO and PA-FO membrane were 824.8 mL, 766.0 mL and 226.0 mL, respectively. Fig. 5-6 (c) and (d) showed the water flux and normalized flux of each membrane on OSPW treatment. In Fig. 5-6 (a) and (b), the water flux and normalized flux given by the baseline experiment was also presented as a function of time.

It was evident that PA-RO membrane was not suitable to operate under FO process. The impact of internal concentration polarization (ICP) significantly affected its performance in terms of water flux. Meanwhile, PA-RO membrane showed minimum fouling phenomenon due to the low generated water flux. The initial water flux generated by AQP-FO was slightly above that of CTA-FO; however, based on the flux profile shown in baseline experiment, no distinctive difference can be found between CTA-FO and AQP-FO membranes. During OSPW fouling experiment, AQP-FO membrane exhibited a higher initial water flux than CTA-FO. After 20-hr operating, 54.5% and 61.0% of water flux was compensated for draw solution dilution and membrane fouling for CTA and AQP membrane, respectively. It was found that two FO membranes displayed great anti-fouling performance under current operating condition. Also, it was still important to note that AQP-FO membrane suffered a more severe surface fouling

considering the obtained final volumes of water permeate. This result was in good agreement with our SFA analysis results. Additionally, the presence of divalent ion in OSPW, for instance, calcium might also enhance the organic membrane (B. X. Mi & Elimelech, 2010). Due to the limited research scope, the impact of divalent on membrane fouling cannot be completely excluded.

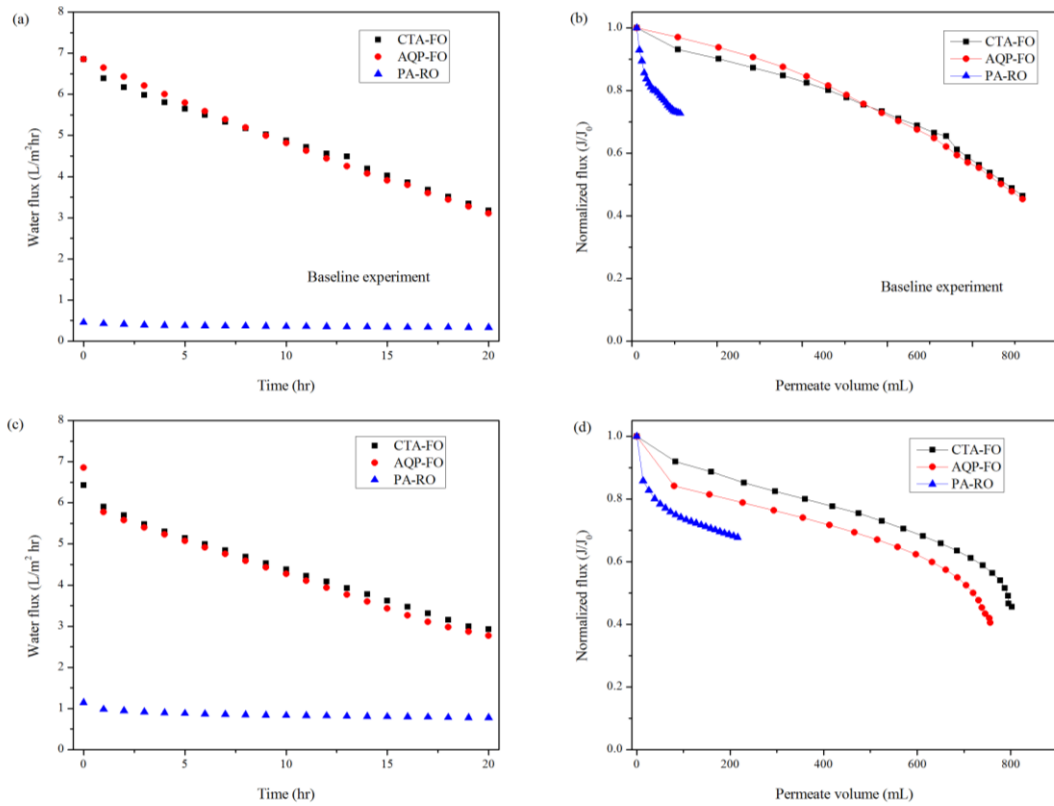


**Figure 5-6** Comparison between three membranes (CTA-FO, AQP-FO and PA-RO) on the treatment of 0.45 μm OSPW. Experimental condition: 1 M NaCl was used as the draw solution and the FO system was operating at a crossflow velocity of 2.3 cm/s.

## 5.4 Conclusions

The fouling mechanism associated with membrane materials and NAs was investigated and compared in terms of performance of treating OSPW, NA model compound adsorption, and force measurement. In the current study, three commercial available FO/RO membranes and three functional groups including -COOH, -OH and -CH<sub>3</sub> were investigated. The interactions between membrane polymer film and functionalized surface were directly measured through SFA. The force measurement was conducted in an aqueous environment at pH 9. It was found that AQP-FO membrane film on mica surface was the most hydrophobic compared to CTA-FO and CA-RO membranes. Because of its comparative high hydrophobicity, AQP-FO membrane demonstrated the strongest adhesive forces when separating its polymer film and hydrophobilized mica surface. Moreover, only repulsive forces were observed between -OH modified surface and all three membrane film surfaces as well as the case of -COOH modified surface, which was likely due to the impact of repulsive electrostatic interaction and steric interaction of two functionalized surfaces in the current pH condition. The results of adsorption experiment did not show enough evidences on the impact of hydrophobic-hydrophobic interaction between membrane and NA model compound, which, on the other hand, confirmed that electro-repulsive force was the governing mechanism of NA model compound adsorption rather than the hydrophobicity. In OSPW fouling test, it was found that PA-RO membrane yielded the lowest water flux because its membrane structure designed for high pressure process led to a severe impact of ICP. Furthermore, comparing the water flux profiles of two FO membranes, CTA-FO membrane performed better than AQP-FO membrane. Along with the SFA analysis, we found that CTA-FO membrane showed a better anti-fouling propensity on

aspect of OSPW organic fouling, especially for the hydrophobic organic compound, for instance, NAs.

## 5.5 Reference

- Allen, E. W. (2008). Process water treatment in Canada's oil sands industry: I. Target pollutants and treatment objectives. *Journal of Environmental Engineering and Science*, 7(2), 123-138.
- Castrillon, S. R. V., Lu, X. L., Shaffer, D. L., & Elimelech, M. (2014). Amine enrichment and poly(ethylene glycol) (PEG) surface modification of thin-film composite forward osmosis membranes for organic fouling control. *Journal of Membrane Science*, 450, 331-339. doi: DOI 10.1016/j.memsci.2013.09.028
- Cath, T. Y., Childress, A. E., & Elimelech, M. (2006). Forward osmosis: Principles, applications, and recent developments. *Journal of Membrane Science*, 281(1-2), 70-87. doi: DOI 10.1016/j.memsci.2006.05.048
- Gormly, S. (2014). Forward osmosis: introduction and applications for wastewater processing, energy conservation and energy generation. *Membranes for Clean and Renewable Power Applications*, 13, 379-395. doi: Doi 10.1533/9780857098658.5.379
- Hickenbottom, K. L., Hancock, N. T., Hutchings, N. R., Appleton, E. W., Beaudry, E. G., Xu, P., & Cath, T. Y. (2013). Forward osmosis treatment of drilling mud and fracturing wastewater from oil and gas operations. *Desalination*, 312, 60-66. doi: DOI 10.1016/j.desal.2012.05.037
- Hurwitz, G., Guillen, G. R., & Hoek, E. M. V. (2010). Probing polyamide membrane surface charge, zeta potential, wettability, and hydrophilicity with contact angle measurements. *Journal of Membrane Science*, 349(1-2), 349-357.

- Israelachvili, J., Min, Y., Akbulut, M., Alig, A., Carver, G., Greene, W., . . . Zeng, H. (2010). Recent advances in the surface forces apparatus (SFA) technique. *Reports on Progress in Physics*, 73(3).
- Israelachvili, J. N. (2011). Chapter 12 - Force-Measuring Techniques *Intermolecular and Surface Forces (Third Edition)* (pp. 223-252). San Diego: Academic Press.
- Israelachvili, J. N., & Adams, G. E. (1978). Measurement of forces between two mica surfaces in aqueous electrolyte solutions in the range 0-100 nm. [10.1039/F19787400975]. *Journal of the Chemical Society, Faraday Transactions 1: Physical Chemistry in Condensed Phases*, 74(0), 975-1001. doi: 10.1039/f19787400975
- Jiang, Y., Liang, J., & Liu, Y. (2016). Application of forward osmosis membrane technology for oil sands process-affected water desalination. *Water Science and Technology*, 73(7), 1-8. doi: 10.2166/wst.2016.014
- Kim, E. S., Liu, Y., & El-Din, M. G. (2011). The effects of pretreatment on nanofiltration and reverse osmosis membrane filtration for desalination of oil sands process-affected water. *Separation and Purification Technology*, 81(3), 418-428. doi: DOI 10.1016/j.seppur.2011.08.016
- Kim, E. S., Liu, Y., & El-Din, M. G. (2012). Evaluation of Membrane Fouling for In-Line Filtration of Oil Sands Process-Affected Water: The Effects of Pretreatment Conditions. *Environmental Science & Technology*, 46(5), 2877-2884. doi: Doi 10.1021/Es2038135
- Lu, X. L., Castrillon, S. R. V., Shaffer, D. L., Ma, J., & Elimelech, M. (2013). In Situ Surface Chemical Modification of Thin-Film Composite Forward Osmosis Membranes for Enhanced Organic Fouling Resistance. *Environmental Science & Technology*, 47(21), 12219-12228. doi: Doi 10.1021/Es403179m

- Mi, B., & Elimelech, M. (2008). Chemical and physical aspects of organic fouling of forward osmosis membranes. *Journal of Membrane Science*, 320(1-2), 292-302. doi: DOI 10.1016/j.memsci.2008.04.036
- Mi, B. X., & Elimelech, M. (2010). Organic fouling of forward osmosis membranes: Fouling reversibility and cleaning without chemical reagents. *Journal of Membrane Science*, 348(1-2), 337-345. doi: DOI 10.1016/j.memsci.2009.11.021
- Moustafa, A. M. A., Kim, E. S., Alpatova, A., Sun, N., Smith, S., Kang, S., & El-Din, M. G. (2014). Impact of polymeric membrane filtration of oil sands process water on organic compounds quantification. *Water Science and Technology*, 70(5), 771-779. doi: 10.2166/wst.2014.282
- Murib, M. S., Yeap, W. S., Eurlings, Y., van Grinsven, B., Boyen, H. G., Conings, B., . . . Wagner, P. (2016). Heat-transfer based characterization of DNA on synthetic sapphire chips. *Sensors and Actuators B-Chemical*, 230, 260-271.
- Nguyen, T. P. N., Yun, E. T., Kim, I. C., & Kwon, Y. N. (2013). Preparation of cellulose triacetate/cellulose acetate (CTA/CA)-based membranes for forward osmosis. *Journal of Membrane Science*, 433, 49-59. doi: DOI 10.1016/j.memsci.2013.01.027
- Qin, D. T., Liu, Z. Y., Sun, D. R. D. L., Song, X. X., & Bai, H. W. (2015). A new nanocomposite forward osmosis membrane custom-designed for treating shale gas wastewater. *Scientific Reports*, 5.
- Salgin, S., Salgin, U., & Soyer, N. (2013). Streaming Potential Measurements of Polyethersulfone Ultrafiltration Membranes to Determine Salt Effects on Membrane Zeta Potential. *International Journal of Electrochemical Science*, 8(3), 4073-4084.



- Shi, C., Chan, D. Y. C., Liu, Q. X., & Zeng, H. B. (2014). Probing the Hydrophobic Interaction between Air Bubbles and Partially Hydrophobic Surfaces Using Atomic Force Microscopy. *Journal of Physical Chemistry C*, 118(43), 25000-25008.
- Xue, J., Zhang, Y., Liu, Y., & Gamal El-Din, M. (2016). Treatment of raw and ozonated oil sands process-affected water under decoupled denitrifying anoxic and nitrifying aerobic conditions: a comparative study. *Biodegradation*, 27(4-6), 247-264. doi: 10.1007/s10532-016-9770-9
- Zeng, H., Tian, Y., Anderson, T. H., Tirrell, M., & Israelachvili, J. N. (2008). New SFA techniques for studying surface forces and thin film patterns induced by electric fields. *Langmuir*, 24(4), 1173-1182.
- Zeng, H. B., Maeda, N., Chen, N. H., Tirrell, M., & Israelachvili, J. (2006). Adhesion and friction of polystyrene surfaces around T(g). *Macromolecules*, 39(6), 2350-2363.
- Zhu, S., Li, M., & Gamal El-Din, M. (2017). Forward osmosis as an approach to manage oil sands tailings water and on-site basal depressurization water. *Journal of Hazardous Materials*, 327, 18-27. doi: <http://dx.doi.org/10.1016/j.jhazmat.2016.12.025>

## **6 Chapter 6 General conclusions and recommendations**

### **6.1 Thesis overview**

Large quantities of OSPW generated from Clark hot water process are currently stored in tailing ponds. Similar to the produced water in unconventional oil and gas, OSPW contains both organic and inorganic species: organic species are made up of NAs, PAHs, benzene, toluene, ethylbenzene, BTEX and phenols, while the inorganic species contain dissolved salts, heavy metals, carbonates and suspended solids (clay, silts, etc.). To eliminate its environmental impact, different treatment approaches on biological, chemical and physicochemical aspects have been investigated for safe discharge and recycle, among which FO is gaining more research interests. As a membrane technology process, FO has several advantages over conventional pressure-driven membrane processes including little or no requirement of hydraulic pressure, less membrane fouling propensity, and reduced energy input. However, membrane fouling, draw solution selection, membrane fabrication, recovery of water permeate etc. are still practical obstacles hindering the wide application of FO process. To date, several studies have been conducted using FO to treat oil and gas wastewaters; however, few investigations focusing on applying FO as OSPW treatment method have been reported. As such, significant research gaps still exist on OSPW treatment using FO.

To better understand FO process on OSPW treatment, the current research evaluated the efficiency of FO process as an OSPW management approach in terms of membrane fouling and organic removal. In the first stage, on-site waste basal depressurization water (BDW) was employed as the draw solution and both short and long-term OSPW desalination experiments were carried out to evaluate membrane fouling phenomenon and NA rejection. In the second stage, the effects of pH and draw solutions on the rejection of NA model compounds including

cyclohexane carboxylic acid (CHA), 1-adamantaneacetic acid (AAA) and the refined Merichem mixture of NAs in forward osmosis were studied. In the third stage, aquaporin (AQP)-based and cellulose triacetate (CTA)-based forward osmosis membranes were compared in terms of membrane characteristics; NA model compounds adsorption and rejection, membrane fouling, and NA and inorganic salt rejections. In the last stage, SFA analysis along with adsorption and membrane fouling experiment were carried out to examine the mechanism of membrane fouling in aspect of membrane materials.

## **6.2 Conclusions**

The main conclusions of each chapter are listed as follows:

### **Chapter 2 Forward osmosis as an approach to manage oil sands tailings water and on-site basal depressurization water**

- Applying BDW as the draw solution and OSPW as the feed solution, the accumulated permeate water volumes were 2622.3 mL and 2800.6 mL in FO and PRO mode after long-term operation, which suggested 40% of OSPW volume can be reduced. Given the high rejection and reduced OSPW volume, this process introduced an energy effective water management concept that not only aims to OSPW treatment but also the management of other process waters. However, the sustainability of process is limited likely due to the low water flux and membrane fouling.

### **Chapter 3 Rejection of naphthenic acids by forward osmosis: Effect of pH value and draw solutes**

- For CTA membrane, electrostatic repulsion mechanism dominated CHA and AAA rejection from pH 3 to 9. From pH 6 to 9, the rejection of Merichem NAs was stable (>

92%) likely due to its larger size and electrostatic repulsion force of membrane. At pH 9, the overall rejection of three NA model compounds was above 95% when using 100 mg/L model compound aqueous solution as feed and 1M NaCl as the draw solution. The water flux observed during the rejection experiment was comparatively pH-independent; however, more severe flux decline was found when using AAA and Merichem NA aqueous solution. The rejection study with respect to various inorganic draw solutes suggested that the tested draw solutes did not significantly affect the rejection of CHA at pH 9 and the corresponding water flux was maintained at a similar level, except for CaCl<sub>2</sub>. The specific reverse salt flux of NaCl revealed that exposure to three aqueous NA model compounds solutions might alternate the membrane surface hydrophobicity.

#### **Chapter 4 Forward osmosis desalination of oil sands produced water: comparison between cellulose triacetate-based and aquaporin-based membranes**

- AQP-FO membrane demonstrated higher water permeability than the CTA-FO membrane. In terms of NaCl rejection, solute permeability and structure parameter, the two membranes showed no significant difference. At pH = 9, low adsorption of NA model compounds was observed on each of the membranes due to the electrostatic repulsive force. Moreover, the rejection efficiency for the two FO membranes was above 90% and that of AQP was slightly below CTA because of the promoted compound diffusion by water flux. The results also indicated less water flux decline found on CTA membrane in treatment of OSPW, showing that the CTA membrane was more anti-fouling under low crossflow velocity.

## **Chapter 5 Probing oil sand process-affected water fouling mechanism of forward osmosis membrane: impact of membrane materials and functional groups in naphthenic acids**

- AQP-FO membrane film on mica surface was the most hydrophobic compared to CTA-FO and CA-RO membranes. Because of its comparative high hydrophobicity, AQP-FO membrane demonstrated the strongest adhesive forces. Moreover, only repulsive forces were observed between –OH modified surface and all three membrane film surfaces as well as the case of -COOH modified surface, which was likely due to the impact of repulsive electrostatic interaction and steric interaction of two functionalized surfaces at pH 9. The results of adsorption experiment did not show enough evidences on the impact of hydrophobic-hydrophobic interaction between membrane and NA model compounds, which, on the other hand, confirmed that electro-repulsive force was the governing mechanism of NA model compound adsorption rather than their hydrophobicity. In OSPW fouling test, it was found that PA-RO membrane yielded the lowest water flux because its membrane structure designed for high pressure process led to a severe impact of ICP. Furthermore, comparing the water flux profiles of two FO membranes, CTA-FO membrane performed better than AQP-FO membrane.

### **6.3 Recommendations**

The following recommendations were drawn based on the results obtained in each chapter.

## **Chapter 2 Forward osmosis as an approach to manage oil sands tailings water and on-site basal depressurization water**

- Given the high rejection and reduced OSPW volume, the current process using BDW as the draw solution introduced an energy effective water management concept that not only

aims to OSPW treatment but also the management of other process waters. However, the sustainability of process is limited likely due to the low water flux and membrane fouling. To unravel those obstacles, future works is required to optimize the operating condition and eliminate the impact of membrane fouling. In future work, other types of concentrated streams, such as the rejection stream or retentate from electrodialysis (ED) process and reverse osmosis (RO) etc., are recommended be screened, assessed and identified as draw solutions in OSPW desalination to increase the desalination efficiency and lower the operational cost. The concentrated OSPW obtained from our process can be send to further treatments, for example advanced oxidation (AOPs). The diluted BDW can be send back to the oil sands mining process as potential process waters (i.e. boiler feed) after further treatment (i.e., RO) to reduce the fresh water intake.

Also, FO process can be integrated with other membrane processes to build a continuous system for OSPW treatment. The conceptual schematic of the integrated system is shown in Fig. 6-1. In this system, microfiltration (MF), ED and FO are integrated: OSPW or other types of oil sands produced water is micro-filtered through MF and then, flows to the ED system. One side of ED system generates clean permeate and a concentrated water stream is produced on the other side which can be used as the draw solution in FO system. In the individual FO module, the feed solution could also be oil sands produced water (i.e., OSPW). Subsequently, the ED concentrated stream will be continuously diluted by the water molecules transported from oil sands produced water in the FO module. The concentrated feed solution can be sent to further treatments including RO, ozonation etc.

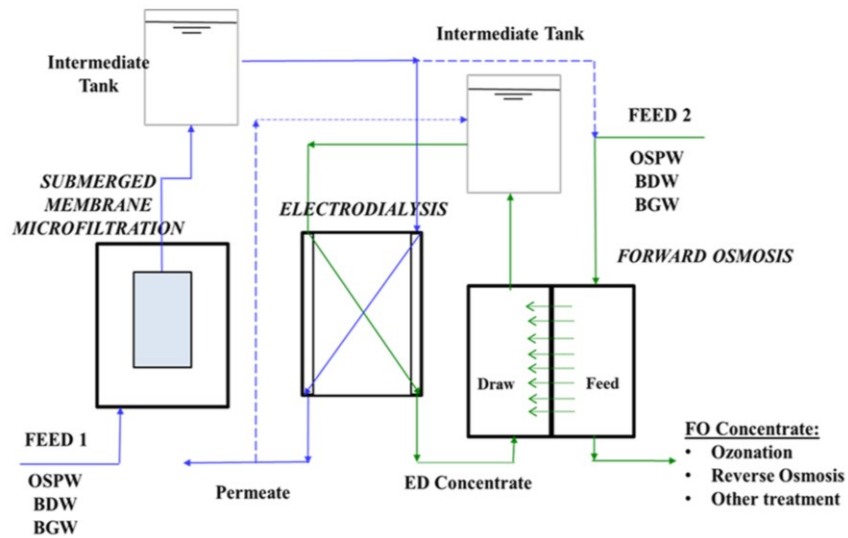


**Figure 6-1** The conceptual schematic of the integrated system

**Chapter 3 Rejection of naphthenic acids by forward osmosis: Effect of pH value and draw solutes**

- The specific reverse salt flux of NaCl revealed that exposure to three aqueous NA model compounds solutions might alternate the membrane characteristics which need to be further investigated.
- Our results cannot exclude the impact of draw solute diffusion on CHA rejection. To further investigate the effect of draw solution diffusion on CHA, higher CHA and draw solute concentration are recommended to employ.

**Chapter 4 Forward osmosis desalination of oil sands produced water: comparison between cellulose triacetate-based and aquaporin-based membranes**

- AQP-FO membrane showed a slight advantage in inorganic salt rejection, compared to CTA-FO membrane. However, compared to membrane selection, the rejection of NAs and salt was more related to pretreatment methods and produced water type.

- Low crossflow velocity was applied in current research and alternative of operating condition may lead to a different result.

**Chapter 5 Probing oil sand process-affected water fouling mechanism of forward osmosis membrane: impact of membrane materials and functional groups in naphthenic acids**

- CTA-FO membrane showed better anti-fouling propensity in aspect of OSPW organic fouling, especially for the hydrophobic organic compound, for instance, NAs.
- Only -OH and -COOH functional group are not attributed to adhesive force, in another word, membrane organic fouling and hydrophobic-hydrophobic interaction was the dominant mechanism for membrane fouling.
- Previous publications suggested that the co-existence of  $\text{Ca}^{2+}$  and -COOH can enhance the membrane fouling, which is recommended to be examined by SFA analysis.



## 7. Bibliography

- Achilli, A., Cath, T. Y., & Childress, A. E. (2010). Selection of inorganic-based draw solutions for forward osmosis applications. *Journal of Membrane Science*, 364(1-2), 233-241. doi: 10.1016/j.memsci.2010.08.010
- Afzal, A., Drzewicz, P., Perez-Estrada, L. A., Chen, Y., Martin, J. W., & El-Din, M. G. (2012). Effect of Molecular Structure on the Relative Reactivity of Naphthenic Acids in the UV/H<sub>2</sub>O<sub>2</sub> Advanced Oxidation Process. *Environmental Science & Technology*, 46(19), 10727-10734.
- Allen, E. W. (2008a). Process water treatment in Canada's oil sands industry: I. Target pollutants and treatment objectives. *Journal of Environmental Engineering and Science*, 7(2), 123-138.
- Allen, E. W. (2008b). Process water treatment in Canada's oil sands industry: II. A review of emerging technologies. *Journal of Environmental Engineering and Science*, 7(5), 499-524. doi: Doi 10.1139/S08-020
- Alpatova, A., Kim, E. S., Dong, S. M., Sun, N., Chelme-Ayala, P., & El-Din, M. G. (2014). Treatment of oil sands process-affected water with ceramic ultrafiltration membrane: Effects of operating conditions on membrane performance. *Separation and Purification Technology*, 122, 170-182. doi: DOI 10.1016/j.seppur.2013.11.005
- Anderson, J. C., Wiseman, S. B., Wang, N., Moustafa, A., Perez-Estrada, L., El-Din, M. C., . . . Giesy, J. P. (2012). Effectiveness of Ozonation Treatment in Eliminating Toxicity of Oil Sands Process-Affected Water to *Chironomus dilutus*. *Environmental Science & Technology*, 46(1), 486-493. doi: Doi 10.1021/Es202415g

- Arkhangelsky, E., Kuzmenko, D., & Gitis, V. (2007). Impact of chemical cleaning on properties and functioning of polyethersulfone membranes. *Journal of Membrane Science*, 305(1-2), 176-184.
- Arkhangelsky, E., Lay, S. S., Wicaksana, F., Al-Rabiah, A. A., Al-Zahrani, S. M., & Wang, R. (2014). Impact of intrinsic properties of foulants on membrane performance in osmotic desalination applications. *Separation and Purification Technology*, 123, 87-95. doi: DOI 10.1016/j.seppur.2013.12.013
- Blandin, G., Vervoort, H., Le-Clech, P., & Verliefde, A. R. D. (2016). Fouling and cleaning of high permeability forward osmosis membranes. *Journal of Water Process Engineering*, 9, 161-169. doi: <http://dx.doi.org/10.1016/j.jwpe.2015.12.007>
- Boo, C., Elimelech, M., & Hong, S. (2013). Fouling control in a forward osmosis process integrating seawater desalination and wastewater reclamation. *Journal of Membrane Science*, 444, 148-156. doi: 10.1016/j.memsci.2013.05.004
- Boo, C., Lee, S., Elimelech, M., Meng, Z. Y., & Hong, S. (2012). Colloidal fouling in forward osmosis: Role of reverse salt diffusion. *Journal of Membrane Science*, 390, 277-284. doi: 10.1016/j.memsci.2011.12.001
- Campos, J. C., Borges, R. M. H., Oliveira, A. M., Nobrega, R., & Sant'Anna, G. L. (2002). Oilfield wastewater treatment by combined microfiltration and biological processes. *Water Research*, 36(1), 95-104.
- Castrillon, S. R. V., Lu, X. L., Shaffer, D. L., & Elimelech, M. (2014). Amine enrichment and poly(ethylene glycol) (PEG) surface modification of thin-film composite forward osmosis membranes for organic fouling control. *Journal of Membrane Science*, 450, 331-339. doi: DOI 10.1016/j.memsci.2013.09.028

- Cath, T. Y., Childress, A. E., & Elimelech, M. (2006). Forward osmosis: Principles, applications, and recent developments. *Journal of Membrane Science*, 281(1-2), 70-87. doi: 10.1016/j.memsci.2006.05.048
- Cath, T. Y., Hancock, N. T., Lundin, C. D., Hoppe-Jones, C., & Drewes, J. E. (2010). A multi-barrier osmotic dilution process for simultaneous desalination and purification of impaired water. *Journal of Membrane Science*, 362(1-2), 417-426. doi: DOI 10.1016/j.memsci.2010.06.056
- Chung, T. S., Li, X., Ong, R. C., Ge, Q. C., Wang, H. L., & Han, G. (2012). Emerging forward osmosis (FO) technologies and challenges ahead for clean water and clean energy applications. *Current Opinion in Chemical Engineering*, 1(3), 246-257.
- Clesceri, L. S., Greenberg, A. E., Eaton, A. D., & American Public Health Association. (1998). *Standard methods for the examination of water and wastewater /edited by Lenore S. Clesceri, Arnold E. Greenberg, Andrew D. Eaton* (20th ed.). Washington, DC: American Public Health Association.
- Coday, B. D., Almaraz, N., & Cath, T. Y. (2015). Forward osmosis desalination of oil and gas wastewater: Impacts of membrane selection and operating conditions on process performance. *Journal of Membrane Science*, 488, 40-55. doi: 10.1016/j.memsci.2015.03.059
- Coday, B. D., Hoppe-Jones, C., Wandera, D., Shethji, J., Herron, J., Lampi, K., . . . Cath, T. Y. (2016). Evaluation of the transport parameters and physiochemical properties of forward osmosis membranes after treatment of produced water. *Journal of Membrane Science*, 499, 491-502.

- Coday, B. D., Xu, P., Beaudry, E. G., Herron, J., Lampi, K., Hancock, N. T., & Cath, T. Y. (2014). The sweet spot of forward osmosis: Treatment of produced water, drilling wastewater, and other complex and difficult liquid streams. *Desalination*, 333(1), 23-35. doi: 10.1016/j.desal.2013.11.014
- Coday, B. D., Yaffe, B. G. M., Xu, P., & Cath, T. Y. (2014). Rejection of Trace Organic Compounds by Forward Osmosis Membranes: A Literature Review. *Environmental Science & Technology*, 48(7), 3612-3624. doi: 10.1021/es4038676
- Couillard, D. (1994). The Use of Peat in Waste-Water Treatment. *Water Research*, 28(6), 1261-1274.
- Cui, Y., Liu, X. Y., Chung, T. S., Weber, M., Staudt, C., & Maletzko, C. (2016). Removal of organic micro-pollutants (phenol, aniline and nitrobenzene) via forward osmosis (FO) process: Evaluation of FO as an alternative method to reverse osmosis (RO). *Water Research*, 91, 104-114. doi: 10.1016/j.watres.2016.01.001
- Deriszadeh, A., Harding, T. G., & Husein, M. M. (2009). Improved MEUF removal of naphthenic acids from produced water. *Journal of Membrane Science*, 326(1), 161-167.
- Dong, S. M., Kim, E. S., Alpatova, A., Noguchi, H., Liu, Y., & El-Din, M. G. (2014). Treatment of oil sands process-affected water by submerged ceramic membrane microfiltration system. *Separation and Purification Technology*, 138, 198-209. doi: 10.1016/j.seppur.2014.10.017
- Duong, P. H. H., & Chung, T. S. (2014). Application of thin film composite membranes with forward osmosis technology for the separation of emulsified oil-water. *Journal of Membrane Science*, 452, 117-126. doi: 10.1016/j.memsci.2013.10.030

- El-Din, M. G., Fu, H. J., Wang, N., Chelme-Ayala, P., Perez-Estrada, L., Drzewicz, P., . . . Smith, D. W. (2011). Naphthenic acids speciation and removal during petroleum-coke adsorption and ozonation of oil sands process-affected water. *Science of the Total Environment*, 409(23), 5119-5125.
- Fang, Y. Y., Bian, L. X., Bi, Q. Y., Li, Q., & Wang, X. L. (2014). Evaluation of the pore size distribution of a forward osmosis membrane in three different ways. *Journal of Membrane Science*, 454, 390-397. doi: DOI 10.1016/j.memsci.2013.12.046
- Frank, R. A., Kavanagh, R., Burnison, B. K., Arsenault, G., Headley, J. V., Peru, K. M., . . . Solomon, K. R. (2008). Toxicity assessment of collected fractions from an extracted naphthenic acid mixture. *Chemosphere*, 72(9), 1309-1314.
- Gallup, D. L., Isacoff, E. G., & Smith, D. N. (1996). Use of Amborsorb(R) carbonaceous adsorbent for removal of BTEX compounds from oil-field produced water. *Environmental Progress*, 15(3), 197-203.
- Garcia-Garcia, E., Pun, J., Hodgkinson, J., Perez-Estrada, L. A., El-Din, M. G., Smith, D. W., . . . Belosevic, M. (2012). Commercial naphthenic acids and the organic fraction of oil sands process water induce different effects on pro-inflammatory gene expression and macrophage phagocytosis in mice. *Journal of Applied Toxicology*, 32(12), 968-979. doi: 10.1002/jat.1687
- Garcia-Garcia, E., Pun, J., Perez-Estrada, L. A., Din, M. G. E., Smith, D. W., Martin, J. W., & Belosevic, M. (2011). Commercial naphthenic acids and the organic fraction of oil sands process water downregulate pro-inflammatory gene expression and macrophage antimicrobial responses. *Toxicology Letters*, 203(1), 62-73.

- Ge, Q. C., Ling, M. M., & Chung, T. S. (2013). Draw solutions for forward osmosis processes: Developments, challenges, and prospects for the future. *Journal of Membrane Science*, 442, 225-237. doi: 10.1016/j.memsci.2013.03.046
- Geise, G. M., Paul, D. R., & Freeman, B. D. (2014). Fundamental water and salt transport properties of polymeric materials. *Progress in Polymer Science*, 39(1), 1-42. doi: DOI 10.1016/j.progpolymsci.2013.07.001
- Gormly, S. (2014). Forward osmosis: introduction and applications for wastewater processing, energy conservation and energy generation. *Membranes for Clean and Renewable Power Applications*, 13, 379-395. doi: Doi 10.1533/9780857098658.5.379
- Hancock, N. T., & Cath, T. Y. (2009). Solute Coupled Diffusion in Osmotically Driven Membrane Processes. *Environmental Science & Technology*, 43(17), 6769-6775. doi: Doi 10.1021/Es901132x
- Hao, C. Y., Headley, J. V., Peru, K. A., Frank, R., Yang, P., & Solomon, K. R. (2005). Characterization and pattern recognition of oil-sand naphthenic acids using comprehensive two-dimensional gas chromatography/time-of-flight mass spectrometry. *Journal of Chromatography A*, 1067(1-2), 277-284. doi: 10.1016/j.chroma.2005.01.041
- Headley, J. V., Peru, K. M., McMartin, D. W., & Winkler, M. (2002). Determination of dissolved naphthenic acids in natural waters by using negative-ion electrospray mass spectrometry. *Journal of Aoac International*, 85(1), 182-187.
- Hickenbottom, K. L., Hancock, N. T., Hutchings, N. R., Appleton, E. W., Beaudry, E. G., Xu, P., & Cath, T. Y. (2013). Forward osmosis treatment of drilling mud and fracturing wastewater from oil and gas operations. *Desalination*, 312, 60-66. doi: 10.1016/j.desal.2012.05.037

- Holloway, R. W., Maltos, R., Vanneste, J., & Cath, T. Y. (2015). Mixed draw solutions for improved forward osmosis performance. *Journal of Membrane Science*, 491, 121-131. doi: 10.1016/j.memsci.2015.05.016
- Holowenko, F. M., MacKinnon, M. D., & Fedorak, P. M. (2002). Characterization of naphthenic acids in oil sands wastewaters by gas chromatography-mass spectrometry. *Water Research*, 36(11), 2843-2855. doi: Pii S0043-1354(01)00492-4
- Huang, C. K., Shi, Y. J., El-Din, M. G., & Liu, Y. (2015). Treatment of oil sands process-affected water (OSPW) using ozonation combined with integrated fixed-film activated sludge (IFAS). *Water Research*, 85, 167-176.
- Hurwitz, G., Guillen, G. R., & Hoek, E. M. V. (2010). Probing polyamide membrane surface charge, zeta potential, wettability, and hydrophilicity with contact angle measurements. *Journal of Membrane Science*, 349(1-2), 349-357.
- Islam, M. S., Zhang, Y. Y., McPhedran, K. N., Liu, Y., & El-Din, M. G. (2015). Next-Generation Pyrosequencing Analysis of Microbial Biofilm Communities on Granular Activated Carbon in Treatment of Oil Sands Process-Affected Water. *Applied and Environmental Microbiology*, 81(12), 4037-4048.
- Israelachvili, J., Min, Y., Akbulut, M., Alig, A., Carver, G., Greene, W., . . . Zeng, H. (2010). Recent advances in the surface forces apparatus (SFA) technique. *Reports on Progress in Physics*, 73(3).
- Israelachvili, J. N. (2011). Chapter 12 - Force-Measuring Techniques *Intermolecular and Surface Forces (Third Edition)* (pp. 223-252). San Diego: Academic Press.
- Israelachvili, J. N., & Adams, G. E. (1978). Measurement of forces between two mica surfaces in aqueous electrolyte solutions in the range 0-100 nm. [10.1039/F19787400975]. *Journal*

- of the Chemical Society, Faraday Transactions 1: Physical Chemistry in Condensed Phases*, 74(0), 975-1001. doi: 10.1039/f19787400975
- Jiang, Y., Liang, J., & Liu, Y. (2016). Application of forward osmosis membrane technology for oil sands process-affected water desalination. *Water Science and Technology*, 73(7), 1-8. doi: 10.2166/wst.2016.014
- Jin, X., Shan, J. H., Wang, C., Wei, J., & Tang, C. Y. Y. (2012). Rejection of pharmaceuticals by forward osmosis membranes. *Journal of Hazardous Materials*, 227, 55-61. doi: 10.1016/j.jhazmat.2012.04.077
- Kannel, P. R., & Gan, T. Y. (2012). Naphthenic acids degradation and toxicity mitigation in tailings wastewater systems and aquatic environments: A review. *Journal of Environmental Science and Health Part a-Toxic/Hazardous Substances & Environmental Engineering*, 47(1), 1-21. doi: 10.1080/10934529.2012.629574
- Kim, C., Lee, S., & Hong, S. (2012). Application of osmotic backwashing in forward osmosis: mechanisms and factors involved. *Desalination and Water Treatment*, 43(1-3), 314-322. doi: 10.1080/19443994.2012.672215
- Kim, E. S., Dong, S., Liu, Y., & Gamal El-Din, M. (2013). Desalination of oil sands process-affected water and basal depressurization water in Fort McMurray, Alberta, Canada: application of electrodialysis. [Research Support, Non-U.S. Gov't]. *Water Science and Technology*, 68(12), 2668-2675. doi: 10.2166/wst.2013.533
- Kim, E. S., Liu, Y., & El-Din, M. G. (2011). The effects of pretreatment on nanofiltration and reverse osmosis membrane filtration for desalination of oil sands process-affected water. *Separation and Purification Technology*, 81(3), 418-428. doi: DOI 10.1016/j.seppur.2011.08.016



- Kim, E. S., Liu, Y., & El-Din, M. G. (2012). Evaluation of Membrane Fouling for In-Line Filtration of Oil Sands Process-Affected Water: The Effects of Pretreatment Conditions. *Environmental Science & Technology*, 46(5), 2877-2884. doi: Doi 10.1021/Es2038135
- Kim, Y., Lee, S., Shon, H. K., & Hong, S. (2015). Organic fouling mechanisms in forward osmosis membrane process under elevated feed and draw solution temperatures. *Desalination*, 355, 169-177. doi: 10.1016/j.desal.2014.10.041
- Klamerth, N., Moreira, J., Li, C., Singh, A., McPhedran, K. N., Chelme-Ayala, P., . . . El-Din, M. G. (2015). Effect of ozonation on the naphthenic acids' speciation and toxicity of pH-dependent organic extracts of oil sands process-affected water. *Science of the Total Environment*, 506, 66-75. doi: 10.1016/j.scitotenv.2014.10.103
- Lee, J., Kim, B., & Hong, S. (2014). Fouling distribution in forward osmosis membrane process. *Journal of Environmental Sciences-China*, 26(6), 1348-1354. doi: Doi 10.1016/S1001-0742(13)60610-5
- Lee, S., Boo, C., Elimelech, M., & Hong, S. (2010). Comparison of fouling behavior in forward osmosis (FO) and reverse osmosis (RO). *Journal of Membrane Science*, 365(1-2), 34-39. doi: 10.1016/j.memsci.2010.08.036
- Li, X. S., Chou, S. R., Wang, R., Shi, L., Fang, W. X., Chaitra, G., . . . Fane, A. G. (2015). Nature gives the best solution for desalination: Aquaporin-based hollow fiber composite membrane with superior performance. *Journal of Membrane Science*, 494, 68-77.
- Linares, R. V., Li, Z., Sarp, S., Bucs, S. S., Amy, G., & Vrouwenvelder, J. S. (2014). Forward osmosis niches in seawater desalination and wastewater reuse. *Water Research*, 66, 122-139. doi: 10.1016/j.watres.2014.08.021

- Linares, R. V., Yangali-Quintanilla, V., Li, Z. Y., & Amy, G. (2011). Rejection of micropollutants by clean and fouled forward osmosis membrane. *Water Research*, 45(20), 6737-6744. doi: 10.1016/j.watres.2011.10.037
- Liu, Y. L., & Mi, B. X. (2012). Combined fouling of forward osmosis membranes: Synergistic foulant interaction and direct observation of fouling layer formation. *Journal of Membrane Science*, 407, 136-144. doi: 10.1016/j.memsci.2012.03.028
- Lu, X. L., Castrillon, S. R. V., Shaffer, D. L., Ma, J., & Elimelech, M. (2013). In Situ Surface Chemical Modification of Thin-Film Composite Forward Osmosis Membranes for Enhanced Organic Fouling Resistance. *Environmental Science & Technology*, 47(21), 12219-12228. doi: Doi 10.1021/Es403179m
- Lutchmiah, K., Verliefde, A. R. D., Roest, K., Rietveld, L. C., & Cornelissen, E. R. (2014). Forward osmosis for application in wastewater treatment: A review. *Water Research*, 58, 179-197. doi: 10.1016/j.watres.2014.03.045
- Madsen, H. T., Bajraktari, N., Helix-Nielsen, C., Van der Bruggen, B., & Sogaard, E. G. (2015). Use of biomimetic forward osmosis membrane for trace organics removal. *Journal of Membrane Science*, 476, 469-474. doi: 10.1016/j.memsci.2014.11.055
- Mazlan, N. M., Marchetti, P., Maples, H. A., Gu, B., Karan, S., Bismarck, A., & Livingston, A. G. (2016). Organic fouling behaviour of structurally and chemically different forward osmosis membranes - A study of cellulose triacetate and thin film composite membranes. *Journal of Membrane Science*, 520, 247-261.
- McGovern, R. K., Mizerak, J. P., Zubair, S. M., & Lienhard, J. H. (2014). Three dimensionless parameters influencing the optimal membrane orientation for forward osmosis. *Journal of Membrane Science*, 458, 104-110. doi: 10.1016/j.memsci.2014.01.061

- Mi, B., & Elimelech, M. (2008). Chemical and physical aspects of organic fouling of forward osmosis membranes. *Journal of Membrane Science*, 320(1-2), 292-302. doi: 10.1016/j.memsci.2008.04.036
- Mi, B. X., & Elimelech, M. (2010). Organic fouling of forward osmosis membranes: Fouling reversibility and cleaning without chemical reagents. *Journal of Membrane Science*, 348(1-2), 337-345. doi: DOI 10.1016/j.memsci.2009.11.021
- Mikula, R. J., Kasperski, K. L., Burns, R. D., & MacKinnon, M. D. (1996). Nature and fate of oil sands fine tailings. *Suspensions: Fundamentals and Applications in the Petroleum Industry*, 251, 677-723.
- Minier-Matar, J., Hussain, A., Janson, A., Wang, R., Fane, A. G., & Adham, S. (2015). Application of forward osmosis for reducing volume of produced/Process water from oil and gas operations. *Desalination*, 376, 1-8.
- Mohamed, M. H., Wilson, L. D., Peru, K. M., & Headley, J. V. (2013). Colloidal properties of single component naphthenic acids and complex naphthenic acid mixtures. *Journal of Colloid and Interface Science*, 395, 104-110. doi: 10.1016/j.jcis.2012.12.056
- Motsa, M. M., Mamba, B. B., D'Haese, A., Hoek, E. M. V., & Verliefde, A. R. D. (2014). Organic fouling in forward osmosis membranes: The role of feed solution chemistry and membrane structural properties. *Journal of Membrane Science*, 460, 99-109. doi: 10.1016/j.memsci.2014.02.035
- Moustafa, A. M. A., Kim, E. S., Alpatova, A., Sun, N., Smith, S., Kang, S., & El-Din, M. G. (2014). Impact of polymeric membrane filtration of oil sands process water on organic compounds quantification. *Water Science and Technology*, 70(5), 771-779. doi: 10.2166/wst.2014.282

- Murib, M. S., Yeap, W. S., Eurlings, Y., van Grinsven, B., Boyen, H. G., Conings, B., . . . Wagner, P. (2016). Heat-transfer based characterization of DNA on synthetic sapphire chips. *Sensors and Actuators B-Chemical*, 230, 260-271.
- Nasr, P., & Sewilam, H. (2015). Forward osmosis: an alternative sustainable technology and potential applications in water industry. *Clean Technologies and Environmental Policy*, 17(7), 2079-2090.
- Nguyen, T. P. N., Yun, E. T., Kim, I. C., & Kwon, Y. N. (2013). Preparation of cellulose triacetate/cellulose acetate (CTA/CA)-based membranes for forward osmosis. *Journal of Membrane Science*, 433, 49-59. doi: DOI 10.1016/j.memsci.2013.01.027
- Parida, V., & Ng, H. Y. (2013). Forward osmosis organic fouling: Effects of organic loading, calcium and membrane orientation. *Desalination*, 312, 88-98. doi: 10.1016/j.desal.2012.04.029
- Phillip, W. A., Yong, J. S., & Elimelech, M. (2010). Reverse Draw Solute Permeation in Forward Osmosis: Modeling and Experiments. *Environmental Science & Technology*, 44(13), 5170-5176. doi: 10.1021/es100901n
- Pourrezaei, P., Alpatova, A., Khosravi, K., Drzewicz, P., Chen, Y., Chelme-Ayala, P., & El-Din, M. G. (2014). Removal of organic compounds and trace metals from oil sands process-affected water using zero valent iron enhanced by petroleum coke. *Journal of Environmental Management*, 139, 50-58.
- Qi, S. R., Wang, R., Chaitra, G. K. M., Torres, J., Hu, X., & Fane, A. G. (2016). Aquaporin-based biomimetic reverse osmosis membranes: Stability and long term performance. *Journal of Membrane Science*, 508, 94-103.

- Qin, D. T., Liu, Z. Y., Sun, D. R. D. L., Song, X. X., & Bai, H. W. (2015). A new nanocomposite forward osmosis membrane custom-designed for treating shale gas wastewater. *Scientific Reports*, 5.
- Qin, M. H., & He, Z. (2014). Self-Supplied Ammonium Bicarbonate Draw Solute for Achieving Wastewater Treatment and Recovery in a Microbial Electrolysis Cell-Forward Osmosis-Coupled System. *Environmental Science & Technology Letters*, 1(10), 437-441. doi: 10.1021/ez500280c
- Rastogi, N. K., & Nayak, C. A. (2011). Membranes for forward osmosis in industrial applications. *Advanced Membrane Science and Technology for Sustainable Energy and Environmental Applications*(25), 680-717. doi: Book\_Do1 10.1533/9780857093790
- Ribeiro, A. R., Nunes, O. C., Pereira, M. F. R., & Silva, A. M. T. (2015). An overview on the advanced oxidation processes applied for the treatment of water pollutants defined in the recently launched Directive 2013/39/EU. *Environment International*, 75, 33-51.
- Salgin, S., Salgin, U., & Soyer, N. (2013). Streaming Potential Measurements of Polyethersulfone Ultrafiltration Membranes to Determine Salt Effects on Membrane Zeta Potential. *International Journal of Electrochemical Science*, 8(3), 4073-4084.
- Scholzy, W., & Fuchs, W. (2000). Treatment of oil contaminated wastewater in a membrane bioreactor. *Water Research*, 34(14), 3621-3629.
- Shaffer, D. L., Chavez, L. H. A., Ben-Sasson, M., Castrillon, S. R. V., Yip, N. Y., & Elimelech, M. (2013). Desalination and Reuse of High-Salinity Shale Gas Produced Water: Drivers, Technologies, and Future Directions. *Environmental Science & Technology*, 47(17), 9569-9583. doi: Doi 10.1021/Es401966e

- Shaffer, D. L., Werber, J. R., Jaramillo, H., Lin, S. H., & Elimelech, M. (2015). Forward osmosis: Where are we now? *Desalination*, *356*, 271-284. doi: 10.1016/j.desa.2014.10.031
- She, Q. H., Jin, X., Li, Q. H., & Tang, C. Y. Y. (2012). Relating reverse and forward solute diffusion to membrane fouling in osmotically driven membrane processes. *Water Research*, *46*(7), 2478-2486. doi: DOI 10.1016/j.watres.2012.02.024
- Shen, Y. X., Saboe, P. O., Sines, I. T., Erbakan, M., & Kumar, M. (2014). Biomimetic membranes: A review. *Journal of Membrane Science*, *454*, 359-381.
- Shi, C., Chan, D. Y. C., Liu, Q. X., & Zeng, H. B. (2014). Probing the Hydrophobic Interaction between Air Bubbles and Partially Hydrophobic Surfaces Using Atomic Force Microscopy. *Journal of Physical Chemistry C*, *118*(43), 25000-25008.
- Shi, Y. J., Huang, C. K., Rocha, K. C., El-Din, M. G., & Liu, Y. (2015). Treatment of oil sands process-affected water using moving bed biofilm reactors: With and without ozone pretreatment. *Bioresource Technology*, *192*, 219-227.
- Shu, Z. Q., Li, C., Belosevic, M., Bolton, J. R., & El-Din, M. G. (2014). Application of a Solar UV/Chlorine Advanced Oxidation Process to Oil Sands Process-Affected Water Remediation. *Environmental Science & Technology*, *48*(16), 9692-9701.
- Tang, C. Y. Y., She, Q. H., Lay, W. C. L., Wang, R., & Fane, A. G. (2010). Coupled effects of internal concentration polarization and fouling on flux behavior of forward osmosis membranes during humic acid filtration. *Journal of Membrane Science*, *354*(1-2), 123-133. doi: 10.1016/j.memsci.2010.02.059
- Tellez, G. T., Nirmalakhandan, N., & Gardea-Torresdey, J. L. (2002). Performance evaluation of an activated sludge system for removing petroleum hydrocarbons from oilfield produced water. *Advances in Environmental Research*, *6*(4), 455-470.

- Wang, Y. N., Wicaksana, F., Tang, C. Y., & Fane, A. G. (2010). Direct Microscopic Observation of Forward Osmosis Membrane Fouling. *Environmental Science & Technology*, 44(18), 7102-7109. doi: 10.1021/es101966m
- Wei, J., Qiu, C. Q., Tang, C. Y. Y., Wang, R., & Fane, A. G. (2011). Synthesis and characterization of flat-sheet thin film composite forward osmosis membranes. *Journal of Membrane Science*, 372(1-2), 292-302. doi: 10.1016/j.memsci.2011.02.013
- Xie, M., Nghiem, L. D., Price, W. E., & Elimelech, M. (2012). Comparison of the removal of hydrophobic trace organic contaminants by forward osmosis and reverse osmosis. *Water Research*, 46(8), 2683-2692. doi: 10.1016/j.watres.2012.02.023
- Xie, M., Nghiem, L. D., Price, W. E., & Elimelech, M. (2013). Impact of humic acid fouling on membrane performance and transport of pharmaceutically active compounds in forward osmosis. *Water Research*, 47(13), 4567-4575. doi: 10.1016/j.watres.2013.05.013
- Xie, M., Nghiem, L. D., Price, W. E., & Elimelech, M. (2014). Impact of organic and colloidal fouling on trace organic contaminant rejection by forward osmosis: Role of initial permeate flux. *Desalination*, 336, 146-152. doi: 10.1016/j.desal.2013.12.037
- Xie, M., Price, W. E., Nghiem, L. D., & Elimelech, M. (2013). Effects of feed and draw solution temperature and transmembrane temperature difference on the rejection of trace organic contaminants by forward osmosis. *Journal of Membrane Science*, 438, 57-64. doi: 10.1016/j.memsci.2013.03.031
- Xie, W. Y., He, F., Wang, B. F., Chung, T. S., Jeyaseelan, K., Armugam, A., & Tong, Y. W. (2013). An aquaporin-based vesicle-embedded polymeric membrane for low energy water filtration. *Journal of Materials Chemistry A*, 1(26), 7592-7600. doi: 10.1039/C3ta10731k

- Xue, J., Zhang, Y., Liu, Y., & Gamal El-Din, M. (2016). Treatment of raw and ozonated oil sands process-affected water under decoupled denitrifying anoxic and nitrifying aerobic conditions: a comparative study. *Biodegradation*, 27(4-6), 247-264. doi: 10.1007/s10532-016-9770-9
- Xue, J. K., Zhang, Y. Y., Liu, Y., & El-Din, M. G. (2016). Treatment of oil sands process-affected water (OSPW) using a membrane bioreactor with a submerged flat-sheet ceramic microfiltration membrane. *Water Research*, 88, 1-11.
- Yashina, A., Meldrum, F., & deMello, A. (2012). Calcium carbonate polymorph control using droplet-based microfluidics. *Biomicrofluidics*, 6(2).
- Yeo, S. Y., Wang, Y., Chilcott, T., Antony, A., Coster, H., & Leslie, G. (2014). Characterising nanostructure functionality of a cellulose triacetate forward osmosis membrane using electrical impedance spectroscopy. *Journal of Membrane Science*, 467, 292-302. doi: 10.1016/j.memsci.2014.05.035
- Yip, N. Y., Tiraferri, A., Phillip, W. A., Schiffman, J. D., & Elimelech, M. (2010). High Performance Thin-Film Composite Forward Osmosis Membrane. *Environmental Science & Technology*, 44(10), 3812-3818. doi: 10.1021/es1002555
- Yong, J. S., Phillip, W. A., & Elimelech, M. (2012). Coupled reverse draw solute permeation and water flux in forward osmosis with neutral draw solutes. *Journal of Membrane Science*, 392, 9-17. doi: 10.1016/j.memsci.2011.11.020
- Zeng, H., Tian, Y., Anderson, T. H., Tirrell, M., & Israelachvili, J. N. (2008). New SFA techniques for studying surface forces and thin film patterns induced by electric fields. *Langmuir*, 24(4), 1173-1182.



- Zeng, H. B., Maeda, N., Chen, N. H., Tirrell, M., & Israelachvili, J. (2006). Adhesion and friction of polystyrene surfaces around T(g). *Macromolecules*, 39(6), 2350-2363.
- Zhang, M. M., Hou, D. X., She, Q. H., & Tang, C. Y. Y. (2014). Gypsum scaling in pressure retarded osmosis: Experiments, mechanisms and implications. *Water Research*, 48, 387-395.
- Zhang, S., Wang, P., Fu, X. Z., & Chung, T. S. (2014). Sustainable water recovery from oily wastewater via forward osmosis-membrane distillation (FO-MD). *Water Research*, 52, 112-121. doi: 10.1016/j.watres.2013.12.044
- Zhang, Y. (2016). *Development and application of Fenton and UV-Fenton processes at natural pH using chelating agents for the treatment of oil sands process-affected water* (Doctor of Philosophy ), University of Alberta.
- Zhao, P., Gao, B. Y., Yue, Q. Y., Liu, S. C., & Shon, H. K. (2016). Effect of high salinity on the performance of forward osmosis: Water flux, membrane scaling and removal efficiency. *Desalination*, 378, 67-73.
- Zhao, P., Gao, B. Y., Yue, Q. Y., & Shon, H. K. (2015). The performance of forward osmosis process in treating the surfactant wastewater: The rejection of surfactant, water flux and physical cleaning effectiveness. *Chemical Engineering Journal*, 281, 688-695. doi: 10.1016/j.cej.2015.07.003
- Zhao, S. A. F., & Zou, L. D. (2011). Relating solution physicochemical properties to internal concentration polarization in forward osmosis. *Journal of Membrane Science*, 379(1-2), 459-467. doi: 10.1016/j.memsci.2011.06.021

- Zhao, S. F., Zou, L., Tang, C. Y. Y., & Mulcahy, D. (2012). Recent developments in forward osmosis: Opportunities and challenges. *Journal of Membrane Science*, 396, 1-21. doi: 10.1016/j.memsci.2011.12.023
- Zheng, Y., Huang, M. H., Chen, L., Zheng, W., Xie, P. K., & Xu, Q. (2015). Comparison of tetracycline rejection in reclaimed water by three kinds of forward osmosis membranes. *Desalination*, 359, 113-122. doi: 10.1016/j.desal.2014.12.009
- Zhou, X. S., Gingerich, D. B., & Mauter, M. S. (2015). Water Treatment Capacity of Forward-Osmosis Systems Utilizing Power-Plant Waste Heat. *Industrial & Engineering Chemistry Research*, 54(24), 6378-6389. doi: 10.1021/acs.iecr.5b00460
- Zhu, S., Li, M., & Gamal El-Din, M. (2017). Forward osmosis as an approach to manage oil sands tailings water and on-site basal depressurization water. *Journal of Hazardous Materials*, 327, 18-27. doi: <http://dx.doi.org/10.1016/j.jhazmat.2016.12.025>
- Zubot, W., MacKinnon, M. D., Chelme-Ayala, P., Smith, D. W., & El-Din, M. G. (2012). Petroleum coke adsorption as a water management option for oil sands process-affected water. *Science of the Total Environment*, 427, 364-372.

## 8. Appendices

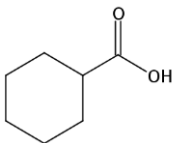
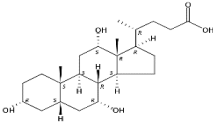
**Table 8-1** Ion composition of OSPW and BDW before and after desalination.

| Analyte                    | Concentrations      |            |           |                  |          |            | CEQG <sup>a</sup><br>(µg/L) |
|----------------------------|---------------------|------------|-----------|------------------|----------|------------|-----------------------------|
|                            | Before desalination |            | FO mode   |                  | PRO mode |            |                             |
|                            | OSPW                | <b>BDW</b> | OSPW      | <b>BDW</b>       | OSPW     | <b>BDW</b> |                             |
| Aluminum<br>(µg/L)         | 15.8±22.7           | 56.2±0.5   | 59.9±0.4  | 45.3±0.2         | 39.8±1.1 | 39.4±0.8   | 100                         |
| <b>Chromium,</b><br>(µg/L) | 2.5±0.9             | 9.9±0.2    | 7.1±0.4   | 4.9±0.1          | 6.6±0.1  | 4.7±0.2    | <b>8.9</b>                  |
| <b>Copper</b>              | 27.6±0.4            | 60.1±0.5   | 39.7±0.4  | 36.5±1           | 58.3±0.6 | 50.1±0.2   | <b>16</b>                   |
| Zinc                       | 9.9±0.3             | 5.8±0.3    | 8.8±0.0   | 6.1±0.3          | 15.4±0.2 | 4.9±0.0    | 30                          |
| Nickel                     | 5.5±0.3             | 1.5±0.5    | 11.6±0.4  | 3.1±1.0          | 12.5±0.2 | 1.9±0.6    | 25                          |
| Lead                       | 0.3±0.1             | 0.4±0.0    | 0.7±0.0   | 0.2±0.0          | 1±0.2    | 0.3±0.0    | 1                           |
| <b>Arsenic</b>             | 2.2±0.2             | 21.3±0.5   | 11.1±0.1  | 7.1±0.2          | 9.5±0.1  | 7.6±0.2    | <b>5</b>                    |
| <b>Silver</b>              | 0.6±0.1             | 0.3±0.0    | 0.2±0.0   | <DL <sup>b</sup> | 0.2±0.0  | 0.1±0.0    | <b>0.25</b>                 |
| Cadmium                    | 0.2±0.0             | <DL        | 0.3±0.0   | <DL              | 0.4±0.0  | <DL        | 0.09                        |
| <b>Titanium</b>            | 65.0±1.9            | 21.9±0.3   | 71.8±0.4  | 20.0±0.2         | 79.8±0.6 | 18.3±0.5   | <b>0.8</b>                  |
| <b>Selenium</b>            | 1.7±0.9             | 59.6±4.9   | 24.6±2.9  | 16.1±2.1         | 28.5±1.4 | 17.2±0.9   | <b>1</b>                    |
| Molybdenum                 | 106.9±1.1           | 5.9±1.4    | 184.6±4.9 | 13.3±0.1         | 210±3.3  | 9.1±1.0    | 73                          |

a. Canadian Environmental Quality Guidelines (CEQG): Water quality guidelines for the protection of aquatic life.

b. Under detect limitation

**Table 8-2** Characteristic of CHA and CA at pH = 9

| Model compound          | cyclohexanecarboxylic acid (CHA)  | Cholic acid (CA)   |
|-------------------------|---|--|
| Molecular weight, g/mol | 128.17  | 408.57   |
| Log D                   | -1.94   | 0.65   |
| pKa                     | 4.91±0.10   | 4.94±0.10  |
| Solubility, g/L (25°C)  | 1000  | 666  |
| Chemical structure      |  |  |

Data source: SciFinder Scholar calculated using Advanced Chemistry

The typical approach force–distance curves (logarithmic coordinates) could be described by Derjaguin-Landau-Verwey-Overbeek (DLVO) model and hydration model or Alexander–de Gennes (AdG) scaling model. The fitting curves (orange) shown in all the figures were obtained base on Derjaguin-Landau-Verwey-Overbeek (DLVO) model and hydration model. The dark yellow lines were the fitting curves based on AdG scaling model.

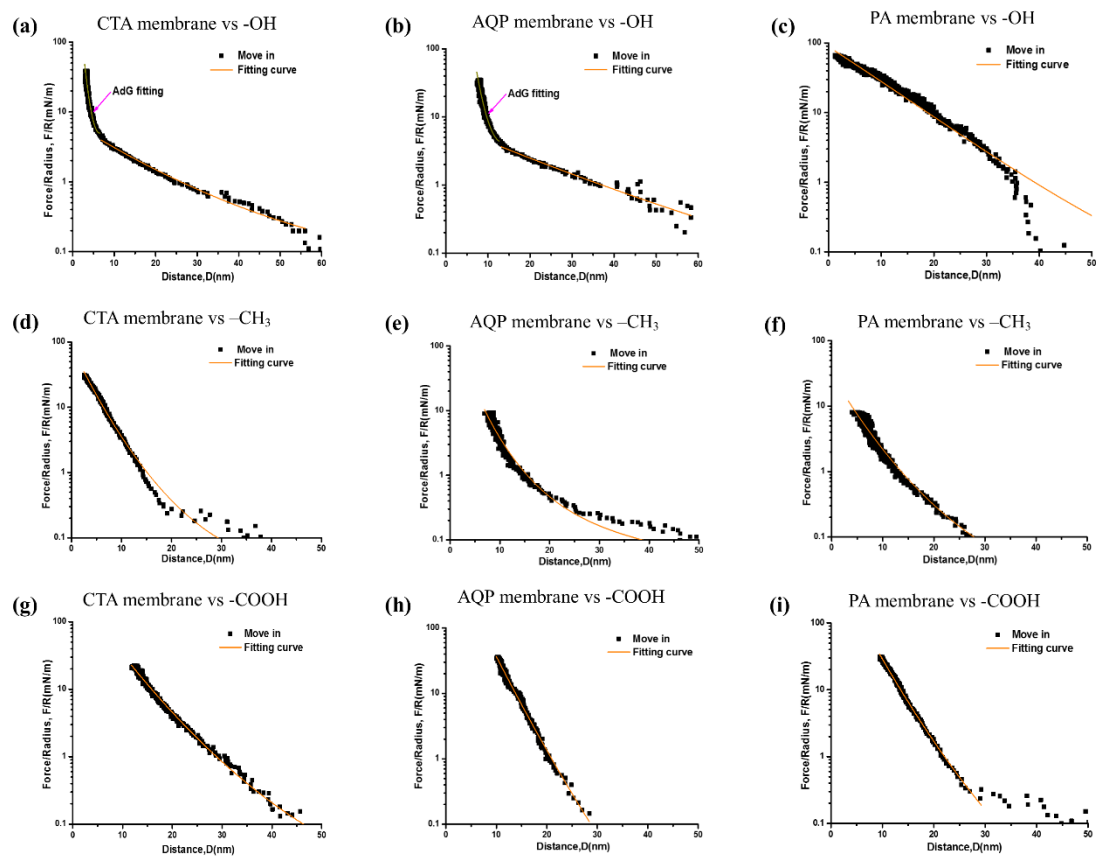


**Figure 8-1** Curve fitting of SFA force measurement